Fall 12-20-2013

Buckling, Postbuckling and Imperfection Sensitivity Analysis of Different Type of Cylindrical Shells by Hui's Postbuckling Method

Hailan Xu
hxu1@uno.edu

Buckling, Postbuckling and Imperfection Sensitivity Analysis of Different Type of Cylindrical Shells by Hui's Postbuckling Method

A Dissertation

Submitted to the Graduate Faculty of the
University of New Orleans
In partial fulfillment of the
Requirements for the degree of

Doctor of Philosophy
In
Engineering and Applied Science
Mechanical Engineering

by

Hailan Xu

BEng., Shenzhen University, 2009
MEng., University of New Orleans, 2011

December, 2013

ACKNOWLEDGEMENTS

I would like to thank for my major supervisor Prof. David Hui for his intellectual guidance, support and patience throughout my PhD study in all these years. I am very grateful to have the opportunity to work with him, and able to expend my knowledge to a very broad field, from material science to mechanical engineering, from nano technology to postbuckling. Besides, I would like to thank Prof. Hui for offering me graduate research assistantship and find the teaching assistantship position for me, and also the possibility to travel and visit other universities and research centers in Texas and German, and also to attend the ICCE conference in Alaska.

I am appreciative and thankful to my department head, Prof. Paul Schilling, for his offering me the teaching assistantship position which make me not only have the research experience, but also the teaching experience, and also I would like to thank for his valuable suggestions and helps regarding my enrollment and financial problems in the University of New Orleans (UNO). Additionally, I would like to thank for my department coordinator Dr. Kazim M. Akyuzlu and Dr. Martin Guillot for their kindly guidance and suggestion on my M.S. and PhD programs. I also would like to thanks all the professors that taught me during my course of studies. I am especially grateful to Dr. Ting Wang, Dr. Carsie A. Hall, Dr. Paul Herrington, Dr. Melody Verges, and Dr. Weilie Zhou for all that they have taught me and all the help they offered. Moreover, special thanks to Prof. Dongming Wei from Department of Mathematics for his assistance and encouragement during my learning in UNO. His kindness

and patience in teaching have led me to overcome a lot of obstacles during my studies and able to enjoy the fun in learning.

I also would like to thank for Dr. Richard Degenhardt, the Professor of PFH Private University of Applied Sciences Gottingen (PFH) and DLR in German, for his advice, and offering me the opportunity to study three months in German. During that time, I have made my major progress of my thesis, without his enthusiasm and guidance, this research project and dissertation would not be complete so fast. I also would like to thank for Dr. Mircea Chipara, the Associate Professor of University of Texas-Pan America for his advices, patience and encouragement during my time in Texas, it was him who taught me who to do the experimental research in Nano-technology.

I would also like to express a great deal of thanks to my colleagues, Dr. Yun Zhai, Mr. He Huang, Dr. Yu Liu, in UNO, also Dr. Mariano Arbeloand, Ms, Saullo Castro in PFH for cooperation and support every time when I have troubles on my research. Especially for Dr. Yu Liu, who helped me a lot on MATLAB programming which is the main software I used in this research, and also Dr. Mariano Arbeloand who taught me how to use ABAQUS, without their patience and help, this research would not have been complete so smoothly. Also I appreciate the friendship with Dr. Yun Zhai, Mr. He Huang and Dr. Yu Liu.

I am also indebted to the technician, Mr. Claude Zerigue of Mechanical Engineering Department in the University of New Orleans. His assistances on setting up and using

equipment help me a lot on my teaching assistantship. I also like to thank for Dr. Baobao Chao of AMRI in UNO for his kindness help on Electron Microscopes.

Finally, I would like to utter my immense gratitude to my parents for their encouragement and support on my study for these five years.

TABLE OF CONTENTS

LIST OF FIGURES

LIST OF TABLES

NOMENCLATURE

Dimensional Quantities

(A_s, A_r)	=	Area of any one stringer or ring
$\left(A_{ij}^*, B_{ij}^*, D_{ij}^*\right)$	=	Laminate stiffness matrix
C	=	$Eh/(1-v^2)$
D	=	$Eh^3/[12(1-v^2)]$, Flexural rigidity of the skin
(d_s, d_r)	=	Distance between adjacent stringers or adjacent rings; meaningful only for equally spaced stiffeners.
E	=	Young's modulus of the skin
(E_s, E_r)	=	Young's modulus of stringer or ring
E_1	=	Young's Modulus of 1- direction
E_2	=	Young's Modulus of 2- direction
(e_s, e_r)	=	Eccentricity of stringer or ring measured from stiffener centroid to the skin middle surface
F	=	Stress function of the smeared shell
(G_s, G_r)	=	Shear modulus of stringer or ring
G_{12}	=	Shear Modulus
h	=	Skin thickness
(I_s, I_r)	=	Out-of-plane moment of inertia of a stringer or a ring with respect to its centroid

(I_t^s, I_t^r)	=	In-plane moment of inertia of a stringer or a ring with respect to its centroid
(J_s, J_r)	=	Torsional constant such that $(G_s J_s, G_r J_r)$ are the torsional rigidity of a stringer or a ring
L	=	length of the shell
$(L_A^*(), L_B^*(), L_D^*())$	=	Differential operator of laminate cylindrical shells
$\left(L_D(), L_Q(), L_H()\right)$	=	Differential operator of stiffened cylindrical shells
$\left(M_x^{sk}, M_y^{sk}, M_{xy}^{sk}\right)$	=	Bending stress resultants of the skin
$\left(N_x, N_y, N_{xy}\right)$	=	Membrane stress resultants of the skin of the shell
(N_s, N_r)		Membrane stress resultants of stringer and ring
P	=	Lateral pressure
(Q_s, Q_r)	=	Height of a stringer or a ring; meaningful only for rectangular shaped stiffeners
R	=	Radius of the cylindrical shell
S	=	Surface area
t	=	Thickness of each laminate
(U, V, W)	=	Axial, circumferential and out-of-plane displacements of the skin middle surface
X	=	Axial coordinate measured from one end of the shell
Y	=	Circumferential coordinate

Non-dimensional quantities

a	=	Postbuckling coefficient related to the cubic term of the potential energy of a single-mode system
$a_{ij}^*, b_{ij}^*, d_{ij}^*$	=	Non-dimensional laminate stiffness matrix
$(A_{xx}, A_{yy}, A_{xy}, A_{yx})$	=	Defined in Table 5.1
b	=	Postbuckling coefficient related to the quartic term of the potential energy of a single-mode system
b_a	=	Postbuckling b coefficient evaluate at the actual applied load
b_{gen}	=	Postbuckling b coefficient calculated by Koiter's general theory
b_{imp}	=	Postbuckling b coefficient calculated by Hui's postbuckling method
$(\bar{B}_{xx}, \bar{B}_{yy}, \bar{B}_{xy}, \bar{B}_{yx})$	=	Defined in Table 5.1
(d_{xx}, d_{yy}, d_{xy})	=	Defined in eqns. (5.9) and (5.10)
(e_x, e_y, e_{xy})	=	Linear strains of the skin middle surface
f	=	$F/(Eh^3)$; Non-dimensional stress function
(f_I, f_{II})	=	Non-dimensional stress function for the buckling state and second order field
(h_{xx}, h_{yy}, h_{xy})	=	Defined in eqns. (5.13) and (5.14)
$(L_a^*(\,), L_b^*(\,), L_d^*(\,))$	=	Non-dimensional differential operator of laminate cylindrical shell

$\left(L_d(),L_q(),L_h()\right)$	=	Non-dimensional differential operator of stiffened cylindrical shell
(M_s,M_r)	=	Number of stringers or rings in a stiffened cylindrical shell
n	=	Number of circumferential full-waves of the buckling mode
$\bar{N}$	=	$n(h/R)^{1/2}$
p	=	$f_{,xx}$; Non-dimensional applied lateral pressure
p_a	=	Non-dimensional actual applied lateral pressure
p_c	=	Non-dimensional classical buckling lateral preseeure
$\left(q_{xx},q_{yy},q_{xy}\right)$	=	Defined in eqns. (5.11) and (5.12)
w	=	W/h ; Non-dimensional out-of-plane displacement
(w_s,w_c,f_s,f_c)	=	See equation (3.10) and (3.11)
(w^*,w_A,w_B,f_A,f_B)	=	Second order field, see equation (3.23) and (3.24)
(x,y)	=	$(X,Y)/(Rt)^{1/2}$, non-dimensional axial and circumferential direction
Z_H	=	$L/(Rh)^{1/2}$; reduced-Batdorf parameter

Non-dimensional quantities (Greek letter)

(α_s, α_r)	=	Ratio of the cross-sectional area of the stringer or ring to that of the skin
(β_s, β_r)	=	Out-of-plane bending stiffness ratio
(γ_s, γ_r)	=	Ratio of eccentricity of stringer or ring to the skin thickness
(δ_s, δ_r)	=	Torsional rigidity ratio
$(\varepsilon_s, \varepsilon_r)$	=	Axial and circumferential strains of a stringer or ring at its centroid
$(\varepsilon_x, \varepsilon_y, \varepsilon_{xy})$	=	Nonlinear strains of the skin middle surface
λ	=	Non-dimensional applied load
λ_a	=	Non-dimensional actual applied load
λ_c	=	Non-dimensional classical buckling load
λ_i	=	Non-dimensional buckling load of imperfect system
μ	=	Imperfection amplitude normalized with the shell thickness
v	=	Poisson's ratio
v_{12}	=	Poisson's ratio of laminate shells
ξ	=	Amplitude of the buckling mode normalized with respect to the skin thickness
σ	=	$N_x R/(Eh^2)$,Non-dimensional axial load
σ_a	=	Non-dimensional actual applied axial load
σ_c	=	Non-dimensional classical buckling axial load
τ	=	$N_{xy} R/(Eh^2)$, non-dimensional applied torsional load

τ_a	=	Non-dimensional actual applied torsional load
τ_c	=	Non-dimensional classical buckling torsional load

ABSTRACT

Buckling and postbuckling has been critical design parameters for many engineering structures. In recent years, this topic has continued to be of major concern due to (1) the discovery of new materials with amazingly superior properties, (2) increasingly more stringent safety requirements, (3) lighter, and more durable requirements. Such applications can be routinely found in aerospace, naval, civil, and electrical, and nuclear engineering structures and especially in the vehicle industries. Koiter is the first one to show that the imperfection-sensitivity of a structure is determined by its initial postbuckling behavior. In Koiter's 1945 general postbuckling theory, it defines the initial postbuckling behavior and imperfection sensitivity behavior by the postbuckling b coefficient. Hui and Chen (1986) were the first to show that the well-known Koiter's General Theory of Elastic Stability of 1945 can be significantly improved by evaluating the postbuckling b coefficient at the actual applied load, rather than at the classical buckling load. The reason for such significant improvement in predicting the imperfection sensitivity is due to the fact that for an imperfection-sensitive structure, the slope of the buckling load versus imperfection amplitude curve approaches negative "infinity" as the imperfection amplitude approaches to zero. Thus for "finite" amplitude of the geometric imperfection, the applied load is significantly lower than the classical buckling load, leading to significant overestimate of imperfection using Koiter's General theory of 1945. Such improvement method was demonstrated to be (1) very simple to apply with no tedious algebra, (2) significant reduction in imperfection sensitivity and (3) although it is still asymptotically valid, there exists a significant extension of validity

involving larger imperfection amplitudes. Strictly speaking, Koiter's theory of 1945 is valid only for vanishingly small imperfection amplitudes. Hence such improved method is termed Hui's Postbuckling method.

This study deals with the Postbuckling and imperfection sensitivity of different kinds of cylinders by using the Hui's postbuckling method. For unstiffened cylinder and laminate cylinder, the solution of Hui's postbuckling method is compared with ABAQUS simulation result. A parameter variation of stringer/ring stiffened cylinder is also evaluated. A positive shift of the postbuckling b coefficient has been observed, which indicates a significant overestimate of the imperfection sensitivity by Koiter's general stability theory. More importantly, the valid region is significantly increased by using Hui's postbuckling method compared with the Koiter's general stability theory.

Keywords: Buckling; Postbuckling; Imperfection Sensitivity; Cylindrical Shell

CHAPTER 1

INTRODUCTION

1.1 Motivation and Scope

1.1.1 History

Thin-walled cylinders are widely used in various engineering approaches. Especially speaking, stiffened and unstiffened metallic cylinders are utilized extensively in navigation, aviation, space vehicles, and also in the construction of liquid storage tanks, pressure vessels, tubes and pipes. Usually they are subject to three kinds of loads, which are axial load, external or internal pressure and torsional load. Therefore the buckling strength of the thin-wall structure is very important in the safety design of such configurations. The first theoretical investigations on the stability of structures with axially loaded cylinders were present by Lorenz [1] [2], Timoshenko [3] [4], and Southwell [5]. The first experimental studies on this topic are performed by Robertson [6], Flugge [7], Wilson and Newmark [8], Lundquist [9]. In the beginning, many assumptions were adapted in the theoretical investigation to reduce the governing equation into a linear eigenvalue problem, which is also called the classical buckling problem. But there is an unacceptable difference between the classical buckling load and experimental buckling load for the thin-walled cylinders. Lots of efforts were made to explain this difference between the analytical and experimental study.

In the analytical study, some simplification assumptions were reevaluated and removed later. Then the studies were focus on the following directions: (1) the effect of prebuckling deformations [10] [11] [12]; (2) the effect of in-plane boundary conditions [13] [14] [15] [16]; (3) the effect of initial geometric imperfections.

In the beginning, the subject to imperfection sensitivity study of the strict postbuckling analyses was perfect structures [17] [18] [19] [20] [21] [22]. Then people start to evaluate the imperfection sensitivity of the imperfect structures with non-linear kinematic relations. Donnell [23] was the first one to evaluate the stability of imperfection structures. Many reports were published by following his analyzing method [24] [25] [26] [27] [28] [29], but the results were not satisfying. Koiter [30] is the first one to present the general postbuckling theory which can take the presence of simple imperfections and interactions of different buckling modes into account when calculating the buckling load of structures. But his theory was not well known until translated in English in 1967. His theory is only valid near the classical buckling load and for very small imperfections. From then on, many breakthroughs have been made in the field of elastic stability theory by those pioneer researchers. Numerous papers were published based on Koiter's theory. These results can be found in many reviews such as Huthinson and Koiter [31]; Budiansky and Hutchinson [32]; Simitses [33]. Through all the theoretical investigation of cylindrical shells, people start to realize that the major reason leading to the difference between theoretical and experiment is the presence of unavoidable geometric imperfections. The fact that the cylindrical structures are extremely sensitive to the initial geometric imperfections has reinforced this effect.

Many experimental studies were performed in parallel to the theoretical investigations. The results were presented to prove the correctness of Koiter's theory such as Nash [34], Weingarten [35], Yamaki and Kodama [36], Kodama et al. [37] . Moreover, Thielemann and Esslinger [38] [39] extended their research to include theoretical postbuckling calculation on the basis of the experimental results.

Some researchers also paid attention to the buckling and postbuckling behavior of stiffened cylindrical shells, since this is an efficient way to improve the properties of the cylindrical shell. Huthcinson and Amazigo [40] presented the postbuckling analysis of stringer stiffened cylindrical shell under axial compression. Besides, an independent investigation of buckling of the above structures under compression incorporating the effects of the torsional rigidity of the stiffeners was performed by Singer, Baruch and Harari [41] and summarized by Singer [42]. Sheinman and Simitses [43] examined the buckling of stiffened cylindrical shells under torsion. Also some experimental studies were carried out for the stiffened cylindrical shells [44] [45] [46] [47] [48]. It has been shown that stringer stiffened reinforcements will decrease the influence of the initial imperfections. External reinforcement is relatively more sensitive to the initial imperfections. This conclusion can be found in many papers [49] [50] [51] [52] [53] [54] [29] [55]. Some researchers also compared the theoretical result with experiment result of the stringer stiffened cylindrical shells [56] [57] [58]. Moreover, some researchers presented the work of buckling and postbuckling of stiffened cylindrical shells under combined load [59] [60] [61] [62].

Due to the requirement of light-weight, high-strength properties, the research of postbuckling of composite cylindrical shells became a hot topic. Tennyson and Muggeridge [63] [64] are the first to investigate the buckling of imperfect anisotropic laminated cylindrical shells. Many researchers followed their study, and extend it to more complicate situations. Shen [65] [66] [67] [68] [69] has presented many results of postbuckling of laminated cylindrical shells using boundary layer theory. People can found many results for buckling of thick laminated cylindrical shells in a complete review by Simitses [70].

Because of the power of commercial finite element software, people start to use these software to solve many complex imperfection sensitivity problems of cylindrical shells. For example the imperfection caused by single or multy perturbation load [71] [72] [73] and stochastic imperfection [74] [75] [76]. Although the finite element method can achieve a relatively high accuracy, it costs much more time than the asymptotic method.

1.1.2 Motivation

Hui and Chen [77] and Hui [78] showed that the well-known Koiter's [30] General Theory of Elastic Stability of 1945 can be significantly improved by evaluating the postbuckling b coefficient (as first defined by Budiansky and Hutchinson [79] in 1966) at the actual applied load, rather than at the classical buckling load. The reason for such significant improvement in predicting the imperfection sensitivity is that, for an imperfection-sensitive structure, the slope of the buckling load versus imperfection amplitude curve approaches negative "infinity" as the imperfection amplitude approaches to zero. Thus, for "finite" amplitude of the geometric imperfection, the applied load is significantly lower than the classical buckling load, causing significant overestimation of imperfection using Koiter's General theory of 1945. Such improved theory was demonstrated to be (1) very simple to apply with no tedious algebra, (2) significant reduction in imperfection sensitivity and (3) although it is still asymptotically valid, there exists a significant extension of the range of validity involving larger imperfection amplitudes. Strictly speaking, Koiter's theory of 1945 is valid only for vanishingly small imperfection amplitudes. Hence such improved method is termed as Hui's Postbuckling method.

But does the improved method also work for closed cylindrical shell? What is the range of validity of the improved method? These questions must be answered before this method can be used in practical. This is the major motivation for this thesis. In this thesis, we will use the Hui's postbuckling method to analyze the postbuckling and imperfection sensitivity of different kinds of cylinders to demonstrate this method works for closed cylindrical shell. We

will also compare the result with finite element result and determine the valid region of the improved method. The other motivation is: nowadays, people usually use the finite element method to solve such problems. Despite this method is very accurate, it is computationally expensive. The traditional asymptotic method is much faster, about 20 times faster than the finite element approach. Also, the commercial software is very expensive compared with Hui's postbuckling method which can be accessed by free codes. So this research can provide a rough but fast and cheap way for the preliminary design.

1.2 Buckling and Postbuckling

1.2.1 Concept of Buckling and Postbuckling

In mechanical point of view, buckling is a disproportionate increase in displacement resulting from a small increase in load, which is characterized by mathematical instability, leading to a failure mode. The buckling is caused by a bifurcation in the solution to the equations of the equilibrium path. At that point, further load can be sustained in either undeformed state or laterally deformed state. This type of problems always can be represented as an eigenvalue problem. Postbuckling is the behavior of the equilibrium path for the laterally deformed state after the structure buckled. The equilibrium paths represent configurations of equilibrium.

1.2.2 Imperfection

Imperfection denotes the shape difference between the ideal product and design. All the products will have imperfections, since there are always manufacture residues. The imperfection concept used in this thesis is defined to be lateral displacements occurred before the closed cylindrical shell sustains the applied load. The imperfection can be separated into three kinds of categories, (1) imperfection which is identical to the buckling mode. (2) Imperfection caused by other load [71] [72] [73]. (3) Stochastic imperfection [74] [75] [76] [80]. The imperfection which is identical to the buckling mode is easy to be applied to the equation, but this type of imperfection is hard to approach from the experiment. Also, this type of imperfection is the worst case imperfection which should have the lowest buckling

load compared with the other imperfection types with the same amplitude. The imperfection caused by other loads is more practical. For example, a small lateral perturbation load presents on the cylinder under compression. The imperfection will concentrate on where the lateral load applied. The stochastic imperfection is also practical, especially for the manufacturing. The product always has small stochastic imperfections due to the residues. The imperfection we are using in this thesis is identical to the first buckling mode, which is also the restriction to both Koiter's General postbuckling theory and Hui's postbuckling method.

1.2.3 Imperfection Sensitivity

Imperfection sensitivity is a property which denotes the stability behavior of the structure. If the buckling load of the structure decreases when it has imperfection, we call this structure is imperfection sensitive (unstable). If the buckling load do not change with the imperfection, we call this structure is imperfection insensitive (stable). Usually, for imperfection sensitive structure, we characterize the sensitivity by the knock down factor (KDF) which is the buckling load of imperfect system divided by the buckling load of perfect system. We can analyze the imperfection behavior of the structure by calculating KDFs for finite number of imperfections and then we can create the curve called knock down curve (KDC). This curve is essential to the imperfection sensitive analysis.

1.3 Koiter's General Stability Theory

1.3.1 Background

Koiter is the first one to show that the imperfection-sensitivity of a structure is determined by its initial postbuckling behavior. He used an asymptotic approach to characterize the total buckling behavior into the combination of prebuckling, buckling and initial postbuckling behavior by a single parameter called b coefficient. He also found the relation between the buckling load and imperfection, which is asymptotically valid for small imperfections. But his theory is not well known until his thesis was translated into English in 1967 [30]. After that, lots of researchers have published many papers based on his theory [81] [40] [82] [83] [84]. The original notation in Koiter's thesis is a little bit hard to understand and fortunately, Budiansky [81] has reformulated with the notation which is more commonly used.

1.3.2 Limitation of Koiter's General Stability Theory

Koiter's general postbuckling theory is using an asymptotic perturbation approach, but there are some limitations (or assumption) for this theory. First, the general theory assumes that the deformation of the structure in the prebuckling state is neglectable, and this limitation was later removed by Fitch [85]. Second, it assumes that the shape of imperfection of the structure should be identical to the buckling mode. Third, the Koiter's general postbuckling theory is only valid for sufficiently small imperfection amplitude, which is less than 10 percent of the skin thickness. It is called the immediate postbuckling and this is pointed out by Koiter and Pignataro [86] in the case of simultaneous buckling mode interaction of integrally stiffened flat plates under compression.

1.3.3 Derive Equations for Koiter's Postbuckling theory

In order to make this thesis more self-contained, and provide a convenient compendium formulas for future use, in this section, we will briefly introduce the Koiter's [30] general stability theory, following by Budiansky's [81] reformulation. Here we will derive the postbuckling formula for cylindrical shell as an example. This will be clearer to understand. The first variation of potential energy for a cylindrical shell can be,

$$\delta P.E. = \int_S (M\delta K + N\delta\varepsilon) dS \tag{1.1}$$

Where

$$M = \begin{bmatrix} M_x \\ M_y \\ M_{xy} \end{bmatrix} = \begin{bmatrix} -D(W_{,XX} + vW_{,YY}) \\ -D(W_{,YY} + vW_{,XX}) \\ -D(1-v)W_{,XY} \end{bmatrix} \tag{1.2}$$

$$K = \begin{bmatrix} K_x \\ K_y \\ 2K_{xy} \end{bmatrix} = \begin{bmatrix} -W_{,XX} \\ -W_{,YY} \\ -2W_{,XY} \end{bmatrix} \tag{1.3}$$

$$\varepsilon = \begin{bmatrix} \varepsilon_x \\ \varepsilon_y \\ 2\varepsilon_{xy} \end{bmatrix} = \begin{bmatrix} U_{,X} + \frac{1}{2}W_{,X}^2 \\ V_{,Y} + \frac{W}{R} + \frac{1}{2}W_{,Y}^2 \\ U_{,Y} + V_{,X} + W_{,X}\,W_{,Y} \end{bmatrix} \tag{1.4}$$

$$N = \begin{bmatrix} N_x \\ N_y \\ N_{xy} \end{bmatrix} = \begin{bmatrix} C(\varepsilon_x + v\varepsilon_y) \\ C(\varepsilon_y + v\varepsilon_x) \\ C(1-v)\varepsilon_{xy} \end{bmatrix} \tag{1.5}$$

We can also write the stress-resultants in terms of an Airy stress function as,

$$N = \begin{bmatrix} N_x \\ N_y \\ N_{xy} \end{bmatrix} = \begin{bmatrix} F_{,yy} \\ F_{,xx} \\ -F_{,xy} \end{bmatrix} \tag{1.6}$$

The calculus of variations then leads to the equilibrium equations

$$\begin{aligned} D\left(W_{,xxxx} + 2W_{xxyy} + W_{,yyyy}\right) + \frac{F_{,xx}}{R} - F_{,yy}\, W_{,xx} \\ - F_{,xx}\, W_{,yy} + 2F_{,XY}\, W_{,XY} = -P \end{aligned} \tag{1.7}$$

where P is the external (inward) pressure.

With the equation (1.4) and (1.5) we can get the compatibility equation as,

$$\begin{aligned} \frac{1}{Eh}\left(F_{,XXXX} + 2F_{,XXYY} + F_{,YYYY}\right) - \frac{W_{,XX}}{R} \\ = (W_{,XY})^2 - W_{,XX}\, W_{,YY} \end{aligned} \tag{1.8}$$

The equilibrium and compatibility equations (1.7) and (1.8) are the famous Karman-Donnell equations.

Now we will assume that the applied load is in prebuckling state which is governed by the linear theory. If λ denotes a scalar measure of the magnitude of the external loading, it can be represented as,

$$\delta P.E. = \lambda \int_S N_0 \delta e dS \tag{1.9}$$

Where

$$N_0 = \lambda \begin{bmatrix} N_{0x} \\ N_{0y} \\ N_{0xy} \end{bmatrix} \tag{1.10}$$

$$e = \begin{bmatrix} e_x \\ e_y \\ 2e_{xy} \end{bmatrix} = \begin{bmatrix} U_{,X} \\ V_{,Y} \\ U_{,Y} + V_{,X} \end{bmatrix} \tag{1.11}$$

Then the equation (1.1) can be written as,

$$\int_S \left\{ \begin{bmatrix} M_x \\ M_y \\ M_{xy} \end{bmatrix}^T \begin{bmatrix} \delta K_x \\ \delta K_y \\ 2\delta K_{xy} \end{bmatrix} + \begin{bmatrix} N_x \\ N_y \\ N_{xy} \end{bmatrix}^T \begin{bmatrix} \delta e_x \\ \delta e_y \\ 2\delta e_{xy} \end{bmatrix} + \begin{bmatrix} N_x \\ N_y \\ N_{xy} \end{bmatrix}^T \begin{bmatrix} W_{,X}\, \delta W_{,X} \\ W_{,Y}\, \delta W_{,Y} \\ W_{,X}\, \delta W_{,Y} + W_{,Y}\, \delta W_{,X} \end{bmatrix} \right\} dS = \lambda \int_S \begin{bmatrix} N_{0x} \\ N_{0y} \\ N_{0xy} \end{bmatrix}^T \begin{bmatrix} e_x \\ e_y \\ 2e_{xy} \end{bmatrix} dS \tag{1.12}$$

The e is the linear part of ε. Now suppose that a bifurcation of the equilibrium state can occur at the critical load λ_c, then we can write the expansion

$$\begin{bmatrix} U \\ W \\ N \\ F \\ M \\ K \\ \varepsilon \\ e \end{bmatrix} = \lambda \begin{bmatrix} U_0 \\ W_0 \\ N_0 \\ F_0 \\ 0 \\ 0 \\ \varepsilon_0 \\ e_0 \end{bmatrix} + \xi \begin{bmatrix} U_1 \\ W_1 \\ N_1 \\ F_1 \\ M_1 \\ K_1 \\ \varepsilon_1 \\ e_1 \end{bmatrix} + \xi^2 \begin{bmatrix} U_2 \\ W_2 \\ N_2 \\ F_2 \\ M_2 \\ K_2 \\ \varepsilon_2 \\ e_2 \end{bmatrix} + \ldots \tag{1.13}$$

where $\lambda \to \lambda_c$ as $\xi \to 0$, the first, second and third column on the right hand side of the above equation represent the prebuckling mode, classical buckling mode and initial postbuckling mode respectively, ξ can be represented as the contribution of classical buckling mode to the initial postbuckling state.

With equation (1.4), (1.11) and (1.13) we can derive the relation as follow,

$$\begin{bmatrix} \varepsilon_{0x} \\ \varepsilon_{0y} \\ 2\varepsilon_{0xy} \end{bmatrix} = \begin{bmatrix} e_{0x} \\ e_{0y} \\ 2e_{0xy} \end{bmatrix} \tag{1.14}$$

$$\begin{bmatrix} \varepsilon_{1x} \\ \varepsilon_{1y} \\ 2\varepsilon_{1xy} \end{bmatrix} = \begin{bmatrix} e_{1x} \\ e_{1y} \\ 2e_{1xy} \end{bmatrix} \tag{1.15}$$

$$\begin{bmatrix} \varepsilon_{2x} \\ \varepsilon_{2y} \\ 2\varepsilon_{2xy} \end{bmatrix} = \begin{bmatrix} e_{2x} + W_{1,X}^2 \\ e_{2y} + W_{1,Y}^2 \\ 2e_{2xy} + W_{1,X}\, W_{1,Y} \end{bmatrix} \tag{1.16}$$

$$\begin{bmatrix} \varepsilon_{3x} \\ \varepsilon_{3y} \\ 2\varepsilon_{3xy} \end{bmatrix} = \begin{bmatrix} e_{3x} + W_{1,X}\, W_{2,X} \\ e_{3y} + W_{1,Y}\, W_{2,Y} \\ 2e_{3xy} + W_{1,X}\, W_{2,Y} + W_{1,Y}\, W_{2,X} \end{bmatrix} \tag{1.17}$$

Substitute equation (1.13) into equation (1.12), we can get,

$$\begin{aligned}
&\int_S \left\{ \begin{bmatrix} M_{1x} \\ M_{1y} \\ M_{1xy} \end{bmatrix}^T \begin{bmatrix} \delta K_x \\ \delta K_y \\ 2\delta K_{xy} \end{bmatrix} + \begin{bmatrix} N_{1x} \\ N_{1y} \\ N_{1xy} \end{bmatrix}^T \begin{bmatrix} \delta e_x \\ \delta e_y \\ 2\delta e_{xy} \end{bmatrix} \right. \\
&\left. + \lambda \begin{bmatrix} N_{0x} \\ N_{0y} \\ N_{0xy} \end{bmatrix}^T \begin{bmatrix} W_{1,X}\, \delta W_{,X} \\ W_{1,Y}\, \delta W_{,Y} \\ W_{1,X}\, \delta W_{,Y} + W_{1,Y}\, \delta W_{,X} \end{bmatrix} \right\} dS \\
&+ \xi \int_S \left\{ \begin{bmatrix} M_{2x} \\ M_{2y} \\ M_{2xy} \end{bmatrix}^T \begin{bmatrix} \delta K_x \\ \delta K_y \\ 2\delta K_{xy} \end{bmatrix} + \begin{bmatrix} N_{2x} \\ N_{2y} \\ N_{2xy} \end{bmatrix}^T \begin{bmatrix} \delta e_x \\ \delta e_y \\ 2\delta e_{xy} \end{bmatrix} \right. \\
&+ \left(\lambda \begin{bmatrix} N_{0x} \\ N_{0y} \\ N_{0xy} \end{bmatrix}^T \begin{bmatrix} W_{2,X}\, \delta W_{,X} \\ W_{2,Y}\, \delta W_{,Y} \\ W_{2,X}\, \delta W_{,Y} + W_{2,Y}\, \delta W_{,X} \end{bmatrix} \right. \\
&\left. \left. + \begin{bmatrix} N_{1x} \\ N_{1y} \\ N_{1xy} \end{bmatrix}^T \begin{bmatrix} W_{1,X}\, \delta W_{,X} \\ W_{1,Y}\, \delta W_{,Y} \\ W_{1,X}\, \delta W_{,Y} + W_{1,Y}\, \delta W_{,X} \end{bmatrix} \right) \right\} dS \\
&+ \xi^2 \int_S \left\{ \begin{bmatrix} M_{3x} \\ M_{3y} \\ M_{3xy} \end{bmatrix}^T \begin{bmatrix} \delta K_x \\ \delta K_y \\ 2\delta K_{xy} \end{bmatrix} + \begin{bmatrix} N_{3x} \\ N_{3y} \\ N_{3xy} \end{bmatrix}^T \begin{bmatrix} \delta e_x \\ \delta e_y \\ 2\delta e_{xy} \end{bmatrix} \right. \\
&+ \left(\lambda \begin{bmatrix} N_{0x} \\ N_{0y} \\ N_{0xy} \end{bmatrix}^T \begin{bmatrix} W_{3,X}\, \delta W_{,X} \\ W_{3,Y}\, \delta W_{,Y} \\ W_{3,X}\, \delta W_{,Y} + W_{3,Y}\, \delta W_{,X} \end{bmatrix} \right. \\
&+ \begin{bmatrix} N_{1x} \\ N_{1y} \\ N_{1xy} \end{bmatrix}^T \begin{bmatrix} W_{2,X}\, \delta W_{,X} \\ W_{2,Y}\, \delta W_{,Y} \\ W_{2,X}\, \delta W_{,Y} + W_{2,Y}\, \delta W_{,X} \end{bmatrix} \\
&\left. \left. + \begin{bmatrix} N_{2x} \\ N_{2y} \\ N_{2xy} \end{bmatrix}^T \begin{bmatrix} W_{1,X}\, \delta W_{,X} \\ W_{1,Y}\, \delta W_{,Y} \\ W_{1,X}\, \delta W_{,Y} + W_{1,Y}\, \delta W_{,X} \end{bmatrix} \right) \right\} dS + \cdots = 0
\end{aligned} \tag{1.18}$$

By letting $\xi \to 0$, we can get a variation equation for the buckling state which is,

$$\int_S \left\{ \begin{bmatrix} M_{1x} \\ M_{1y} \\ M_{1xy} \end{bmatrix}^T \begin{bmatrix} \delta K_x \\ \delta K_y \\ 2\delta K_{xy} \end{bmatrix} + \begin{bmatrix} N_{1x} \\ N_{1y} \\ N_{1xy} \end{bmatrix}^T \begin{bmatrix} \delta e_x \\ \delta e_y \\ 2\delta e_{xy} \end{bmatrix} + \lambda_c \begin{bmatrix} N_{0x} \\ N_{0y} \\ N_{0xy} \end{bmatrix}^T \begin{bmatrix} W_{1,X}\, \delta W_{,X} \\ W_{1,Y}\, \delta W_{,Y} \\ W_{1,X}\, \delta W_{,Y} + W_{1,Y}\, \delta W_{,X} \end{bmatrix} \right\} dS = 0 \tag{1.19}$$

and a consequence of this relation is the "energy" equation

$$\int_S \left\{ \begin{bmatrix} M_{1x} \\ M_{1y} \\ M_{1xy} \end{bmatrix}^T \begin{bmatrix} K_{1x} \\ K_{1y} \\ 2K_{1xy} \end{bmatrix} + \begin{bmatrix} N_{1x} \\ N_{1y} \\ N_{1xy} \end{bmatrix}^T \begin{bmatrix} e_{1x} \\ e_{1y} \\ 2e_{1xy} \end{bmatrix} \right\} dS = -\lambda_c \int_S \left\{ \begin{bmatrix} N_{0x} \\ N_{0y} \\ N_{0xy} \end{bmatrix}^T \begin{bmatrix} W_{1,X}^2 \\ W_{1,Y}^2 \\ 2W_{1,X}\, W_{1,Y} \end{bmatrix} \right\} dS \tag{1.20}$$

By applying the orthogonality condition,

$$\int_S \left\{ \begin{bmatrix} M_{1x} \\ M_{1y} \\ M_{1xy} \end{bmatrix}^T \begin{bmatrix} K_{ix} \\ K_{iy} \\ 2K_{ixy} \end{bmatrix} + \begin{bmatrix} N_{1x} \\ N_{1y} \\ N_{1xy} \end{bmatrix}^T \begin{bmatrix} e_{ix} \\ e_{iy} \\ 2e_{ixy} \end{bmatrix} \right\} dS = -\lambda_c \int_S \left\{ \begin{bmatrix} N_{0x} \\ N_{0y} \\ N_{0xy} \end{bmatrix}^T \begin{bmatrix} W_{1,X}\, W_{i,X} \\ W_{1,Y}\, W_{i,Y} \\ W_{1,X}\, W_{i,Y} + W_{1,Y}\, W_{i,X} \end{bmatrix} \right\} dS = 0 \tag{1.21}$$

For $i > 1$, the reason for $i \neq 1$ is because the buckling mode is not possible to be orthogonal to itself.

Note that from the equations (1.2) to (1.5), we can get the following symmetric relation,

$$\begin{bmatrix} M_{ix} \\ M_{iy} \\ M_{ixy} \end{bmatrix}^T \begin{bmatrix} K_{jx} \\ K_{jy} \\ 2K_{jxy} \end{bmatrix} = \begin{bmatrix} M_{jx} \\ M_{jy} \\ M_{jxy} \end{bmatrix}^T \begin{bmatrix} K_{ix} \\ K_{iy} \\ 2K_{ixy} \end{bmatrix} \tag{1.22}$$

$$\begin{bmatrix} N_{ix} \\ N_{iy} \\ N_{ixy} \end{bmatrix}^T \begin{bmatrix} \varepsilon_{jx} \\ \varepsilon_{jy} \\ 2\varepsilon_{jxy} \end{bmatrix} = \begin{bmatrix} N_{jx} \\ N_{jy} \\ N_{jxy} \end{bmatrix}^T \begin{bmatrix} \varepsilon_{ix} \\ \varepsilon_{iy} \\ 2\varepsilon_{ixy} \end{bmatrix} \tag{1.23}$$

For all i and j. With the use of equations (1.19) to (1.21), and choose

$$\begin{bmatrix} \delta U \\ \delta V \\ \delta W \end{bmatrix} = \begin{bmatrix} U_1 \\ V_1 \\ W_1 \end{bmatrix} \tag{1.24}$$

The equation (1.18) then gives,

$$\begin{aligned} &(\lambda - \lambda_c) \int_S \left\{ \begin{bmatrix} N_{0x} \\ N_{0y} \\ N_{0xy} \end{bmatrix}^T \begin{bmatrix} W_{1,X}^2 \\ W_{1,Y}^2 \\ 2W_{1,X}\, W_{1,Y} \end{bmatrix} \right\} dS \\ &+ \frac{3\xi}{2} \int_S \left\{ \begin{bmatrix} N_{1x} \\ N_{1y} \\ N_{1xy} \end{bmatrix}^T \begin{bmatrix} W_{1,X}^2 \\ W_{1,Y}^2 \\ 2W_{1,X}\, W_{1,Y} \end{bmatrix} \right\} dS \\ &+ \xi^2 \int_S \left\{ 2 \begin{bmatrix} N_{1x} \\ N_{1y} \\ N_{1xy} \end{bmatrix}^T \begin{bmatrix} W_{1,X}\, W_{2,X} \\ W_{1,Y}\, W_{2,Y} \\ W_{1,X}\, W_{2,Y} + W_{1,Y}\, W_{2,X} \end{bmatrix} \right. \\ &\left. + \begin{bmatrix} N_{2x} \\ N_{2y} \\ N_{2xy} \end{bmatrix}^T \begin{bmatrix} W_{1,X}^2 \\ W_{1,Y}^2 \\ 2W_{1,X}\, W_{1,Y} \end{bmatrix} \right\} dS + \cdots = 0 \end{aligned} \tag{1.25}$$

Then we can write the above equation as,

$$\frac{\lambda}{\lambda_c} = 1 + a\xi + b\xi^2 + \cdots \tag{1.26}$$

Where,

$$a = -\frac{3}{2\lambda_c}\left(\int_S \left\{\begin{bmatrix} N_{1x} \\ N_{1y} \\ N_{1xy} \end{bmatrix}^T \begin{bmatrix} W_{1,X}^2 \\ W_{1,Y}^2 \\ 2W_{1,X}\,W_{1,Y} \end{bmatrix}\right\} dS \div \int_S \left\{\begin{bmatrix} N_{0x} \\ N_{0y} \\ N_{0xy} \end{bmatrix}^T \begin{bmatrix} W_{1,X}^2 \\ W_{1,Y}^2 \\ 2W_{1,X}\,W_{1,Y} \end{bmatrix}\right\} dS\right) \tag{1.27}$$

$$b = -\frac{1}{\lambda_c}\left(\int_S \left\{2\begin{bmatrix} N_{1x} \\ N_{1y} \\ N_{1xy} \end{bmatrix}^T \begin{bmatrix} W_{1,X}\,W_{2,X} \\ W_{1,Y}\,W_{2,Y} \\ W_{1,X}\,W_{2,Y} + W_{1,Y}\,W_{2,X} \end{bmatrix} + \begin{bmatrix} N_{2x} \\ N_{2y} \\ N_{2xy} \end{bmatrix}^T \begin{bmatrix} W_{1,X}^2 \\ W_{1,Y}^2 \\ 2W_{1,X}\,W_{1,Y} \end{bmatrix}\right\} dS \div \int_S \left\{\begin{bmatrix} N_{0x} \\ N_{0y} \\ N_{0xy} \end{bmatrix}^T \begin{bmatrix} W_{1,X}^2 \\ W_{1,Y}^2 \\ 2W_{1,X}\,W_{1,Y} \end{bmatrix}\right\} dS\right) \tag{1.28}$$

The coefficient a depends only on W_1 and F_1, and vanishes if the postbuckling behavior is independent of the sign of the buckling mode. When $a = 0$, the initial postbuckling behavior only depends on b, which requires the determination of W_2 and $F_{2,xx}$.

When $a = 0$ and $b < 0$, the structure is unstable and imperfection-sensitive. This can be demonstrated by the repetition of the above analysis, with equation (1.4) changing to,

$$\varepsilon = \begin{bmatrix} \varepsilon_x \\ \varepsilon_y \\ 2\varepsilon_{xy} \end{bmatrix} = \begin{bmatrix} e_x + \frac{1}{2} W_{,X}^2 + W_{,X} \widetilde{W}_{,X} \\ e_y + \frac{1}{2} W_{,Y}^2 + W_{,Y} \widetilde{W}_{,Y} \\ e_{xy} + W_{,X} W_{,Y} + \left(W_{,X} \widetilde{W}_{,Y} + W_{,Y} \widetilde{W}_{,X} \right) \end{bmatrix} \tag{1.29}$$

where $\widetilde{W}$ is the initial normal displacement for the imperfection. Let $\widetilde{W} = \mu W_1$. The expension form can be rewrote as,

$$\begin{aligned} \begin{bmatrix} W \\ F \end{bmatrix} = \lambda \begin{bmatrix} W_0 \\ F_0 \end{bmatrix} + \xi \begin{bmatrix} W_1 \\ F_1 \end{bmatrix} + \xi^2 \begin{bmatrix} W_2 \\ F_2 \end{bmatrix} + \ldots \\ + \mu\xi \begin{bmatrix} W_{(1,1)} \\ F_{(1,1)} \end{bmatrix} + \mu\xi^2 \begin{bmatrix} W_{(2,1)} \\ F_{(2,1)} \end{bmatrix} + \ldots \\ + \mu^2\xi \begin{bmatrix} W_{(1,2)} \\ F_{(1,2)} \end{bmatrix} + \mu^2\xi^2 \begin{bmatrix} W_{(2,2)} \\ F_{(2,2)} \end{bmatrix} + \ldots \end{aligned} \tag{1.30}$$

where $\lim_{\xi \to 0}\left[\lim_{\mu \to 0} \lambda\right] = \lambda_c$, but $\lim_{\xi \to 0} \lambda = 0$ when $\mu \neq 0$. Consequently we can get,

$$\left(1 - \frac{\lambda}{\lambda_c}\right)\xi + a\xi^2 + b\xi^3 + \cdots = \frac{\lambda}{\lambda_c}\mu + \cdots \tag{1.31}$$

for $a = 0$, the equilibrium path will be,

$$\left(1 - \frac{\lambda}{\lambda_c}\right)\xi + b\xi^3 = \frac{\lambda}{\lambda_c}\mu \tag{1.32}$$

Figure 1.1 shows the sketches of λ/λ_c vs. ξ given by equation (1.32) with $a = 0$ and $b < 0$ for $\mu = 0$ and $\mu \neq 0$.

Let λ_i be the buckling load of the imperfect system, and Koiter first showed for negative b coefficient,

$$\mu = \frac{2\sqrt{-3b}[1 - (\lambda_i/\lambda_c)\,]^{3/2}}{3(\lambda_i/\lambda_c)} \tag{1.33}$$

Figure 1.2 shows the knock down curve for various b coefficients by equation (1.33).

The above equation can produce the knock down curve which is valid for the imperfection amplitude up to few percent of the skin thickness. It can also be called as initial postbuckling region.

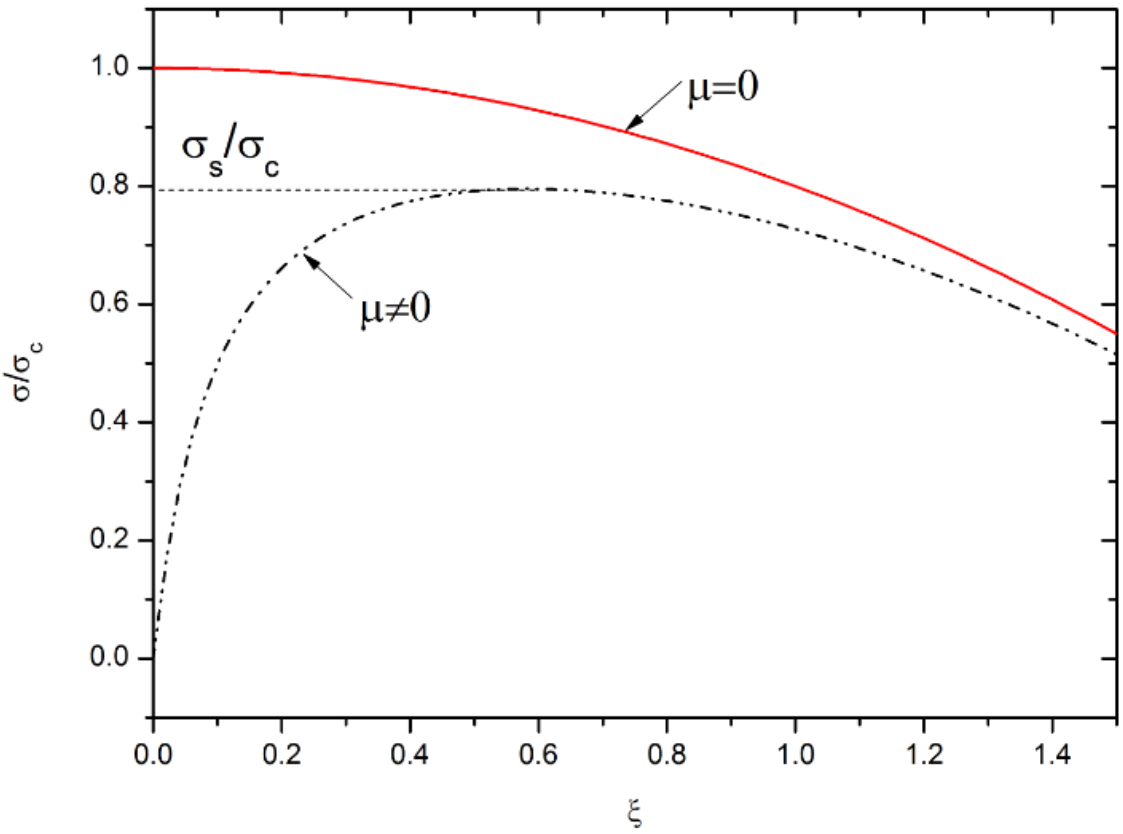

Figure 1.1 Influence of small imperfection

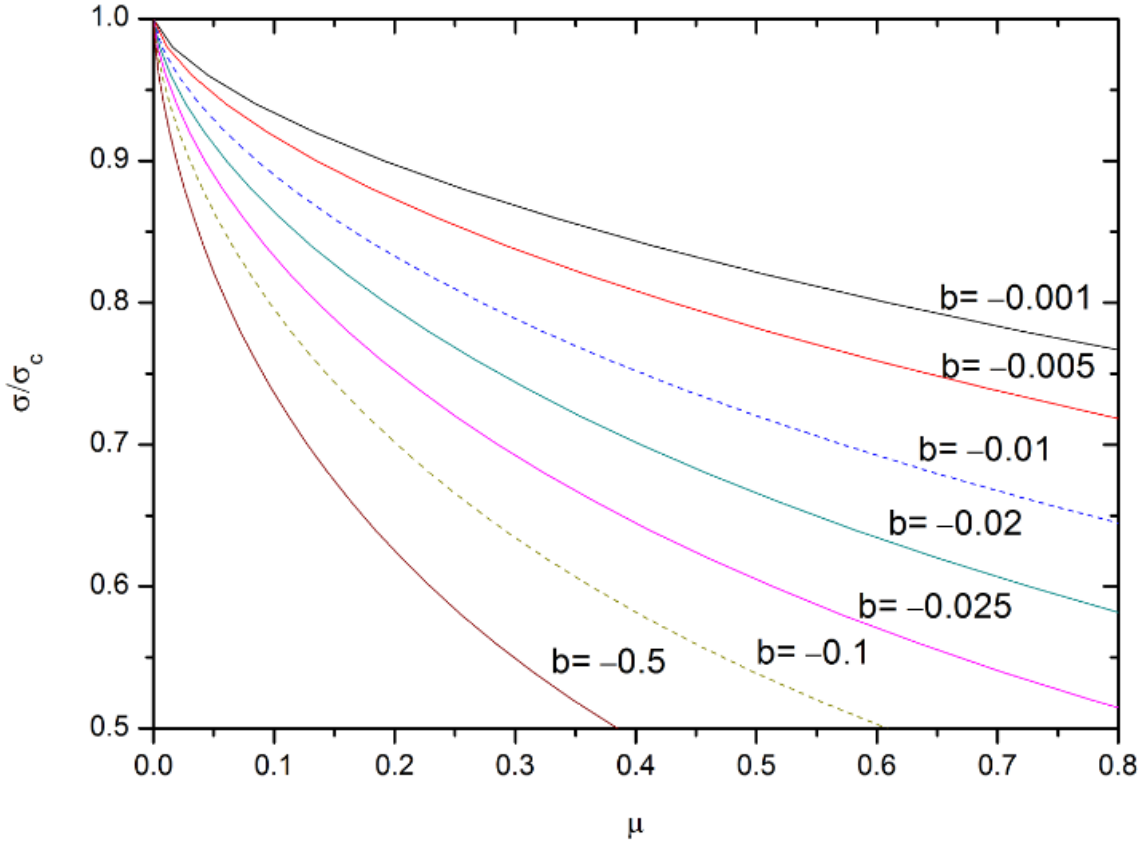

Figure 1.2 Imperfection-sensitivity curves for various b coefficients

1.4 Different Kinds of Cylindrical shell Problems

1.4.1 Introduction to Unstiffened Cylinder under axial compression

For unstiffened cylinder with isotropic homogeneous material, many studies showed that the postbuckling behavior of cylindrical shells is determined by the magnitude of loads associated with buckle of finite depth. They find that the post buckling loads evaluated by approximate energy methods are usually smaller than the classical buckling load. Occasionally, similar approach has also been used in cylinders with imperfection. The perfect and imperfect circular cylinder under torsion has been studied in this way by Loo [25] and Nash [87]. Koiter is the first to present a different approach which determines the initial postbuckling behavior using an asymptotic approximation of the displacement and the stress function. It changes the nonlinear Donnell type PDE (partial differential equation) into a linear ODE (ordinary differential equation) sets. Then it requires only solving the linear problems to find out the stability immediately after buckling. The analysis in this thesis is based on the work of Budiansky [81] who presented an initial postbuckling behavior of isotropic homogeneous cylindrical shells under torsion by using Koiter's general postbuckling theory. In this study, we consider the unstiffened closed cylindrical shell under axial compression using Hui's postbuckling method, and compare the result with Koiter's general theory and finite element result. The finite element result is generated by ABAQUS.

1.4.2 Introduction to Laminate Cylinder

The cross-ply cylindrical shell is introduced here since there is extensively use of light-weight composite materials in modern industry such as aviation, aerospace, and navel. So the buckling and postbuckling of laminated cylindrical shells is very important. Lots of papers were published in this area. Such as: Booton [88] which considered the effects of axisymmetric geometric imperfection on torsional or combined-load buckling of laminated cylindrical shells; Hui [82] which consider the asymmetric postbuckling behavior of symmetrically laminated cylindrical panel; Hui and Du [89] which present the postbuckling study on antisymmetric cross-ply cylindrical shells under torsion. People also can found more articles in this area in the review articles by Tennyson [90] and Simitses [70]. But none of these papers were using the Hui's postbuckling method to evaluate the postbuckling behavior. The study in this thesis is to exam the imperfection sensitivity behavior of antisymmetric cross-play laminated cylindrical shells under axial compression using the Hui's postbuckling theory. This study is based on the work of Hui and Du [89], but in here the external load is axial compression, and some of the results are reproduced to confirm the MATLAB program is right. The postbuckling behavior and imperfection sensitivity behavior of antisymmetric cross-ply cylindrical shells under axial compression is evaluated using both Koiter's general theory and Hui's postbuckling method. Also the results are compared with the finite element result by ABAQUS.

1.4.3 Introduction to Stringer/Ring Stiffened Cylinder

Isotropic homogeneous closed cylindrical shells are often reinforced by stiffeners, such as stringers (axially) and/or ring (circumferentially), in order to satisfy the light-weight requirements of these structures. These stiffened cylindrical shells are frequently used as load-carrying structures such as aircraft fuselages and submarines. These structures are designed to withstand external loads like axial compression, lateral-hydrostatic pressure and torsion. After Van der Neut [91] observed that the buckling load of an outside stringer stiffened cylinder under axial compression is much higher than the buckling load of an unstiffened cylinder, the stiffened cylinder has been extensively researched. Hedgepeth and Hall [92] presented an extensive study of the eccentricity of the stringers effects on axial buckling. Baruch and Singer [93] have investigated the buckling of stiffened cylindrical shells under hydrostatic pressure. Hui [94] has presented the interaction between local and overall buckling modes in axially stiffened cylindrical shells. These studies were based on linear buckling theory, which is called classical buckling. The imperfection sensitivity study of stiffened cylindrical shells under axial compression was presented by Hutchinson and Amazigo [40], by using the Koiter's general stability theory. In this thesis, we are focusing on the analysis of isotropic homogeneous stiffened cylindrical shells under axial compression which is based on the result presented by Hutchinson and Amazigo [40]. In this study, some results of Hutchinson and Amazigo [40] were reproduced for comparison purpose. We also apply the Hui's postbuckling method to the same problem and do a parameter variation analysis on stringer or ring stiffened cylindrical shells under torsion.

1.5 Finite element method

1.5.1 Introduction to finite element method

The finite element method (FEM) is a numerical technique for finding approximate solutions to boundary value problems for differential equations. It uses variational methods (the calculus of variations) to minimize an error function and produce a stable solution. Analogous to the idea that connecting many tiny straight lines can approximate a larger circle, FEM encompasses all the methods for connecting many simple element equations over many small subdomains, named finite elements, to approximate a more complex equation over a larger domain. The finite element method is treated as the most accurate way to do the structure analysis, but it is not computational efficient. Usually it needs lots of computational resources and time to calculate the results. In this research we use the commercial finite element software ABAQUS to calculate the results as a comparison.

1.5.2 Element selection in ABAQUS

The shell element used in ABAQUS is S8R5. In ABAQUS documentation, S8R5 is said to be a thin conventional shell element in ABAQUS, which imposes the Kirchhoff constraint. It works for the shell which thickness is less than 1/15 characteristic length. So this element is ideal to this research since the Donnell type governing equation we used in Koiter's theory and Hui's method are also using the Kirchhoff assumption and also only valid for thin shells. The Kirchhoff assumption is: (1) Normals to the undeformed middle plane are assumed to remain straight, normal, and inextensional during the deformation, so that the transverse

normal and shearing strains may be neglected in deriving the shell kinematic relations; (2) Transverse normal stresses are assumed to be small compared with the other normal stress components, so that they may be neglected in the stress-strain relations.

1.5.3 Procedure for the ABAQUS simulation

In ABAQUS simulation, we do the Eigen-buckling first to get the imperfection shape, and apply the first buckling mode shape to a perfect cylinder as an imperfection, and then do the postbuckling analysis which is a general static process. For Eigen-buckling analysis, we are using Lanczos method to get the eigenvalues. For the postbuckling analysis, ABAQUS uses Newton's method to solve the nonlinear equilibrium equations. Newton's method has a finite radius of convergence. Too large an increment can prevent any solution from being obtained because the initial state is too far away from the equilibrium state that is being sought—it is outside the radius of convergence. Since the buckling analysis always has a large negative increment of load when the structure buckles, so we need a small damping factor in postbuckling analysis to let ABAQUS can overcome this sudden drop. Usually we set the damping factor as 10E-9 to 10E-10, to prevent an inaccurate result.

In order to get the most accurate result using the minimum computational resource, we are always checking the mesh convergence first. Figure 1.3 shows the buckling load versus Degree of freedom (DOF) result. Concerning about the computational efficiency, we choose the DOF around 67000 in this research.

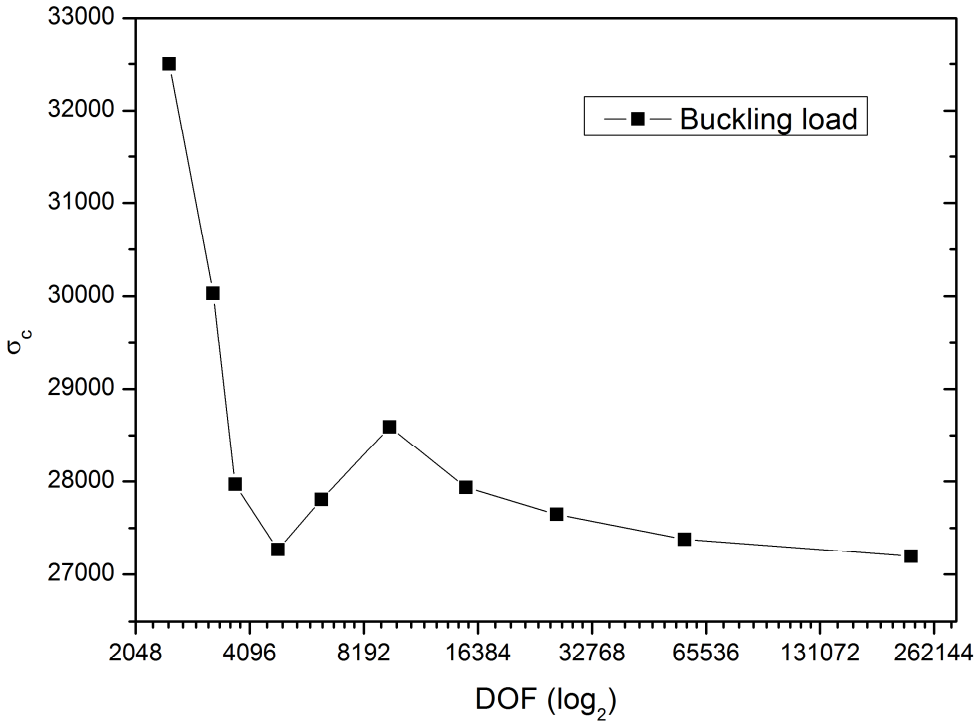

Figure 1.3 Buckling load versus DOF

1.6 Outline of the Thesis

In this thesis, we will first briefly mention about the general Koiter's theory, and then introduce the Hui's postbuckling method. Then we will evaluate the postbuckling behavior and imperfection sensitivity for unstiffened cylinders using Hui's postbuckling method, and compare it with Koiter's general theory and ABAQUS simulation results. After that we will evaluate the postbuckling behavior and imperfection sensitivity for antisymmetric cross-ply laminated cylindrical shells under axial compression using Hui's postbuckling method. Later we will compare with Koiter's general theory and ABAQUS simulation results. Finally, we will evaluate the postbuckling and imperfection sensitivity of stringer/ring stiffened cylindrical shells under both axial compression and torsion using Hui's postbuckling method with some parameter variation. All the curves plotted in this thesis are curve fitted by B-Phline technique except the knock down curves.

CHAPTER 2

HUI'S POSTBUCKLING METHOD

2.1 Introduction

2.1.1 Background

In order to extent the valid range of the Koiter's theory, we need to introduce some modification in this theory. This idea was motivated by Koiter's remarks, which means the general theory of elastic stability can be improved. Koiter [95] [96] pointed out a suggestion that, "A better accuracy, however, may be achieved for larger values of $|\lambda_1 - 1|$ and $|\lambda - 1|$, if each of the coefficients C_1 and C_2 (which is the b coefficient defined by Budiansky and Hutchison [79]) is evaluated at the actual load factor λ, although we are unable to estimate the extended range of validity; we recommend to evaluate both C_1 and C_2 at the actual values of the load factor in a systematic numerical evaluation of the theory". But he never thoroughly investigated in this idea. From the above Koiter's notation, there is a possibility to improve valid range of the Koiter's general postbuckling theory. Although there are lots of paper's published on imperfection-sensitivity of structures such as Budiansky [81], Hutchinson and Amazigo [40], Citerley [60] [97] [98] [99], Hui [83] [84] [100], Hui and Du [89] [101], they were using the Koiter's general theory. Hui and Chen [77] and Hui [78] were the first to thoroughly investigate the idea and apply it to the imperfection sensitivity analysis.

Only these 2 papers involve the calculations of the postbuckling coefficients at the actual load. Hui [78] used the actual load to calculate the postbuckling coefficient of infinite beams. Hui and Chen [77] evaluated the imperfection sensitivity of the cylindrical panels under actual load. So we can call this method as 'Hui's postbuckling method' or 'Improved Koiter's postbuckling theory". But no literatures were found to evaluate the imperfection sensitivity of closed cylindrical shells under actual load and also this improved method was not verified by other methods. This thesis is the first one to apply the Hui's postbuckling method to different kinds of cylinders. Also, this is the first time to verify the result of Hui's postbuckling method by the finite element result using commercial software ABAQUS.

2.1.2 Brief introduction to the idea of Hui's postbuckling method

In Koiter's general theory, the b coefficient is evaluated at the critical buckling load. The following equation shows the idea of Koiter's theory,

$$PE_{Koiter}(\mu) = g_0(\mu) + \lambda_c g_1(\mu) \tag{2.1}$$

We can see, this idea only works when the imperfection μ is close to zero, since λ_c changes a lot when μ is away from zero. That's why Koiter's theory only works when the imperfection is very small. Hui's method is to improve the valid region of Koiter's theory to make this theory more practical. It evaluates the potential energy at the actual applied load rather than the critical buckling load. So Hui's method changes the equation (2.1) into the following explanation.

$$PE_{Hui}(\mu) = g_0(\mu) + \lambda(\mu) g_1(\mu) \tag{2.2}$$

When μ is close to zero, $PE_{Hui}(\mu) = PE_{Koiter}(\mu)$. But when μ is away from zero, $PE_{Hui}(\mu)$ is more accurate than $PE_{Koiter}(\mu)$ since λ changes very fast when μ is small.

2.1.3 Advantages and Limitations of Hui's postbuckling Method

There are three advantages of Hui's postbuckling method, (1) compared with Koiter's general postbuckling theory, Hui's postbuckling method significantly increases the valid region. (2) It predicts the imperfection sensitivity more accurately than Koiter's general postbuckling theory. (3) Although the finite element simulation is the most accurate method, Hui's postbuckling method is much faster than finite element method.

But there are also some limitations which we need to notice, (1) Like the Koiter's general theory, the imperfection must be identical to the buckling mode. (2) It is only valid to thin wall structures.

2.2 Details of Applying Hui's Postbuckling Method

2.2.1 Methodology

The studies in this thesis are based on a solution of the Donnell-type nonlinear equilibrium and compatibility equations using Hui's postbuckling method. The nonlinear PDEs are reduced to sets of linear ODEs by using the Koiter-type perturbation method asymptotically corresponding to the buckling and initial-postbuckling regimes. These ODEs discretized by using a central finite difference scheme (see APPENDIX A). The resulting eigenvalue problem and the postbuckling coefficients are calculated out by using MATLAB program developed by ourselves. Special care is taken to ensure that, first, the differential equations for the second-order problems are solved by retaining the actual value of the applied load rather than classical buckling load, second, the value of first order displacement and stress function are modified with respect to the rate of the actual value of the applied load and classical buckling load, third, the postbuckling coefficient is also evaluated at the actual applied load. This procedure is call the Hui's postbuckling method, and will yield the improved postbuckling b coefficient as a function of the applied load. The improved imperfection sensitivity curve is fitted by the least square method between 0 and 0.25 times of the shell thickness in order to yield the improved postbuckling coefficient. The finite element result is reached by commercial software ABAQUS. The imperfection limit is set to be one shell thickness. All the examples are using the clamp boundary condition for the simplicity reason in finite element simulation in ABAQUS.

2.2.2 General Steps

In this section, we will introduce the details in applying the Hui's postbuckling method by using the Donnell type equilibrium equation and compatibility equation for the plates,

$$\begin{aligned} D(W_{,XXXX} + 2W_{,XXYY} + W_{,YYYY}) \\ = F_{,YY} W_{,XX} + F_{,XX} W_{,YY} - 2F_{,XY} W_{,XY} \\ + P \end{aligned} \tag{2.3}$$

$$\begin{aligned} \frac{1}{Eh}(F_{,XXXX} + 2F_{,XXYY} + F_{,YYYY}) \\ = (W_{,XY})^2 - W_{,XX} W_{,YY} \end{aligned} \tag{2.4}$$

where W is the out of plane displacement, F is the stress function, P is the out of plane force.

According to Koiter's [30] theory of elastic stability, the total displacement and the total stress function can be expressed as the sum of the prebuckling state, the buckling state and the initial postbuckling state as follow,

$$W = W_0 + \xi W_I + \xi^2 W_{II} \tag{2.5}$$

$$F = F_0 + \xi F_I + \xi^2 F_{II} \tag{2.6}$$

where ξ is the amplitude of the buckling mode normalized with respect to the skin thickness.

The followings are the general steps to apply the Hui's postbuckling method,

Step 1. Calculating the prebuckling state

$$\begin{aligned} W_0 &= 0 \\ \sigma &= -N_{0x} = -F_{0,YY} \\ p &= -N_{0y} = -F_{0,XX} \\ \tau &= N_{0xy} = -F_{0,XY} \end{aligned} \tag{2.7}$$

where σ, p and τ are stress in x, y, z direction respectively before buckling.

Step 2. Calculating the classical buckling load (first order field)

Substituting the equation (2.5) to equation (2.3) and (2.4), collecting the terms which is linear to ξ, then we can get the GDEs for the first order field,

$$\begin{aligned} D(W_{I,XXXX} + 2W_{I,XXYY} + W_{I,YYYY}) + \sigma W_{,XX} + pW_{,YY} \\ - 2\tau W_{,XY} = 0 \end{aligned} \tag{2.8}$$

$$F_{I,XXXX} + 2F_{I,XXYY} + F_{I,YYYY} = 0 \tag{2.9}$$

By using the separable solution, we can change the above PDEs to ODE sets, and the result will be an general eigenvalue problem $(A - \lambda B)x = 0$. We can use a build in function in MATLAB or Sifted Inverse Power Method (see APPENDIX B) to find the smallest real positive eigenvalue and corresponding eigenvector. The eigenvalue we found is the classical buckling load σ_c, p_c, or τ_c. The eigenvector is nomalized to make the largest out-of-plane displacement of the buckling mode to be unity.

Step 3. Calculate the initial postbuckling state (second order field)

Substituting the equation (2.5) to equation (2.3) and (2.4), collecting the terms which is linear to ξ^2, then we can get the GDEs for the second order field,

$$\begin{aligned} D(W_{II,XXXX} + 2W_{II,XXYY} + W_{II,YYYY}) + \sigma_c W_{II,XX} \\ + p_c W_{II,YY} - 2\tau_c W_{II,XY} \\ = F_{I,YY} W_{I,XX} + F_{I,XX} W_{I,YY} \\ - 2F_{I,XY} W_{I,XY} \end{aligned} \tag{2.10}$$

$$\begin{aligned} \frac{1}{Eh}(F_{II,XXXX} + 2F_{II,XXYY} + F_{II,YYYY}) \\ = (W_{I,XY})^2 - W_{I,XX} W_{I,YY} \end{aligned} \tag{2.11}$$

By using the separable solution, we can change the above PDEs to ODE sets. Then we can solve the second order field with enough boundary conditions.

Step 4. Calculate the regular postbuckling b_{reg} coefficient for the Koiter's general theory using the following equation

$$\begin{aligned} b_{reg} = \Big\{ 2 \int_S [& F_{I,XX} W_{I,Y} W_{II,Y} + F_{I,YY} W_{I,X} W_{II,X} \\ & - F_{I,XY} (W_{I,X} W_{II,Y} + W_{I,Y} W_{II,X})] dS \\ & + \int_S [F_{II,XX} W_I^2{}_{,Y} + F_{II,YY} W_I^2{}_{,X} \\ & - 2F_{II,XY} W_{I,X} W_{I,Y}] dS \Big\} \\ \div \Big\{ \int_S [& \sigma_c W_I^2{}_{,Y} + p_c W_I^2{}_{,X} \\ & - 2\tau_c W_{I,X} W_{I,Y}] dS \Big\} \end{aligned} \tag{2.12}$$

Step 5. Define the actual load and actual first order field

We can get the actual applied load simply by the following relation,

$$(\sigma_a, p_a, \tau_a) = percent \times (\sigma_c, p_c, \tau_c) \tag{2.13}$$

Where the '$percent$' is the rate between actual load and critical load. If $b_{reg} < 0$, then $percent < 1$, if $b_{reg} > 0$, then $percent > 1$

Also the first order field is modified by the following relation,

$$(\bar{W}_I, \bar{F}_I) = percent \times (W_I, F_I) \tag{2.14}$$

The reason is when you calculating the second order field at the actual applied load, the energy of first order field should also be changed by the actual load.

Step 6. Calculate the second order field under the actual applied load

We can solve the second order field again by changing the classical buckling load to actual applied load,

$$\begin{aligned} D(W_{II,XXXX} + 2W_{II,XXYY} + W_{II,YYYY}) + \sigma_a W_{II,XX} \\ + p_a W_{II,YY} - 2\tau_a W_{II,XY} \\ = \bar{F}_{I,YY}\, \bar{W}_{I,XX} + \bar{F}_{I,XX}\, \bar{W}_{I,YY} \\ - 2\bar{F}_{I,XY}\, \bar{W}_{I,XY} \end{aligned} \tag{2.15}$$

$$\begin{aligned} \frac{1}{Eh}(F_{II,XXXX} + 2F_{II,XXYY} + F_{II,YYYY}) \\ = (\bar{W}_{I,XY})^2 - \bar{W}_{I,XX}\, \bar{W}_{I,YY} \end{aligned} \tag{2.16}$$

By using the separable solution, we can change the above PDEs to ODE sets. Then we can solve the second order field with enough boundary conditions under actual applied load.

Step 7. Calculate the postbuckling b coefficient under actual applied load

b coefficient also needs to be calculated under actual applied load, by applying the actual applied load and second order field calculated in Step 6 and modifying first order field in the following equation,

$$
\begin{aligned}
b_a = \Big\{ 2 \int_S [& \bar{F}_{I,XX}\, \bar{W}_{I,Y}\, W_{II,Y} + \bar{F}_{I,YY}\, \bar{W}_{I,X}\, W_{II,X} \\
& - \bar{F}_{I,XY}\, (\bar{W}_{I,X}\, W_{II,Y} + \bar{W}_{I,Y}\, W_{II,X})]\, dS \\
& + \int_S [F_{II,XX}\, \bar{W}_I^2{}_{,Y} + F_{II,YY}\, \bar{W}_I^2{}_{,X} \\
& - 2F_{II,XY}\, \bar{W}_{I,X}\, \bar{W}_{I,Y}]\, dS \Big\} \\
\div \Big\{ \int_S [& \sigma_a \bar{W}_I^2{}_{,Y} + p_a \bar{W}_I^2{}_{,X} \\
& - 2\tau_a \bar{W}_{I,X}\, \bar{W}_{I,Y}]\, dS \Big\}
\end{aligned}
\tag{2.17}
$$

Step 8. Calculate the actual imperfection and deflection

If $b_{reg} < 0$, then the structure is imperfection sensitive. We use the following equation to calculate the actual imperfection,

$$
\mu_a = \frac{2\sqrt{-3b_a}[1 - percent\,]^{3/2}}{3percent} \tag{2.18}
$$

where μ_a is the imperfection amplitude divide by the shell thickness. As we mentioned above, $percent = \lambda_a/\lambda_c$. Where λ_a represents the actual applied load and λ_c represents

the classical buckling load. We can see, if $\lambda_a = \lambda_c$ the imperfection is 0.

If $b_{reg} > 0$, then the structure is imperfection insensitive, we cannot use equation (2.11) anymore. So we need to use the equation for the load deflection curve to calculate the actual deflection as follow,

$$\xi = [(percent - 1)/b_a\,]^{0.5} \tag{2.19}$$

where ξ is the deflection amplitude divide by the shell thickness.

2.2.3 Algorithm for Getting The Improved Postbuckling b Coefficient

Now we can do the iteration to get the curves we want. Here is the algorithm,

i. Choose a step size n. For a better accuracy, always choose a small number, for example $n = 0.02$.

ii. Let $percent = 1$ to calculate out the b_{reg}.

iii. If $b_{reg} < 0$, let $percent_{new} = percent_{old} - n$; if $b_{reg} > 0$, let $percent_{new} = percent_{old} + n$. Use the $percent_{new}$ to calculate out the b_a, μ_a or δ_a.

iv. Repeat step iii, until the μ_a or δ_a reaches 25% of the shell thickness.

v. Use the least square curve fit to fit the μ_a or ξ_a with equation (2.11) or (2.12) respectively, then we can get b_{imp} for the Hui's postbuckling method.

CHAPTER 3

IMPERFECTION SENSITIVITY OF UNSTIFFENED CYLINDER UNDER AXIAL COMPRESSION USING HUI'S POSTBUCKLING METHOD

3.1 Introduction

Here we are using the Hui's postbuckling method to analyze the postbuckling and imperfection sensitivity behavior of unstiffened cylindrical shell under axial compression. We will compare the solution of Hui's postbuckling method with the Koiter's general postbuckling theory and ABAQUS simulation results. This analysis is based on the work of Budiansky [81], which presented an initial postbuckling behavior of isotropic homogeneous cylindrical shells under torsion. The Donnell type non-linear partial differential equations of the unstiffened cylindrical shell are reduced to a set of linear ordinary differential equations corresponding to the buckling and initial-postbuckling regimes by using the separation of variables technique employed by Budiansky [81]. These equations are discretized using a central-finite difference scheme (see APPENDIX A). By applying the Hui's postbuckling method, three special cares are taken, (i) the applied load in the differential equations of the second order field is using the actual value of the applied load rather than the classical buckling load, (ii) the value of first order displacement and stress function are modified with respect to the rate of the actual value of the applied load and classical buckling load, (iii) The

postbuckling coefficient is also evaluated at the actual applied load. The resulting knock down curve is fitted by the least square curve fit technique for the imperfection amplitude between 0 and 0.25 to get the improved postbuckling b coefficient.

3.2 Governing Equations and First Order Field

3.2.1 Governing Equations

The Donnell type governing PDEs of equilibrium and compatibility equations for an unstiffened cylindrical shell in out-of-plane displacement and stress function are (Budiansky [81]),

$$D(W_{,XXXX}+2W_{,XXYY}+W_{,YYYY})+\frac{1}{R}F_{,XX} = F_{,YY}W_{,XX}+F_{,XX}W_{,YY}-2F_{,XY}W_{,XY} \tag{3.1}$$

$$\frac{1}{Eh}(F_{,XXXX}+2F_{,XXYY}+F_{,YYYY})-\frac{1}{R}W_{,XX} = (W_{,XY})^2-W_{,XX}W_{,YY} \tag{3.2}$$

where, W is the out-of-plane displacement, F is the stress function, X is the axial coordinate, Y is the circumferential coordinate, R is the radius of the cylinder, h is the skin thickness, E is the Young's modulus, $D = Eh^3/[12(1-v^2)]$ is the flexural rigidity, v is the Poisson's ratio.

3.2.2 Non-Dimensionalize

The following non-dimensional quantities are employed,

$$w = W/h,\ f = F/(Eh^3),\ (x,y) = (X,Y)/(Rh)^{1/2} \tag{3.3}$$

Thus, the non-dimensional equilibrium and compatibility equations becomes,

$$\frac{1}{12(1-v^2)}\left(w_{,xxxx} + 2w_{,xxyy} + w_{,yyyy}\right) + f_{,xx} = f_{,yy}\,w_{,xx} + f_{,xx}\,w_{,yy} - 2f_{,xy}\,w_{,xy} \tag{3.4}$$

$$f_{,xxxx} + 2f_{,xxyy} + f_{,yyyy} - w_{,xx} = \left(w_{,xy}\right)^2 - w_{,xx}\,w_{,yy} \tag{3.5}$$

3.2.3 Equations for the First Order Field

According to Koiter's (1945) theory of elastic stability, the total displacement and the total stress function can be expressed as the sum of the prebuckling state. The buckling state and the initial postbuckling state are as follow,

$$\begin{aligned} w &= w_0 + \xi w_I + \xi^2 w_{II} \\ f &= f_0 + \xi f_I + \xi^2 f_{II} \end{aligned} \tag{3.6}$$

where, ξ is the amplitude of the buckling mode normalized with respect to the skin thickness. The prebuckling stress function can be expressed by the membrane stress resultants as follow,

$$\begin{aligned} (\sigma, p, \tau) &= \left(-f_{0,yy}, -f_{0,xx}, -f_{0,xy}\right) \\ &= \frac{R}{Eh^2}(-N_{0x}, 0, 0) \end{aligned} \tag{3.7}$$

Substituting w and f into the equation (3.4) and (3.5) and then collecting terms which are linear in ξ. The equilibrium and compatibility equations for the buckling state are,

$$\begin{aligned} \frac{1}{12(1-\nu^2)}\left(w_{I,xxxx} + 2w_{I,xxyy} + w_{I,yyyy}\right) + f_{I,xx} \\ + \sigma w_{I,xx} = 0 \end{aligned} \tag{3.8}$$

$$f_{I,xxxx} + 2f_{I,xxyy} + f_{I,yyyy} - w_{I,xx} = 0 \tag{3.9}$$

3.2.4 Solve the First Order Field

By the analysis of Budiansky (1967), the general solution of the buckling state can be written in the following separable form,

$$w_I(x,y) = w_c(\mathrm{x})\cos(\bar{N}y) + w_s(x)\sin(\bar{N}y) \tag{3.10}$$

$$f_I(x,y) = f_c(\mathrm{x})\cos(\bar{N}y) + f_s(x)\sin(\bar{N}y) \tag{3.11}$$

where, $\bar{N} = n(h/R)^{1/2}$, n is the number of circumferential full-waves. Substituting $w_I(x,y)$ and $f_I(x,y)$ into the equation (3.8) and (3.9), and collecting the terms involving $\cos(\bar{N}y)$ and $\sin(\bar{N}y)$ respectively, we can get the following ODEs,

$$\frac{1}{12(1-v^2)}(w_{c,xxxx} - 2\bar{N}^2 w_{c,xx} + \bar{N}^4 w_c) + f_{c,xx} + \sigma w_{c,xx} = 0 \tag{3.12}$$

$$f_{c,xxxx} - 2\bar{N}^2 f_{c,xx} + \bar{N}^4 f_c - w_{c,xx} = 0 \tag{3.13}$$

$$\frac{1}{12(1-v^2)}(w_{s,xxxx} - 2\bar{N}^2 w_{c,xx} + \bar{N}^4 w_s) + f_{s,xx} + \sigma w_{s,xx} = 0 \tag{3.14}$$

$$f_{s,xxxx} - 2\bar{N}^2 f_{s,xx} + \bar{N}^4 f_s - w_{s,xx} = 0 \tag{3.15}$$

For the simplicity of simulation in ABAQUS, the clamp boundary condition is applied to both ends of the cylindrical shell,

$$w = w_{,X} = U_{,YY} = V_{,Y} = 0 \qquad at\ X = 0\ and\ L \tag{3.16}$$

For the axially immovable boundary condition $U_{,YY}\,(X = 0) = 0$, it can be derived from the following strain-displacement relationship,

$$2\varepsilon_{xy,Y} - \varepsilon_{y,X} = U_{,YY} - \frac{W_{,X}}{R} + W_{,X}\,W_{,YY} \tag{3.17}$$

The above equation can be written in terms of w and f (using $W_{,Y}\,(X = 0) = 0$),

$$-f_{,xxx}\,(x = 0) + (-2 - v) f_{,xyy}\,(x = 0) = 0 \tag{3.18}$$

The circumferentially immovable boundary condition $V_{,Y}\,(X = 0) = 0$ can be derived from $V_{,Y} = \varepsilon_y - W/R - (1/2)\,(W_{,Y}\,)^2$. Then the $V_{,Y}\,(X = 0) = 0$ boundary condition becomes (using $W(X = 0) = 0, W_{,Y}\,(X = 0) = 0$),

$$f_{,xx}\,(x = 0) - v f_{,yy}\,(x = 0) = 0 \tag{3.19}$$

The same equations are used for $x = L/(Rh)^2$. To the buckling state, the equations for the boundary conditions will be,

$$w_c = w_{c,x} = w_s = w_{s,x} = 0 \qquad at\ x = 0\ and\ L/(Rh)^2$$

$$-f_{c,xxx}\,(x = 0, L/(Rh)^2) + (2 + v)\overline{N} f_{c,x}\,(x = 0, L/(Rh)^2) = 0$$

$$-f_{s,xxx}\,(x = 0, L/(Rh)^2) + (2 + v)\overline{N} f_{s,x}\,(x = 0, L/(Rh)^2) = 0 \tag{3.20}$$

$$f_{c,xx}\,(x = 0, L/(Rh)^2) + v\overline{N}^2 f_c(x = 0, L/(Rh)^2) = 0$$

$$f_{s,xx}\,(x = 0, L/(Rh)^2) + v\overline{N}^2 f_s(x = 0, L/(Rh)^2) = 0$$

The above four governing ODEs and eight boundary conditions are discretized using the central finite difference scheme (see APPENDIX A). The resulting linear system of equations becomes an eigenvalue problem, which can be solved by a build in function in MATLAB or using the inversed power method (see APPENDIX B). The amplitude of the buckling state is normalized by forcing the largest out-of-plane displacement of the buckling state to be unity, which means $[w_c(x) + w_s(x)]^{1/2} = 1$.

3.3 Second Order Field And Postbuckling Coefficient

3.3.1 Equations for the Second Order Field

Substituting w and f into the equation (3.4) and (3.5) and then collecting terms which are linear in ξ^2, the equilibrium and compatibility equations for the initial postbuckling state are,

$$\begin{aligned}\frac{1}{12(1-v^2)}\left(w_{II,xxxx}+2w_{II,xxyy}+w_{II,yyyy}\right)+f_{II,xx}\\ +\sigma_a w_{II,xx}\\ =f_{I,yy}\,w_{I,xx}+f_{I,xx}\,w_{I,yy}-2f_{I,xy}\,w_{I,xy}\end{aligned} \tag{3.21}$$

$$\begin{aligned}f_{II,xxxx}+2f_{II,xxyy}+f_{II,yyyy}-w_{II,xx}\\ =\left(w_{I,xy}\right)^2-w_{I,xx}\,w_{I,yy}\end{aligned} \tag{3.22}$$

where σ_a is the actual applied load.

3.3.2 Solve the Second Order Field

It is clear that the solution for the second order field should be,

$$w_{II}(x,y) = w^*(x) + w_A(x)\cos(2\bar{N}y) + w_B(x)\sin(2\bar{N}y) \tag{3.23}$$

$$f_{II}(x,y) = f^*(x) + f_A(x)\cos(2\bar{N}y) + f_B(x)\sin(2\bar{N}y) \tag{3.24}$$

Then the second order field can be separated into two sets of ODEs. One is $[w^*(x), f^*(x)]$ and the other is $[w_A(x), w_B(x), f_A(x), f_B(x)]$. The first sets of ODEs is,

$$\frac{1}{12(1-v^2)} w^*{}_{,xxxx} + f^*{}_{,xx} + \sigma w^*{}_{,xx} = -\frac{\bar{N}^2}{2}[w_s f_s + w_c f_c]_{,xx} \tag{3.25}$$

$$f^*{}_{,xxxx} - w^*{}_{,xx} = \frac{\bar{N}^2}{4}[w_s^2 + w_c^2]_{,xx} \tag{3.26}$$

The second sets of ODEs will be,

$$E_{12} = \frac{\bar{N}^2}{2}(w_{s,xx} f_s - w_{c,xx} f_c + w_s f_{s,xx} - w_c f_{c,xx} - 2w_{s,x} f_{s,x} + 2w_{c,x} f_{c,x}) \tag{3.27}$$

$$E_{13} = \frac{\bar{N}^2}{2}\left[(w_{s,x})^2 - (w_{c,x})^2 - w_s w_{s,xx} + w_c w_{c,xx}\right] \tag{3.28}$$

$$E_{14} = -\frac{\bar{N}^2}{2}(w_{c,xx} f_s + w_{s,xx} f_c + w_c f_{s,xx} + w_s f_{c,xx} - 2w_{c,x} f_{s,x} - 2w_{s,x} f_{c,x}) \tag{3.29}$$

$$E_{15} = \frac{\bar{N}^2}{2}(w_c w_{s,xx} + w_s w_{c,xx} - 2w_{s,x} w_{c,x}) \tag{3.30}$$

where E_{12}, E_{13}, E_{14} and E_{15} can be obtained from the left hand side of equations (3.12) to (3.15) by replacing $\bar{N}$, w_c, w_s, f_c, f_s by $2\bar{N}$, w_A, w_B, f_A, f_B respectively. The boundary conditions can also be obtained by following the above replacement of the boundary condition equations in the first order field. Note that, the applied load used to calculate the second order field should use the actual applied load rather than the classical buckling load. Moreover, w_c, w_s, f_c, f_s used in the second order field must be multiplied by the ratio of actual load and applied load.

3.3.3 Equations for the Postbuckling Coefficient

The postbuckling b coefficient evaluates the stability of the structures. If the b coefficient is positive then the structure has a stable postbuckling behavior; if the b coefficient is negative, the structure has an unstable postbuckling behavior. The imperfection sensitivity is measured by the magnitude of the postbuckling b coefficient. The path of equilibrium is formulated as,

$$b\xi^3 + \left[1 - \frac{\lambda_i}{\lambda_c}\right]\xi = \mu\frac{\lambda_i}{\lambda_c} \tag{3.31}$$

where, λ_i is the buckling load of the imperfect system, λ_c is the classical buckling load of the perfect system, μ is the imperfection amplitude normalized by the shell thickness. The imperfection amplitude is related to the buckling load by the following formula (only for b<0),

$$\mu = \frac{2\sqrt{-3b}[1 - (\lambda_i/\lambda)]^{3/2}}{3(\lambda_i/\lambda)} \tag{3.32}$$

The formula of postbuckling b coefficient is (Budiansky (1967), Hui and Du (1987a)),

$$b = \frac{C_1 + C_2}{|D_1|} \tag{3.33}$$

where,

$$C_1 = 2\int_{y=0}^{y_0}\int_{x=0}^{Z_H}\{f_{I,yy}\,w_{I,x}\,w_{II,x} + f_{I,xx}\,w_{I,y}\,w_{II,y} - f_{I,xy}\left(w_{I,x}\,w_{II,y} + w_{I,y}\,w_{II,x}\right)\}dxdy \tag{3.34}$$

$$C_2 = \int_{y=0}^{y_0}\int_{x=0}^{Z_H}\{f_{II,yy}\,(w_{I,x})^2 + f_{II,xx}\left(w_{I,y}\right)^2 - 2f_{II,xy}\,w_{I,x}\,w_{I,y}\}dxdy \tag{3.35}$$

$$D_1 = \int_{y=0}^{y_0}\int_{x=0}^{Z_H}(\sigma_a w_{I,x}^2)dxdy \tag{3.36}$$

In the above, $y = 2\pi R/(Rh)^{1/2}$ and the reduced-Batdorf parameter $Z_H = L/(Rh)^{1/2}$. Substituting the buckling state and the postbuckling state into the above formulas, and integrating in the circumferential direction analytically, we can obtain,

$$
\begin{aligned}
C_1 = \bar{N}^2 y_0 \int_{x=0}^{Z_H} \{ & w_{,x}^{*} \left(-f_s w_{s,x} - f_c w_{c,x}\right) \\
& + \frac{1}{2} w_{A,x} \left(f_s w_{s,x} - f_c w_{c,x}\right) \\
& - \frac{1}{2} w_{B,x} \left(f_s w_{c,x} + f_c w_{s,x}\right) \\
& - w_A (f_{s,xx} w_s - f_{c,xx} w_c) \\
& + w_B (f_{s,xx} w_c + f_{c,xx} w_s) \\
& + w_A \left(f_{s,x} w_{s,x} - f_{c,x} w_{c,x}\right) \\
& - w_B \left(f_{s,x} w_{c,x} + f_{c,x} w_{s,x}\right) \\
& - w_{,x}^{*} \left(f_{s,x} w_s + f_{c,x} w_c\right) \\
& - \frac{1}{2} w_{A,x} \left(f_{s,x} w_s - f_{c,x} w_c\right) \\
& - \frac{1}{2} w_{B,x} \left(-f_{s,x} w_c - f_{c,x} w_s\right) \} dx
\end{aligned}
\tag{3.37}
$$

$$
\begin{aligned}
C_2 = \bar{N}^2 y_0 \int_{x=0}^{Z_H} \{ & -f_A [(w_{c,x})^2 - (w_{s,x})^2] \\
& - 2 f_B w_{s,x} w_{c,x} + \frac{1}{2} f_{,x}^{*} (w_c^2 + w_s^2) \\
& + \frac{1}{4} f_{A,xx} (w_s^2 - w_c^2) - \frac{1}{2} f_{B,xx} w_s w_c \\
& + f_{A,x} \left(w_s w_{s,x} - w_c w_{c,x}\right) \\
& - f_{B,x} \left(w_c w_{s,x} + w_s w_{c,x}\right) \} dx
\end{aligned}
\tag{3.38}
$$

$$
D_1 = \bar{N}^2 y_0 \int_{x=0}^{Z_H} \{ \frac{1}{2} \sigma_a [(w_{c,x})^2 + (w_{s,x})^2] \} dx \tag{3.39}
$$

Note that, postbuckling b coefficient is also calculated by using the actual applied load σ_a, then the b coefficient should be a function of applied load numerically.

3.4 Result and Discussion

3.4.1 Example Cases

In here, we are concentrating on demonstrating the improvement of the Hui's postbuckling method by comparing it with the Koiter's general stability theory and ABAQUS simulation. So, we will not do a complete parameter variation of the cylindrical shells. The example problem is chosen to be unstiffened cylindrical shell made of Aluminum materials. The material parameters are,

$E = 70GPa, \ \ v = 0.33$

For the simplicity of simulating in ABAQUS, the clamp boundary condition is applied to both sides of the cylindrical shells,

$w = w_{,X} = U_{,YY} = V_{,Y} = 0 \qquad at\ X = 0\ and\ L$

The geometry of the cylindrical shell can be represented by the reduced-Batdorf parameter Z_H, and four geometric cases are concerned here,

i. Medium cylinder: $R = 30mm, \quad L = 50mm, \quad h = 0.1mm,$

ii. Long cylinder: $R = 30mm, \quad L = 100mm, \quad h = 0.1mm,$

iii. Short cylinder: $R = 30mm, \quad L = 20mm, \quad h = 0.1mm,$

iv. Large cylinder: $R = 1736mm, \quad L = 7013mm, \quad h = 50mm,$

3.4.2 How to Apply the Hui's Postbuckling Method to this Problem

The detail of calculating this problem by the Hui's postbuckling method will be presented in here. The coupled ODEs are discretized in the axial direction using the central finite difference method (see APPENDIX A). The boundary conditions at both ends are also discretized in the same scheme. For a given wave number n, the smallest eigenvalue is found by using the build-in function in MATLAB or inverse power method (see APPENDIX B). Find the minimum eigenvalue through all possible wave numbers, and the resulting eigenvalue and wave number are the classical buckling load λ_c and buckling mode respectively. The actual applied load is defined to be some percent of classical buckling load, such as from 100% to 20% of the classical buckling load λ_c. The actual applied load $\lambda_a = percent * \lambda_c$. For the unstiffened cylinder we do not modify the first order field, which is different from the General Steps we mentioned above. The equation (2.14) should be changed to this,

$$(\overline{w}_c, \overline{w}_s, \bar{f}_c, \bar{f}_s) = (w_c, w_s, f_c, f_s) \tag{3.40}$$

where $(\overline{w}_c, \overline{w}_s, \bar{f}_c, \bar{f}_s)$ is the first order field under the actual applied load. This modification only works for the unstiffened cylinder. For other types of cylinders, we still need to use equation (2.14). Since the interaction between the buckling state and the postbuckling state is very complicate, it is impossible to figure out the exact effect of the changes of applied load to the first order field. But we can assume the influence in such way by empirical analysis. It is easy to accept that if we decrease the applied load, it will also decrease the potential energy

of the first order field. We are assuming this change is linear, so the amplitude of the first order field will decrease by the same percent of the applied load. The second order field and postbuckling b coefficient can be calculated out for each applied load. Then we can get the b coefficient for each applied load. Use that b coefficient to calculate the normalized imperfection amplitude μ by using equation (3.32), in which we let $\lambda_i = \lambda_a$. Then we can get the normalized imperfection amplitude for that applied load. By evaluating several applied loads, we can get the knock down curve numerically. This means the b coefficient is a function of applied load numerically. This curve can be called as the knock down curve of Hui's postbuckling method.

In order to compare the Hui's postbuckling method with the Koiter's general theory, we need to get a single b coefficient for Hui's postbuckling method. This is the reason for us to do the least square curve fit. Fit the knock down curve of the Hui's postbuckling method using equation (3.32) by the least square technique in the range of imperfection amplitude form 0 to 25 percent of the shell thickness. One example is given in Figure 3.1. After we get the improved b coefficient, we can use it to compare with the usual b coefficient calculated by the Koiter's general postbuckling theory.

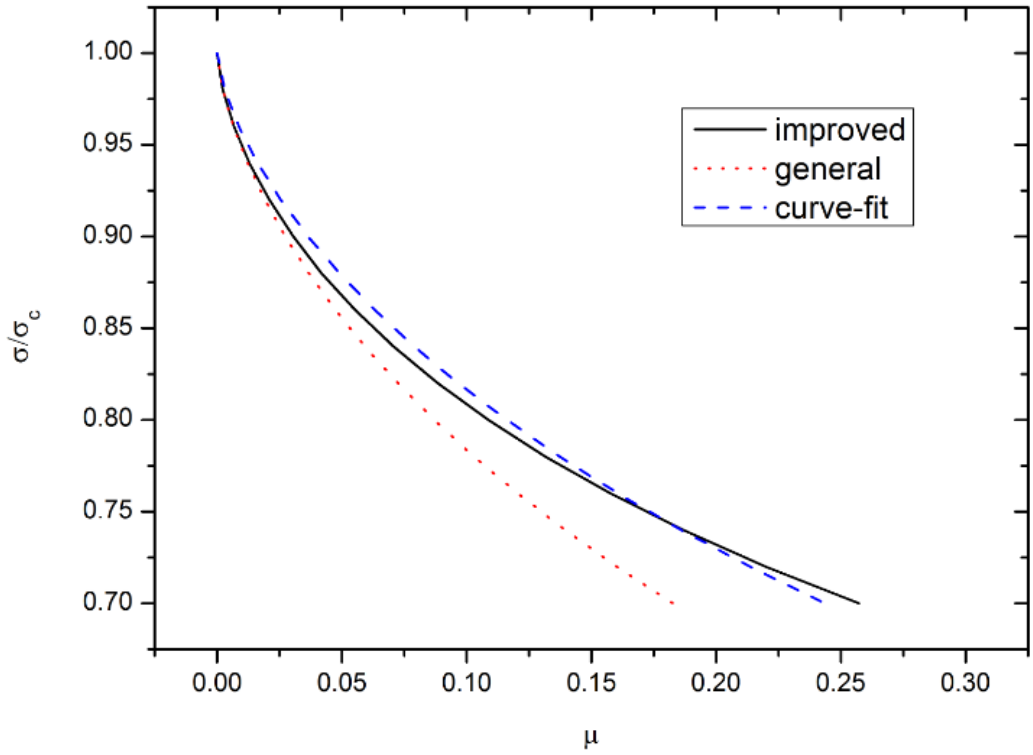

Figure 3.1 Example for least-square curve fit through imperfection form 0 to 25% of shell thickness

3.4.3 Medium Length Cylinder

Figure 3.2 shows the Knock down curves for cylindrical shell under axial compression at the reduced Batdorf parameter $Z_H = 28.8675$ calculated by Hui's postbuckling method, Koiter's general theory, curve fitting for improved b coefficient and the ABAQUS finite element simulation respectively. In ABAQUS simulation, the geometric parameters are set as,

$$R = 30mm, \quad L = 50mm, \quad h = 0.1mm$$

where R is the radius of the cylinder, L is the length of the cylinder, h is the shell thickness of the cylinder. The geometric parameter shows this is a typical medium length cylinder. The classical buckling load calculated by ABAQUS is 0.6137, compared with the classical buckling load calculated by Koiter's theory which is 0.6124, there is less than 1% error, which proved the program for Koiter's theory is right. From the figure, we can see that the knock down curve of Hui's postbuckling method fits the ABAQUS result very well when the imperfection is up to almost 30% of the shell thickness. Then it starts to diverge from the ABAQUS result. Same phenomenon happens to the knock down curve created by the curve fitting of improved b coefficient. In contrast, the knock down curve from the usual b coefficient by Koiter's general stability theory only fits the ABAQUS result when the imperfection is less than 5% of the shell thickness. So the valid region for Hui's postbuckling method is 6 times more than Koiter's general theory. The improved b coefficient from curve fitting of the knock down curve of Hui's postbuckling method is about -1.1385, but the usual b coefficient computed from Koiter's general theory is about -7.9282. There is a significant difference between these two b coefficients. The positive shifting from usual b coefficient to improved b coefficient is almost 86%. This tells us, for the unstiffened cylinder with metallic

material, the Koiter's general stability theory significantly overestimates the imperfection sensitivity of the structure. The Koiter's general theory is only valid when the imperfection is few percentage of the total shell thickness. This is not practical for the real industry application. For the Hui's postbuckling method, the valid region is increased up to the imperfection around 30% of the shell thickness, and the improved b coefficient shows the imperfection sensitivity is much lower than the Koiter's general stability theory. Compared with the commercial finite element software ABAQUS, the Hui's postbuckling method also has its own advantage. Although the result from ABAQUS is the most accurate one, it takes more than 30 times of the time to compute the knock down curve than using the Hui's postbuckling method. Furthermore, ABAQUS is an expensive commercial software, but people can use any free programming language, such as Python or Fortran, to achieve the Hui's postbuckling method. Also the result is good up to 30% imperfection of the shell thickness, which is practical to the real industry. Here we need to note that although the Hui's postbuckling method is more accurate than the Koiter's general stability theory, sometime it may slightly underestimate the buckling load like in this example. So it is important to have some proper safety factors taking into account when practically use it. From ABAQUS simulation result, we can see the buckling load decreases very fast at first. It fits the result from Hui's postbuckling method very well. In this region the imperfection is not that large compared with the geometric size of the cylinder, so the physical behavior fits for the Donnell type equations for the shells. After this region, the ABAQUS simulate curve starts to diverge from the curve of Hui's postbuckling method, and even increases after the imperfection goes to more than 50% of the shell thickness. This may be due to the

imperfection is so large compared with the geometric of the structure, and it starts to deform continuously which exceeds the valid region of the Donnell type equation. So there is no buckling behavior in the valid region of the Donnell type governing deferential equations (GDEs). This is the reason that the result starts to diverge from the Hui's postbuckling method. The reason that the buckling load of ABAQUS simulation starts to increase after some imperfection level may be that the deflection caused by the imperfection is so large which may behave like stiffener. This means it changes the structure shape before buckling starts, so the equations for the unstiffened cylinder are not valid any more.

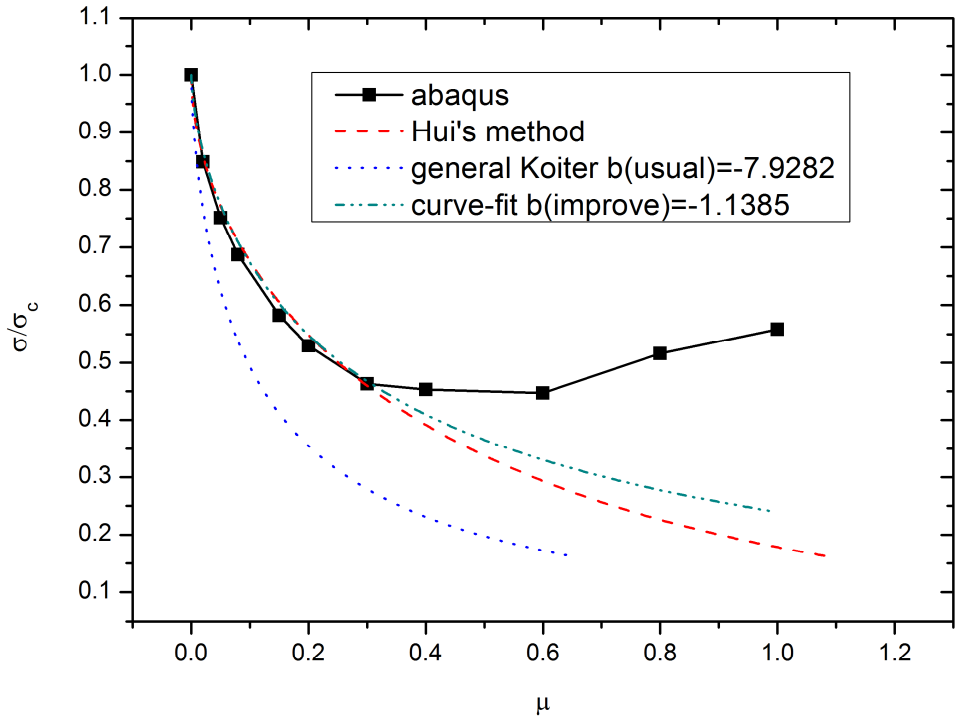

Figure 3.2 Knock down curve for cylindrical shell under axial compression at the reduced Batdorf parameter $Z_H = 28.8675$ calculate by different method

3.4.4 Long Cylinder

Figure 3.3 shows the Knock down curves for cylindrical shell under axial compression at the reduced Batdorf parameter $Z_H = 57.7350$ calculated by Hui's postbuckling method, Koiter's general theory, curve fitting for improved b coefficient and the ABAQUS finite element simulation, respectively. In ABAQUS simulation, the geometric parameter is set as,

$$R = 30mm, \quad L = 100mm, \quad h = 0.1mm$$

The geometric parameter shows this is a long cylinder. The classical buckling load (0.6118) calculated by ABAQUS is same with the classical buckling load calculated by Koiter's theory which is also 0.6118. This proves the program for Koiter's theory is right. The purpose to choose this example is to demonstrate the Hui's postbuckling method is also valid for long cylinders. From the figure, we can see that the knock down curve of Hui's postbuckling method fits the ABAQUS result very well when the imperfection is up to almost 30% of the shell thickness. After that it starts to diverge from the ABAQUS result. We can also get the similar result for the knock down curve created by the curve fitting of improved b coefficient. This result shows the similar properties to the middle length cylinder. Again, the knock down curve from the usual b coefficient by Koiter's general stability theory only fits the ABAQUS result when the imperfection is less than 5% of the shell thickness. So the valid region of Hui's postbuckling method is 6 times more than Koiter's general theory, same as the conclusion for the middle length cylinder. The improved b coefficient from curve fitting of the knock down curve of Hui's postbuckling method is -1.0966, and the usual b coefficient from the Koiter's general stability is -5.4185. We can see there is still a significant difference

between the improved b coefficient and the usual b coefficient. The positive shifting from usual b coefficient to improved b coefficient is about 80%. Again, this shows the Koiter's general stability theory significantly overestimates the imperfection sensitivity of the structures and it is also only valid when the imperfection is few percentage of the total shell thickness. In this example, the knock down curve from Hui's postbuckling method fits even better than the previous one in the valid region which has the imperfection up to 30% of the shell thickness. There is no underestimate situation occurred in this example. This shows that by changing the structure of the cylinder, the fitness will also change. We cannot guarantee the Hui's postbuckling method is always under or overestimating the buckling load. So we always need a safety factor to make sure it will not underestimate the buckling load.

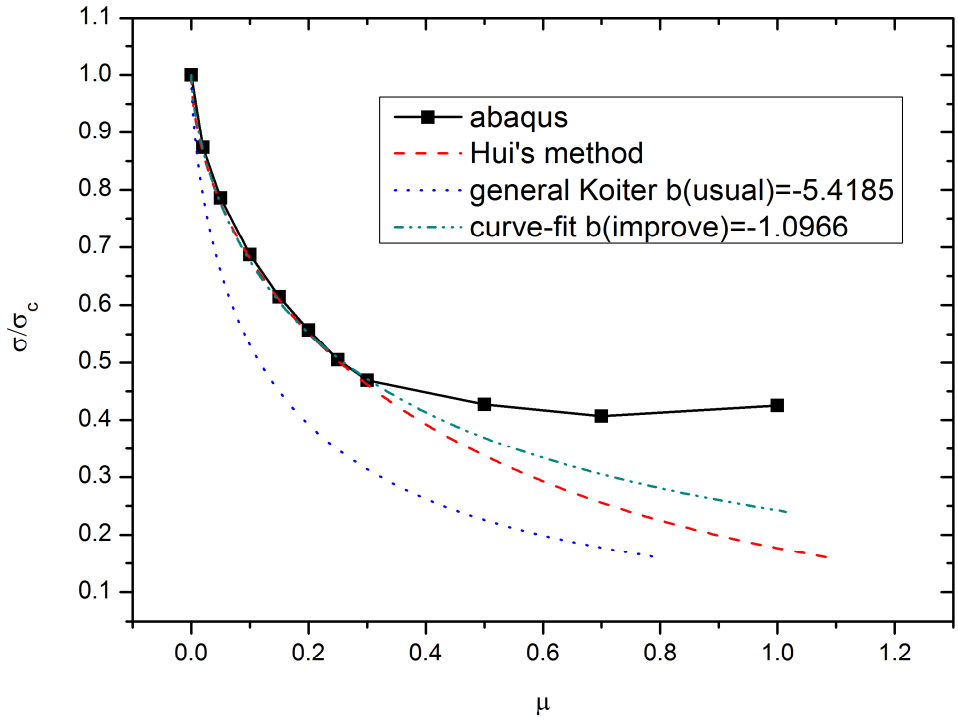

Figure 3.3 Knock down curve for cylindrical shell under axial compression at $Z_H = 57.7350$ calculate by different method

3.4.5 Short Cylinder

Figure 3.4 shows the Knock down curves for cylindrical shell under axial compression at the reduced Batdorf parameter $Z_H = 11.5470$ calculated by Hui's postbuckling method, Koiter's general theory, curve fitting for improved b coefficient and the ABAQUS finite element simulation, respectively. In ABAQUS simulation, the geometric parameter is set as,

$$R = 30mm, \quad L = 20mm, \quad h = 0.1mm$$

The geometric parameter shows this is a short cylinder. The classical buckling load calculated by ABAQUS is 0.6162, compared with the classical buckling load calculated by Koiter's theory which is 0.6178, there is less than 1% error, which proves the program for Koiter's theory is right. The purpose to choose this example is to demonstrate the Hui's postbuckling method is also valid for short cylinders. From the figure, we can see that the knock down curve calculated by Hui's postbuckling method fits the ABAQUS simulate result quite well when the imperfection is up to 18% of the shell thickness. Although the valid region decreases from 30% to 18% from above result, compared with the Koiter's general theory which the valid region is when the imperfection less than 2% of the shell thickness, it is still an significant improvement of valid region for Hui's postbuckling method. So the valid region of Hui's postbuckling method is about 8 times more than Koiter's general theory for this short cylinder. The improved b coefficient from curve fitting of the knock down curve of Hui's postbuckling method is -1.0336, and the usual b coefficient from the Koiter's general stability is -4.8179. We can see there is still a significant difference between the improved b coefficient and the usual b coefficient. The positive shifting from usual b coefficient to

improved b coefficient is about 79%, this shows the Koiter's general stability theory significantly overestimates the imperfection sensitivity of the structures again. In this example, we can see that the Hui's postbuckling method slightly overestimates the buckling load at the imperfection region which is up to 4% of the shell thickness. And when the imperfection is from 5% to 14% of the shell thickness, the Hui's postbuckling method slightly underestimates the buckling load. This proves the conclusion we get from above example. Although the Hui's postbuckling method is more accurate than Koiter's general theory, we cannot guarantee the Hui's postbuckling method always under or overestimates the buckling load. So we always need a safety factor to make sure it will not underestimate the buckling load. This example also shows that the valid region for the Hui's postbuckling method is changing case by case. In above cases the valid region is the imperfection up to 30% of the total shell thickness, but in this case, the valid region is only 18% of the total shell thickness. Depends on our experience, the valid region is always around the imperfection up to 20%-30% of the shell thickness. So in practically use, we usually choose the result within the region which the imperfection is up to 25% of the shell thickness, unless the finite element result is available.

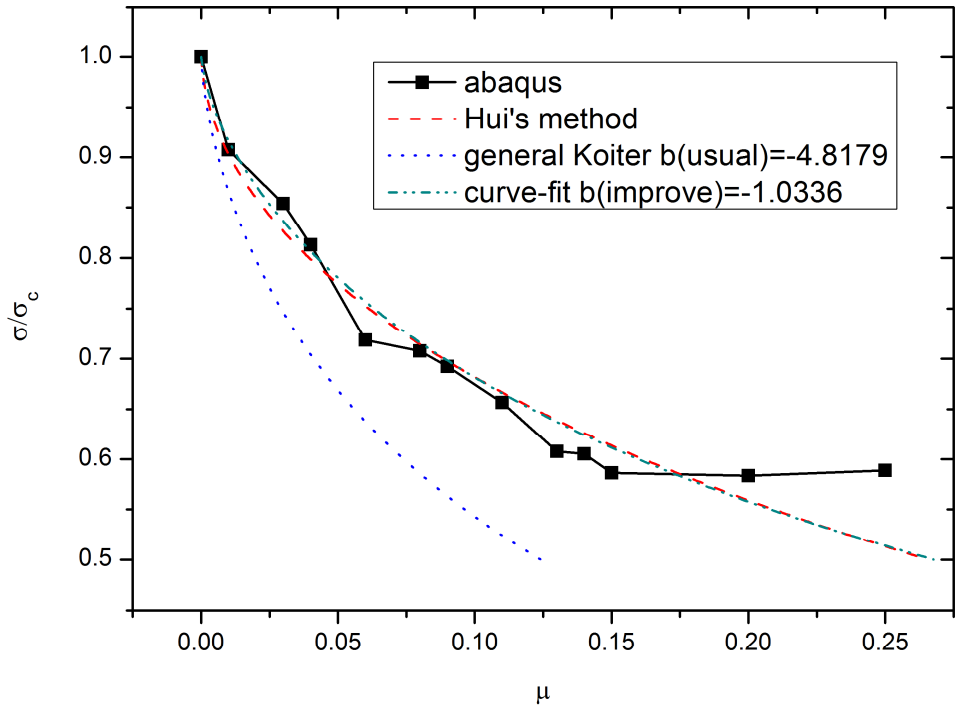

Figure 3.4 Knock down curve for cylindrical shell under axial compression at $Z_H = 11.5470$ calculate by different method

3.4.6 Large Cylinder and Parameter Variation

Table 1 shows the improved b coefficient and usual b coefficient varying by the length of cylinder with $R = 30, h = 0.1$. From the table we can see that the usual b coefficient is very sensitive to the geometry of the cylinder. It goes from -5 to -13 and then to -5, the variation is about 200% about its average. But the improved b coefficient is relatively insensitive with the geometry of the cylinders. The variation is about 20% of its average. We can also see that in the whole varying range of length, the Koiter's general theory is always significantly overestimating the imperfection sensitivity of the structure.

L	Z_H	b(improve)	b(usual)
20	11.5470	−1.03359	−4.81794
30	17.3205	−1.1457	−10.5046
40	23.0940	−1.17314	−13.5785
50	28.8675	−1.13845	−7.92821
60	34.6410	−1.21944	−9.19678
70	40.4145	−0.84459	−6.92347
80	46.1880	−1.01253	−5.33978
90	51.9615	−1.04628	−7.89774
100	57.7350	−1.09655	−5.41846

Table 3.1 Improved b coefficient and usual b coefficient varying by the length of cylinder with the following parameter fixed: $R = 30, h = 0.1$

Figure 3.5 shows the knock down curve of the large unstiffened cylindrical shell under axial compression. Although its length is quite large, the reduced-Batdorf parameter Z_H is only 23.8037 because of the radius and shell thickness. The result shows that the improved method also works for large cylinders, and the fitness is quite well up to 40% of the shell thickness. Compared with the knock down curve by the Koiter's general theory, the valid region for Hui's postbuckling method is significantly increased. Also we can see the Koiter's

general theory significantly overestimates the imperfection sensitivity of the structure by comparing improved b coefficient and general b coefficient which are -1.1810 and -2.9568 respectively.

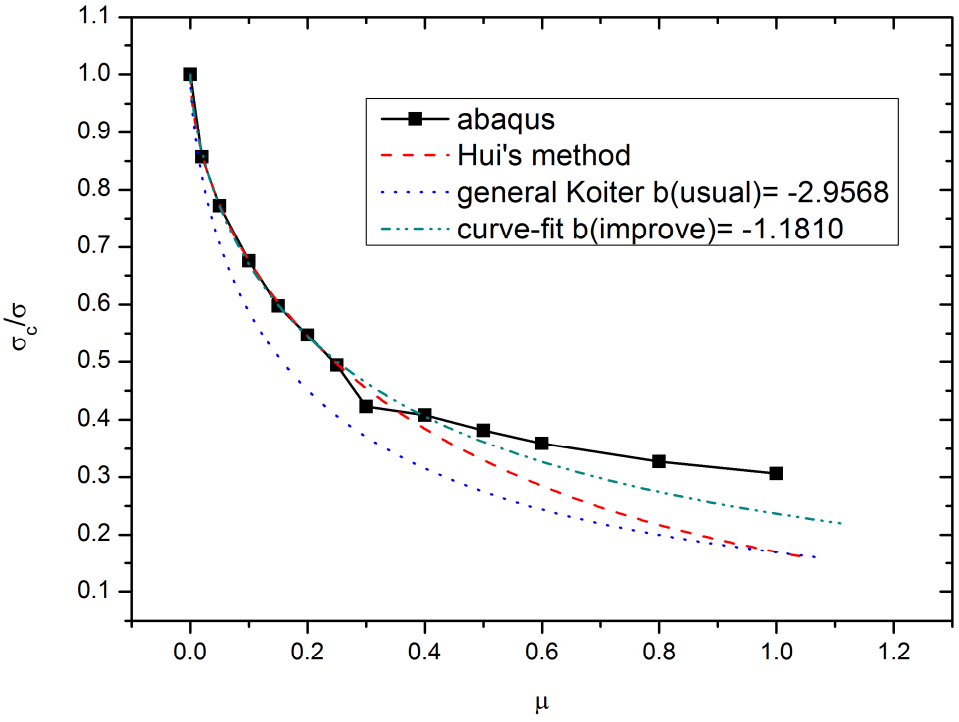

Figure 3.5 Knock down curve for large cylindrical shell under axial compression calculate by different method, $Z_H = 23.8037$

3.5 Conclusion

In this example, we successfully compared the Hui's postbuckling method with ABAQUS simulation and Koiter's general theory by analyzing the postbuckling behavior and imperfection sensitivity of different length of unstiffened cylindrical shell. The result shows the valid region for Hui's postbuckling method is significantly increased compared with the Koiter's general theory. The valid region for the Hui's postbuckling method is the imperfection up to about 25% of the shell thickness. Also, the Koiter's general theory significantly overestimates the imperfection sensitivity of the structures. More than 80% positive shift of postbuckling b coefficient was found through all the cases. Even in a large dimension case, the Hui's postbuckling method fits much better than Koiter's general theory to the ABAQUS result. Although the ABAQUS result is the most accurate one, the time consuming is at least 20 times more than that using Hui's postbuckling method. Furthermore, ABAQUS is also an expensive commercial software. But there will be no cost if we calculate by Hui's postbuckling method using free programming language. We should note that the valid region of Hui's postbuckling method is varying case by case. Sometimes it will slightly underestimate the buckling load. So it is good to have some safety factor which can overcome this situation. Overall, Hui's postbuckling method significantly improves the valid region of Koiter's general theory, so that it is more practical to be used in the real industry.

CHAPTER 4

IMPERFECTION SENSITIVITY OF ANTISYMMETRIC CROSS-PLY CYLINDER UNDER COMPRESSION USING HUI'S POSTBUCKLING MEHOD

4.1 Introduction

Here we are using the Hui's postbuckling method to analyze the postbuckling and imperfection sensitivity of cylindrical shell under axial compression and compare the solution with the Koiter's general postbuckling theory and ABAQUS simulation result. This analysis is based on the work of Hui and Du [89], which presents the initial postbuckling behavior of imperfect, antisymmetric cross-ply cylindrical shells under torsion. In here, the applied load is changed to axial compression to fit the consistence of the thesis. The Donnell type non-linear partial differential equilibrium and compatibility equations of a cylindrical shell are reduced to sets of linear ordinary differential equations corresponding to the buckling and initial-postbuckling regimes by using the separation of variables technique employed by Budiansky [81]. These equations are discretized using a central-finite difference scheme (See APPENDIX A). By applying the Hui's postbuckling method, three special cares are taken, (i) the applied load in the differential equations of the second order field are using the actual value of the applied load rather than the classical buckling load, (ii) the value of first order

displacement and stress function are modified with respect to the rate of the actual value of the applied load and classical buckling load, (iii) The postbuckling coefficient is also evaluated at the actual applied load. The resulting knock down curve is fitted by the least square curve fit technique for the imperfection amplitude between 0 and 0.25 to get the improved postbuckling coefficient.

4.2 Governing Equations and First Order Field

4.2.1 Governing Equations

The governing differential equations for the initial postbuckling of imperfect antisymmetric cross-ply laminate cylindrical shell are nonlinear Donnell type equilibrium and compatibility equations, written in terms of the out-of-plane displacement W and the stress function F, which are (see Hui and Du [89]),

$$L_D^*(W) + L_B^*(F) + \frac{1}{R}\mathrm{F}_{,XX} = F_{,XX}\,W_{,YY} + F_{,YY}\,W_{,XX} - 2F_{,XY}\,W_{,XY} \tag{4.1}$$

$$L_A^*(F) - L_B^*(W) - \frac{1}{R}W_{,XX} = (W_{,XY})^2 - W_{,XX}\,W_{,YY} \tag{4.2}$$

where X and Y are axial and circumferential coordinates respectively, R is the radius of the cylindrical shell, The forth order differential operators $L_A^*(\,)$, $L_B^*(\,)$ and $L_D^*(\,)$ are defined by Tennyson et al. [63] [102].

4.2.2 Non-Dimensionalize

Apply the following non-dimensional quantities to equation (4.1) and (4.2),

$$\begin{gathered}(x,y)=\frac{X,Y}{Rh^{0.5}}\\ w=\frac{W}{h}\\ f=\frac{F}{E_2h^3}\\ \left(a_{ij}^*,b_{ij}^*,\mathrm{d}_{ij}^*\right)=\left[(E_2h)A_{ij}^*,\frac{B_{ij}^*}{h},\frac{D_{ij}^*}{E_2h^3}\right]\end{gathered} \tag{4.3}$$

The non-dimensional equilibrium and compatibility equations become,

$$\begin{aligned}&L_d^*(w)+L_b^*(f)+f_{,xx}\\ &\qquad=f_{,xx}\,w_{,yy}+f_{,yy}\,w_{,xx}-2f_{,xy}\,w_{,xy}\end{aligned} \tag{4.4}$$

$$L_a^*(f)-L_b^*(w)-w_{,xx}=\left(f_{,xy}\right)^2-w_{,xx}\,w_{,yy} \tag{4.5}$$

The non-dimensional differential operators then become (Hui and Du [89]),

$$\begin{aligned}L_a^*(\,)=&\,a_{22}^*(\,)_{,xxxx}+(2a_{12}^*+a_{66}^*)(\,)_{,xxyy}\\ &+a_{11}^*(\,)_{,yyyy}-2a_{26}^*(\,)_{,xxxy}\\ &-2a_{16}^*(\,)_{,xyyy}\end{aligned} \tag{4.6}$$

$$
\begin{aligned}
L_b^*(\,) = {} & b_{21}^*(\,)_{,xxxx} + (b_{11}^* + b_{22}^* - 2b_{66}^*)(\,)_{,xxyy} \\
& + b_{12}^*(\,)_{,yyyy} + (2b_{26}^* - b_{61}^*)(\,)_{,xxxy} \\
& - (2b_{16}^* - b_{62}^*)(\,)_{,xyyy}
\end{aligned} \tag{4.7}
$$

$$
\begin{aligned}
L_d^*(\,) = {} & d_{11}^*(\,)_{,xxxx} + 2(d_{12}^* + 2d_{66}^*)(\,)_{,xxyy} \\
& + d_{22}^*(\,)_{,yyyy} + 4d_{16}^*(\,)_{,xxxy} \\
& + 4d_{26}^*(\,)_{,xyyy}
\end{aligned} \tag{4.8}
$$

4.2.3 Equations for the First Order Field

Following the analysis of Koiter's [30] theory of elastic stability, the out-of-plane displacement and the stress function can be express in the sum of the prebuckling state, the buckling state and the initial postbuckling state (Hui and Du [89]),

$$
\begin{aligned}
w &= w_0 + \xi w_I + \xi^2 w_{II} \\
f &= f_0 + \xi f_I + \varepsilon \xi^2 f_{II}
\end{aligned} \tag{4.9}
$$

where, ξ is the amplitude of the buckling mode nomalized with respect to the total shell thickness h. Then the prebuckling state will be,

$$
\begin{aligned}
(\sigma, p, \tau) &= \left(-f_{0,yy}\,, -f_{0,xx}\,, -f_{0,xy}\right) \\
&= [R/(E_2 h^2)](N_x, 0, 0)
\end{aligned} \tag{4.10}
$$

Applying the equation (4.9) to the non-dimensional equilibrium and compatibility

equations and connecting the term which is linear to ξ, we can get the equation for the buckling state,

$$L_d^*(w_I) + L_b^*(f_I) + f_{I,xx} + \sigma w_{,xx} = 0 \tag{4.11}$$

$$L_a^*(f_I) - L_b^*(w_I) - w_{I,xx} = 0 \tag{4.12}$$

4.2.4 Solve the First Order Field

Following the analysis by Budiansky [81], the solution to the buckling state can be expressed into the following separation form,

$$w_I(x,y) = w_c(\mathrm{x})\cos(\bar{N}y) + w_s(x)\sin(\bar{N}y) \tag{4.13}$$

$$f_I(x,y) = f_c(\mathrm{x})\cos(\bar{N}y) + f_s(x)\sin(\bar{N}y) \tag{4.14}$$

where $\bar{N} = n(h/R)^{1/2}$, n is the number of circumferential full-waves. Substituting $w_I(x,y)$ and $f_I(x,y)$ into the equation (4.10) and (4.11), and collecting the terms involving $\cos(Ny)$ and $\sin(Ny)$ respectively, we can get the following ODEs,

$$\begin{aligned} &L_d^{2*}(w_c) + L_d^{3*}(w_s) + L_b^{2*}(f_c) + L_b^{3*}(f_s) + f_{c,xx} \\ &+ \sigma w_{c,xx} - p\bar{N}^2 w_c - 2\tau\bar{N}w_{s,x} = 0 \end{aligned} \tag{4.15}$$

$$L_d^{2*}(w_s) - L_d^{3*}(w_c) + L_b^{2*}(f_s) - L_b^{3*}(f_c) + f_{s,xx} + \sigma w_{s,xx} - p\bar{N}^2 w_s + 2\tau\bar{N} w_{c,x} = 0 \tag{4.16}$$

$$L_a^{2*}(f_c) + L_a^{3*}(f_s) - L_b^{2*}(w_c) - L_b^{3*}(w_s) - w_{c,xx} = 0 \tag{4.17}$$

$$L_a^{2*}(f_s) + L_a^{3*}(f_c) - L_b^{2*}(w_s) - L_b^{3*}(w_c) - w_{s,xx} = 0 \tag{4.18}$$

The ordinary differential operators in the above equations are defined as,

$$L_a^{2*}(\,) = a_{22}^*(\,)_{,xxxx} - \bar{N}^2(2a_{12}^* + a_{66}^*)(\,)_{,xx} + \bar{N}^4 a_{11}^*(\,) \tag{4.19}$$

$$L_a^{3*}(\,) = -2a_{26}^*\bar{N}(\,)_{,xxx} + 2a_{16}^*\bar{N}^3(\,)_{,x} \tag{4.20}$$

$$L_b^{2*}(\,) = b_{21}^*(\,)_{,xxxx} - \bar{N}^2(b_{11}^* + b_{22}^* - 2b_{66}^*)(\,)_{,xx} + \bar{N}^4 b_{12}^*(\,) \tag{4.21}$$

$$L_b^{3*}(\,) = \bar{N}(2b_{26}^* - b_{61}^*)(\,)_{,xxx} - \bar{N}^3(2b_{16}^* - b_{62}^*)(\,)_{,x} \tag{4.22}$$

$$L_d^{2*}(\,) = d_{11}^*(\,)_{,xxxx} - 2\bar{N}^2(d_{12}^* + 2d_{66}^*)(\,)_{,xx} + \bar{N}^4 d_{22}^*(\,) \tag{4.23}$$

$$L_d^{3*} = 4\bar{N}d_{16}^*(\,)_{,xxx} - 4\bar{N}^3 d_{26}^*(\,)_{,x} \tag{4.24}$$

For the simplicity of simulation in the ABAQUS, the clamp boundary conditions are applied to both end of the cylindrical shell,

$$w = w_{,X} = U_{,YY} = V_{,Y} = 0 \qquad at\ X = 0\ and\ L \tag{4.25}$$

For the axially immovable boundary condition $U_{,YY}\,(X = 0) = 0$, we can get it from the following strain-displacement relationship,

$$2\varepsilon_{xy,Y} - \varepsilon_{y,X} = U_{,YY} - \frac{W_{,X}}{R} + W_{,X}\,W_{,YY} \tag{4.26}$$

the above equation can be written in w and f form (see Hui and Du [89]),

$$\begin{aligned} a_{16}^{*} f_{,yyy} + 2a_{26}^{*} f_{,xxy} - (a_{12}^{*} + a_{66}^{*}) f_{,xyy} \\ - a_{22}^{*} f_{,xxx} + (b_{22}^{*} - 2b_{66}^{*}) w_{,xyy} \\ + (2b_{26}^{*} - b_{61}^{*}) w_{,xxy} + b_{21}^{*} w_{,xxx} \\ + w_{,x} = 0 \\ at\ x = 0\ and\ L/(Rh)^{0.5} \end{aligned} \tag{4.27}$$

The circumferentially immovable boundary condition $V_{,Y}\,(X = 0) = 0$ can be derived from $V_{,Y} = \varepsilon_y - W/R - (1/2)\,(W_{,Y}\,)^2$, then the $V_{,Y}\,(X = 0) = 0$ boundary condition becomes (see Hui and Du [89]),

$$a_{12}^{*} f_{yy} + a_{22}^{*} f_{,xx} - a_{26}^{*} f_{,xy} - b_{21}^{*} w_{,xx} - 2b_{26}^{*} w_{,xy} = 0$$
$$at\ x = 0 \tag{4.28}$$

Note that $w(x = 0) = 0, w_{,y}\,(x = 0) = 0\ and\ w_{,yy}\,(x = 0) = 0$. The above equations for boundary conditions are also available for $x = L/(Rh)^{1/2}$. Substituting the separable form of the buckling mode into the boundary conditions and connecting the terms involving $\cos(Ny)$ and $\sin(Ny)$ respectively, we can get the ODEs for the boundary conditions as follow,

$$w_c = w_s = w_{c,x} = w_{s,x} = 0 \tag{4.29}$$

$$\begin{aligned} a_{16}^{*} N^3 f_c - 2a_{26}^{*} N f_{c,xx} + (a_{12}^{*} + a_{66}^{*}) N^2 f_{s,x} \\ - a_{22}^{*} f_{s,xxx} - (b_{22}^{*} - 2b_{66}^{*}) N^2 w_{s,x} \\ - (2b_{26}^{*} - b_{61}^{*}) N w_{c,xx} + b_{21}^{*} w_{s,xxx} \\ + w_{s,x} = 0 \end{aligned} \tag{4.30}$$

$$\begin{aligned} -a_{16}^{*} N^3 f_s + 2a_{26}^{*} N f_{s,xx} + (a_{12}^{*} + a_{66}^{*}) N^2 f_{c,x} \\ - a_{22}^{*} f_{c,xxx} - (b_{22}^{*} - 2b_{66}^{*}) N^2 w_{c,x} \\ + (2b_{26}^{*} - b_{61}^{*}) N w_{s,xx} + b_{21}^{*} w_{c,xxx} \\ + w_{c,x} = 0 \end{aligned} \tag{4.31}$$

$$\begin{aligned} -a_{12}^{*} N^2 f_s + a_{22}^{*} f_{s,xx} + a_{26}^{*} N f_{c,x} - b_{21}^{*} w_{s,xx} \\ + 2b_{26}^{*} N w_{c,x} = 0 \end{aligned} \tag{4.32}$$

$$\begin{aligned} -a_{12}^{*} N^2 f_c + a_{22}^{*} f_{c,xx} - a_{26}^{*} N f_{s,x} - b_{21}^{*} w_{c,xx} \\ + 2b_{26}^{*} N w_{s,x} = 0 \end{aligned} \tag{4.33}$$

above equations for the boundary are valid at $x = 0\ and\ L/(Rh)^{1/2}$.

The above four governing ODEs and eight boundary conditions are discretized using the central finite difference scheme (see APPENDIX A). The resulting linear system of equations becomes an eigenvalue problem which can be solved by a build-in function in MATLAB or using the inverse power method (see APPENDIX B). The amplitude of the buckling state is normalized by forcing the largest out-of-plane displacement of the buckling state to be unity, which means that $[w_c(x) + w_s(x)]^{1/2} = 1$.

4.3 Second Order Field and Postbuckling Coefficient

4.3.1 Equations for the Second Order Field

Substituting the equations of the total out-of-plane and total stress function into the governing Donnell type equations, respectively, and collecting the terms involving ξ^2, then we can get the equilibrium and compatibility equations for the initial postbuckling state (also called second order field),

$$\begin{aligned} L_d^*(w_{II}) + L_b^*(f_{II}) + f_{II,xx} + \sigma_a w_{II,xx} \\ = f_{I,yy}\, w_{I,xx} + f_{I,xx}\, w_{I,yy} - 2 f_{I,xy}\, w_{I,xy} \end{aligned} \tag{4.34}$$

$$L_a^*(f_{II}) - L_b^*(w_{II}) - w_{II,xx} = \left(w_{I,xy}\right)^2 - w_{I,xx}\, w_{I,yy} \tag{4.35}$$

Note that instead of using σ_c to calculate the second order field, we replace them by the actual applied load σ_a, this is one step for the Hui's postbuckling method. The actual applied load is defined to be some percent of classical buckling load, for example from 100% to 20% of the classical buckling load λ_c. So the actual applied load $\lambda_a = percent * \lambda_c$, also for each applied load the first order field must be modified like in the General Steps (Note this is different from unstiffened cylinder in previous section where we mentioned it is a special case),

$$(\bar{w}_c, \bar{w}_s, \bar{f}_c, \bar{f}_s) = percent * (w_c, w_s, f_c, f_s) \tag{4.36}$$

where, $(\bar{w}_c, \bar{w}_s, \bar{f}_c, \bar{f}_s)$ is the first order field of the buckling state under actual applied load. Same procedure should be taken place when calculating the postbuckling b coefficient.

4.3.2 Solve the Second Order Field

It is clear that the solution for the equilibrium and compatibility equations for the initial postbuckling state can be expressed as the following separable forms (see Budiansky [81]),

$$w_{II}(x,y) = w^*(x) + w_A(x)\cos(2\bar{N}y) + w_B(x)\sin(2\bar{N}y) \tag{4.37}$$

$$f_{II}(x,y) = f^*(x) + f_A(x)\cos(2\bar{N}y) + f_B(x)\sin(2\bar{N}y) \tag{4.38}$$

By substituting the above separable form of solution into the equilibrium and compatibility equations for the second order field, and collecting the terms involving "*", $\cos(2\bar{N}y)$ and $\sin(2\bar{N}y)$ respectively, we can get two sets of ODEs. The first set involves just $w^*(x)$ and $f^*(x)$, the second set involves $w_A(x)$, $w_B(x)$, $f_A(x)$ and $f_B(x)$. The first set is,

$$d_{11}^* w^*{}_{,xxxx} + b_{21}^* f^*{}_{,xxxx} + f^*{}_{,xx} + \sigma_a w^*{}_{,xx} = -\frac{\bar{N}^2}{2}(w_c f_c + w_s f_s)_{,xx} \tag{4.39}$$

$$a_{22}^* f^*{}_{,xxxx} - b_{21}^* w^*{}_{,xxxx} - w^*{}_{,xx} = \frac{\bar{N}^2}{4}(w_s^2 + w_c^2)_{,xx} \tag{4.40}$$

We can see the two in-plane boundary conditions $U_{,yy}\,(x = 0\ and\ L/(Rh)^{1/2}) = 0$ and $V_{,y}\,(x = 0\ and\ L/(Rh)^{1/2}) = 0$ are not available now, so we cannot uniquely define the $f^*(x)$ just with the remaining two out-of-plane boundary conditions $w^*(x = 0\ and\ L/(Rh)^{1/2}) = 0$ and $w^*{}_{,x}\,(x = 0\ and\ L/(Rh)^{1/2}) = 0$. Since the postbuckling b coefficient only relates to the second derivatives of $f^*(x)$, we can apply the additional boundary condition which is the single value requirement of the circumferential displacement. This can be derived from

$$\oint V_{,y}\,dy = 0 \tag{4.41}$$

Form which we can get the following additional boundary condition,

$$\begin{aligned} f^*(x)_{,xx} = \frac{b_{21}^*}{a_{22}^*} w^*(x)_{,xx} + \frac{1}{a_{22}^*} w^*(x) \\ + \frac{\bar{N}^2}{4a_{22}^*}\left(w_s^2(x) + w_c^2(x)\right) \end{aligned} \tag{4.42}$$

Substituting equation (4.40) and (4.42) into equation (4.39) and replacing the term $f^*{}_{,xxxx}$ and $f^*{}_{,xx}$, we can get an ODE involving only $w^*(x)$, which is,

$$\left(d_{11}^{*}+\frac{{b_{21}^{*}}^{2}}{a_{22}^{*}}\right)w^{*},_{xxxx}+\left(\frac{2b_{21}^{*}}{a_{22}^{*}}+\sigma\right)w^{*},_{xx}+\frac{1}{a_{22}^{*}}w^{*}$$
$$=-\frac{\overline{N}^{2}}{2}(w_{s}f_{s}+w_{c}f_{c}),_{xx}$$
$$-\frac{\overline{N}^{2}b_{21}^{*}}{4a_{22}^{*}}(w_{s}^{2}+w_{c}^{2}),_{xx} \qquad (4.43)$$
$$-\frac{\overline{N}^{2}}{4a_{22}^{*}}(w_{s}^{2}+w_{c}^{2}) \quad at\ x$$
$$=0\ and\ \frac{L}{(Rh)^{\frac{1}{2}}}$$

With two out-of-plane boundary conditions $w^{*}(x=0\ and\ L/(Rh)^{1/2})=0$ and $w^{*},_{x}(x=0\ and\ L/(Rh)^{1/2})=0$, we can uniquely solve $w^{*}(x)$, and substitute the solution of $w^{*}(x)$ into equation (4.42) to solve $f^{*}(x),_{xx}$.

The second set of second order field is,

$$L_{II}{}_{d}^{2*}(w_{A})+L_{II}{}_{d}^{3*}(w_{B})+L_{II}{}_{b}^{2*}(f_{A})+L_{II}{}_{b}^{3*}(f_{B})+f_{A},_{xx}$$
$$+\sigma w_{A},_{xx}-4\overline{N}^{2}pw_{A}-4\overline{N}\tau w_{B},_{x}$$
$$=\frac{\overline{N}^{2}}{2}(w_{s},_{xx}f_{s}-w_{c},_{xx}f_{c}+w_{s}f_{s},_{xx} \qquad (4.44)$$
$$-w_{c}f_{c},_{xx}-2w_{s},_{x}f_{s},_{x}+2w_{c},_{x}f_{c},_{x})$$

$$
\begin{aligned}
&L_{II}{}_{d}^{2*}(w_B) - L_{II}{}_{d}^{3*}(w_A) + L_{II}{}_{b}^{2*}(f_B) - L_{II}{}_{b}^{3*}(f_A) + f_{B,xx} \\
&\quad + \sigma w_{B,xx} - 4\bar{N}^2 p w_B + 4\bar{N}\tau w_{A,x} \\
&\quad = \frac{\bar{N}^2}{2}(-w_{c,xx} f_s - w_{s,xx} f_c - w_c f_{s,xx} \\
&\quad - w_s f_{c,xx} + 2w_{c,x} f_{s,x} + 2w_{s,x} f_{c,x})
\end{aligned} \tag{4.45}
$$

$$
\begin{aligned}
&L_{II}{}_{a}^{2*}(f_A) + L_{II}{}_{a}^{3*}(f_B) - L_{II}{}_{b}^{2*}(w_A) - L_{II}{}_{b}^{3*}(w_B) \\
&\quad - w_{A,xx} \\
&\quad = \frac{\bar{N}^2}{2}(w_{s,x}^2 - w_{c,x}^2 - w_s w_{s,xx} \\
&\quad + w_c w_{c,}xx)
\end{aligned} \tag{4.46}
$$

$$
\begin{aligned}
&L_{II}{}_{a}^{2*}(f_B) + L_{II}{}_{a}^{3*}(f_A) - L_{II}{}_{b}^{2*}(w_B) - L_{II}{}_{b}^{3*}(w_A) \\
&\quad - w_{B,xx} \\
&\quad = \frac{\bar{N}^2}{2}(w_c w_{s,xx} + w_s w_{c,xx} - 2w_{s,x} w_{c,x})
\end{aligned} \tag{4.47}
$$

where the linear differential operators $L_{II}{}_{a}^{2*}$, $L_{II}{}_{a}^{3*}$, $L_{II}{}_{b}^{2*}$, $L_{II}{}_{b}^{3*}$, $L_{II}{}_{d}^{2*}$ and $L_{II}{}_{d}^{3*}$ can be got from equation (4.19) to (4.24) by replacing the $\bar{N}$ by $2\bar{N}$ resplectively.

The boundary conditions for the second set can be reached from equations (4.28-4.32) by replacing the $\bar{N}$, w_c, w_s, f_c and f_s by $2\bar{N}$, w_A, w_B, f_A and f_B respectively. The second order filed is descrelized by center finite difference scheme and solved by Gauss elimination method.

4.3.3 Equations for the Postbuckling Coefficient

The postbuckling b coefficient evaluates the stability of the structures. If the b coefficient is positive, then the structure has stable postbuckling behavior; if the b coefficient is negative, the structure has unstable postbuckling behavior. The imperfection sensitivity is measured by the magnitude of the postbuckling b coefficient. The path of equilibrium is formulated as,

$$b\xi^3 + \left[1 - \frac{\lambda_i}{\lambda_c}\right]\xi = \mu\frac{\lambda_i}{\lambda_c} \tag{4.48}$$

where, λ_i is the buckling load of the imperfect system, λ_c is the classical buckling load of the perfect system, μ is the imperfection amplitude divide by the shell thickness. The imperfection amplitude is related to the buckling load by the following formula (only for b<0),

$$\mu = \frac{2\sqrt{-3b}[1 - (\lambda_i/\lambda)]^{3/2}}{3(\lambda_i/\lambda)} \tag{4.49}$$

The formula of postbuckling b coefficient is (Budiansky [81], Hui and Du [89]),

$$b = \frac{C_1 + C_2}{|D_1|} \tag{4.50}$$

where,

$$C_1 = 2\int_{y=0}^{y_0}\int_{x=0}^{Z_H}\{f_{I,yy}\,w_{I,x}\,w_{II,x} + f_{I,xx}\,w_{I,y}\,w_{II,y} - f_{I,xy}\left(w_{I,x}\,w_{II,y} + w_{I,y}\,w_{II,x}\right)\}dxdy \tag{4.51}$$

$$C_2 = \int_{y=0}^{y_0}\int_{x=0}^{Z_H}\{f_{II,yy}\,(w_{I,x})^2 + f_{II,xx}\left(w_{I,y}\right)^2 - 2f_{II,xy}\,w_{I,x}\,w_{I,y}\}dxdy \tag{4.52}$$

$$D_1 = \int_{y=0}^{y_0}\int_{x=0}^{Z_H}(\sigma_a w_I^2{}_{,x} + p_a w_I^2{}_{,y} + 2\tau_a w_{I,x}\,w_{I,y}) \tag{4.53}$$

In the above, $y = 2\pi R/(Rh)^{1/2}$ and the reduced-Batdorf parameter $Z_H = L/(Rh)^{1/2}$. Substituting the buckling state and the postbuckling state, and integrating in the circumferential direction analytically, we can obtain,

$$
\begin{aligned}
C_1 = \bar{N}^2 y_0 \int_{x=0}^{Z_H} \{ & w_{,x}^{*} \left(-f_s w_{s,x} - f_c w_{c,x}\right) \\
& + \frac{1}{2} w_{A,x} \left(f_s w_{s,x} - f_c w_{c,x}\right) \\
& - \frac{1}{2} w_{B,x} \left(f_s w_{c,x} + f_c w_{s,x}\right) \\
& - w_A (f_{s,xx} w_s - f_{c,xx} w_c) \\
& + w_B (f_{s,xx} w_c + f_{c,xx} w_s) \\
& + w_A (f_{s,x} w_{s,x} - f_{c,x} w_{c,x}) \\
& - w_B (f_{s,x} w_{c,x} + f_{c,x} w_{s,x}) \\
& - w_{,x}^{*} (f_{s,x} w_s + f_{c,x} w_c) \\
& - \frac{1}{2} w_{A,x} (f_{s,x} w_s - f_{c,x} w_c) \\
& - \frac{1}{2} w_{B,x} (-f_{s,x} w_c - f_{c,x} w_s) \} dx
\end{aligned} \tag{4.54}
$$

$$
\begin{aligned}
C_2 = \bar{N}^2 y_0 \int_{x=0}^{Z_H} \{ & -f_A [(w_{c,x})^2 - (w_{s,x})^2] \\
& - 2 f_B w_{s,x} w_{c,x} + \frac{1}{2} f_{,x}^{*} (w_c^2 + w_s^2) \\
& + \frac{1}{4} f_{A,xx} (w_s^2 - w_c^2) - \frac{1}{2} f_{B,xx} w_s w_c \\
& + f_{A,x} (w_s w_{s,x} - w_c w_{c,x}) \\
& - f_{B,x} (w_c w_{s,x} + w_s w_{c,x}) \} dx
\end{aligned} \tag{4.55}
$$

$$
D_1 = \bar{N}^2 y_0 \int_{x=0}^{Z_H} \{ \frac{1}{2} \sigma_a [(w_{c,x})^2 + (w_{s,x})^2] \} dx \tag{4.56}
$$

Note that postbuckling b coefficient is also calculated by using the actual applied load σ_a, then the b coefficient should be a function of applied load numerically. In order to compare the Hui's postbuckling method with the Koiter's general theory, we need to get one b coefficient for improved Koiter. This is the reason for us to do the least square curve fit.

Fitting the knock down curve of the Hui's postbuckling method using equation (4.48) by the least square technique in the range of imperfection amplitude form 0 to 25 percent of the shell thickness, we can get the improved b coefficient. Then we can use it to compare with the usual b coefficient calculated by the Koiter's general postbuckling theory.

4.4 Result and Discussion

4.4.1 Example Cases

Here we concentrate on demonstrating the improvement of the Hui's postbuckling method by comparing the result with the Koiter's general stability theory and ABAQUS simulation. So we will not do a complete parameter variation of the composite cylindrical shells in here. The example used here is antisymmetric laminated cross-ply cylindrical shells made of Boron-epoxy materials (see Hui and Du [89]). The material parameters are,

$$\frac{E_1}{E_2} = 10, \qquad \frac{G_{12}}{E_2} = 0.5, \qquad v_{12} = 0.25 \tag{4.57}$$

The clamp boundary condition is applied in both ends of the cylindrical shell. Three cases are considered in here,

i. $_{in}[0^o_t/90^o_t]_{out}$, clamp

ii. $_{in}[90^o_t/0^o_t]_{out}$, clamp

iii. $_{in}[90^o_t/0^o_t/90^o_t/0^o_t]_{out}$, clamp

The geometric properties of above laminated cylindrical shells used in ABAQUS simulation are,

$$R = 30mm, L = 50mm, t = 0.05mm \tag{4.58}$$

where t is the thickness of each layer of the laminate.

For comparison to the unstiffened cylinder, here we also use the large cylinder case, but the material is changed to one kind of carbon fiber, with ten cross-ply $[0^o_t/90^o_t]_5$ layers. The material properties are,

$$E_1 = 142500Mpa, E_2 = 8700Mpa, v_{12} = 0.28, G_{12} = 5100Mpa \tag{4.59}$$

The geometric properties are the same as for unstiffened ones, which are

$$R = 1736mm, L = 7013mm, t = 5mm \tag{4.60}$$

Some results in Hui and Du [89] are reproduced to check the accuracy of my programming. The geometry of the cylindrical shell is described by the reduced-Batdorf parameter $Z_H = L/(Rh)^{1/2}$. Where, h is the total thickness of the laminated cylindrical shell. The postbuckling coefficients of ${}_{in}[0^o_t/90^o_t]_{out}$ and ${}_{in}[90^o_t/0^o_t]_{out}$ antisymmetric cross-ply cylindrical shell under torsion are reproduced and presented in Figure 4.1. The result is identical to the result presented in Hui and Du's work. This shows that the b coefficient changes from positive to negative when Z_H changes from 3.0 to 5.0 for both cases. When Z_H is between 6.0 and 9.0, the b coefficient of both case reaches their maximum negative, which means the most imperfect-sensitivity is occurred in this region for both cases. The most negative value of b coefficient of ${}_{in}[0^o_t/90^o_t]_{out}$ case is about -0.07, and the most negative value for ${}_{in}[90^o_t/0^o_t]_{out}$ case is about -0.055. From the result we can see the ${}_{in}[90^o_t/0^o_t]_{out}$ laminated cylindrical shell is more imperfection sensitive than ${}_{in}[0^o_t/90^o_t]_{out}$

laminated cylindrical shell. So the b coefficient of Koiter's general theory agrees with the one presented by Hui and Du [89] very well.

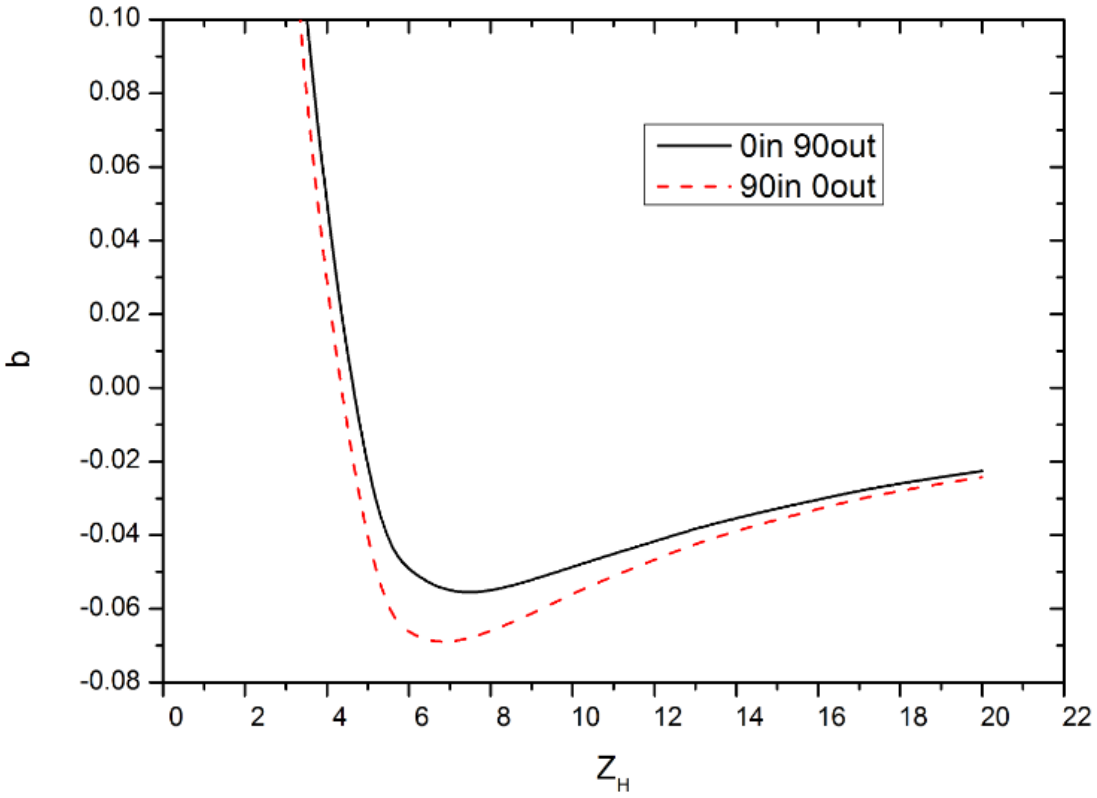

Figure 4.1 Postbuckling b coefficient versus the reduced-Batdorf parameters for antisymmetric cross-ply cylindrical shells under torsion

4.4.2 [0/90] Laminate

Now we can compare the Hui's postbuckling method with the Koiter's general theory and ABAQUS simulation result. Figure 4.2 shows the Knock down factors of $_{in}[0^{o}_{t}/90^{o}_{t}]_{out}$ antisymmetric cross-ply cylindrical shell under axial compression calculated by ABAQUS, Hui's postbuckling method, Koiter's general theory and curve fit of the improved b coefficient, respectively. From the figure, we can see that the curve for the Hui's postbuckling method can fit the ABAQUS result of the imperfection up to 39% of the shell thickness and then it starts to diverge from the ABAQUS result. Furthermore, the Koiter's general theory is only valid when the imperfection of the cylinder is around 10% of the shell thickness. For the comparison purpose, the curve fit for the Hui's postbuckling method is taken place, and the improved b coefficient is calculated out. We can see that the knock down curve for the improved b coefficient is also valid when the imperfection is up to 30% of the shell thickness. Now we can compare the general b coefficient which is -0.4561 with the improved b coefficient which is -0.2347. We can find a 50% positive shift of the postbuckling coefficient by using the Hui's postbuckling method. This means that the general Koiter's theory significantly overestimates the imperfection sensitivity. Also, there is a significant increase of valid region of Koiter's general theory from the imperfection about 10% of the shell thickness to 30% of the shell thickness. The improvement of the valid region is about 300%. This is a significant improvement which means the Hui's postbuckling method is more practical than the original one. The cylinder with imperfection within 10% of the shell thickness is very hard to make. Although the result of ABAQUS simulation is the most accurate one, the time consuming to calculate this knock down curve is at least 30 times more

than using Hui's postbuckling method. Also, ABAQUS is an expensive commercial software. So the efficiency and the low cost are the advantages of the Hui's postbuckling method.

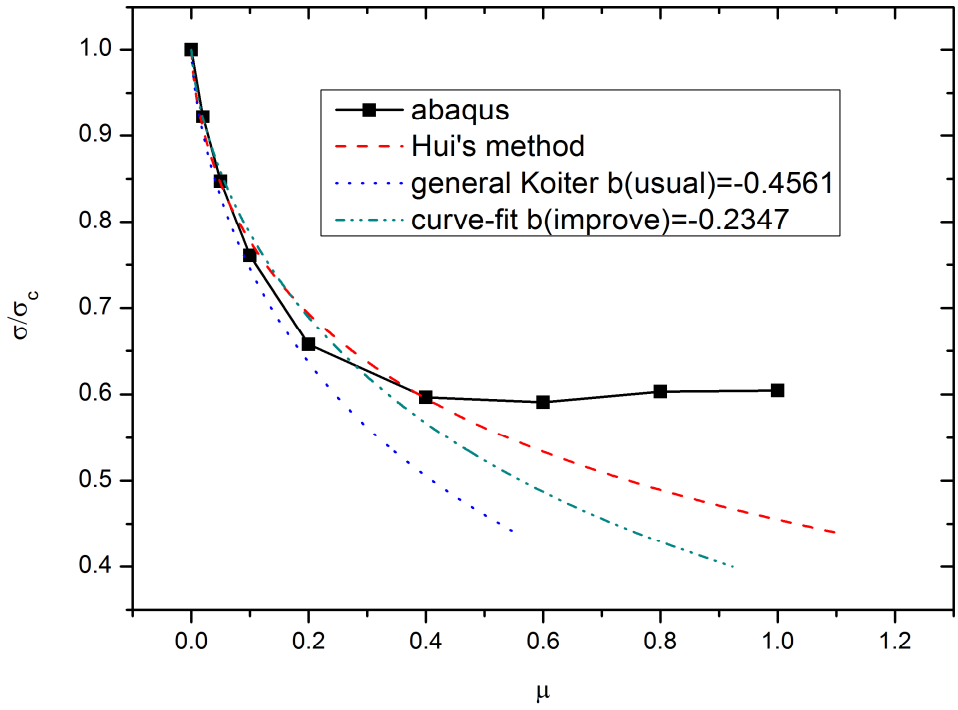

Figure 4.2 Knock down curve for $_{in}[0^{o}_{t}/90^{o}_{t}]_{out}$ antisymmetric cross-ply cylindrical shell under axial compression calculate by different method

4.4.3 [90/0] Laminate

Figure 4.3 shows the Knock down factors of $_{in}[90^{o}_{t}/0^{o}_{t}]_{out}$ antisymmetric cross-ply cylindrical shell under axial compression calculated by ABAQUS, Hui's postbuckling method, Koiter's general theory and curve fit of the improved b coefficient, respectively. The result shows that, the curve for the Hui's postbuckling method fits the ABAQUS result when the imperfection is up to 18% of the shell thickness. Same phenomenon happens for the result calculated by the improved b coefficient from curve fitting. Koiter's general theory is only valid when the imperfection is less than 5% of the shell thickness. Then it starts to diverge from the ABAQUS result. Again, more than 300% percent improvement of valid region was found for the Hui's postbuckling method compared with the original one. But we can also see that, compared with the previous case; the valid region for the Hui's postbuckling method decreases significantly. So the validity region of the Hui's postbuckling method is varying from case by case. This conclusion is also valid for Koiter's general theory, and the improvement of the valid region is still significant. We can also see the general b coefficient is -0.4528, compared with the improved b coefficient which is -0.2290. There is an about 50% positive shift of the postbuckling b coefficient. This also demonstrates the Koiter's general significantly overestimates the imperfection sensitivity.

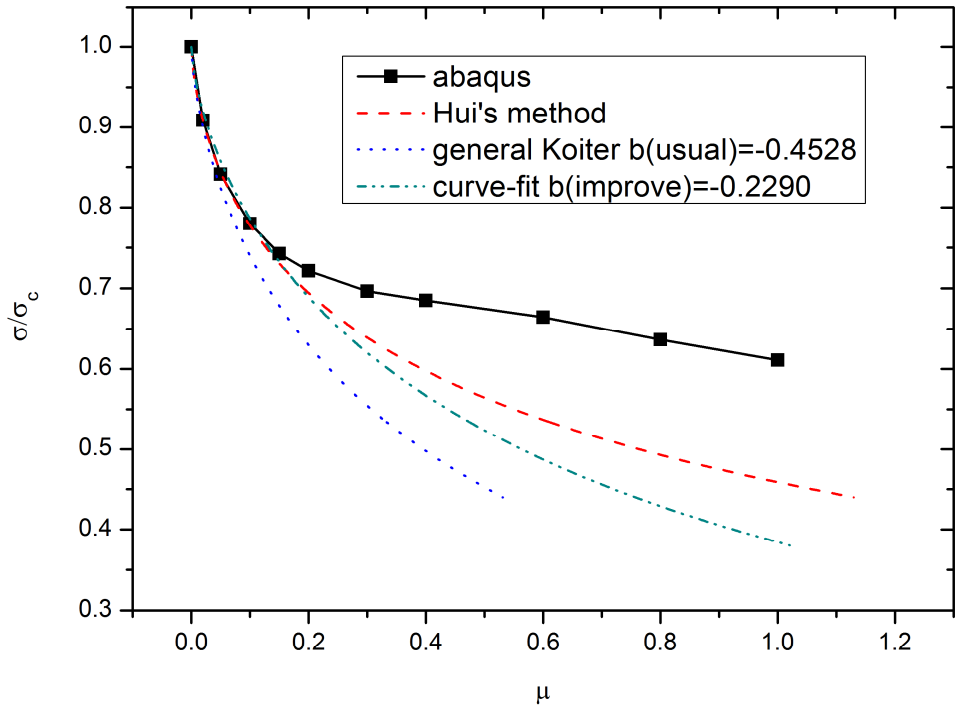

Figure 4.3 Knock down curve for $_{in}[90^{o}_{t}/0^{o}_{t}]_{out}$ antisymmetric cross-ply cylindrical shell under axial compression calculate by different method

Figure 4.4 shows the improved b coefficient and usual b coefficient versus the reduced-Batdorf parameters for $_{in}[90^{o}_{t}/0^{o}_{t}]_{out}$ antisymmetric cross-ply cylindrical shell under axial compression. It is important to note that when b coefficient is positive, the curve fitting process takes place for the equilibrium path of the load-deflection curve which is specified by the equation (1.32). From the result we can see, for stable structure (b coefficient is positive) there is almost no difference between Hui's postbuckling method and Koiter's general theory. After the structure becomes unstable, the improved b coefficient and usual b coefficient start to diverge. The difference of the b coefficient between Hui's postbuckling method and Koiter's general theory is stabilized at about 50% positive shifting of usual b coefficient throughout the whole region of Z_H which considered in here. It is clear shows that the

Koiter's general theory always significantly overestimates the imperfection sensitivity of the structure. But we should note that, the positive shifting is not always 50% for different kinds of cylinders. For some type of cylinder the shift is larger, for example the isotropic cylindrical shell under axial compression, sometimes the shift is not that much (like in this case).

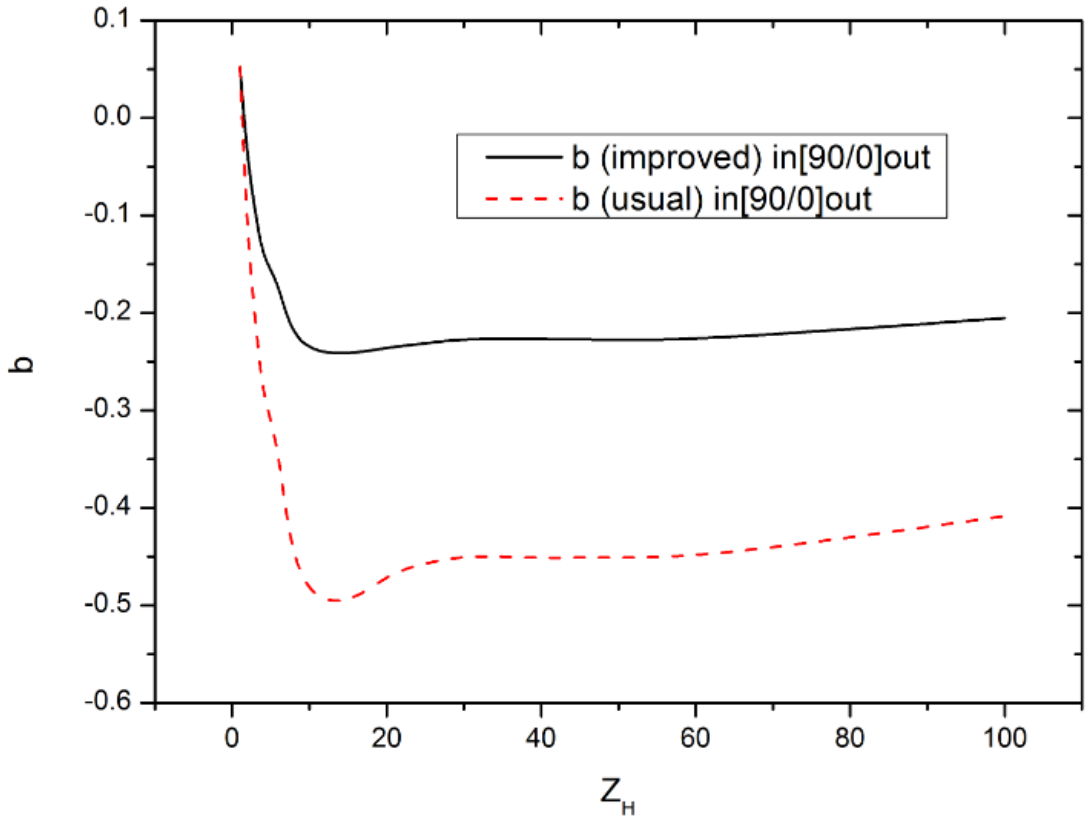

Figure 4.4 Improved b coefficient and usual b coefficient versus the reduced-Batdorf parameters for $_{in}[90^{o}_{t}/0^{o}_{t}]_{out}$ antisymmetric cross-ply cylindrical shell under axial compression

4.4.4 [90/0/90/0] Laminate

Figure 4.5 presents the knock down curves for $_{in}[90^{o}_{t}/0^{o}_{t}/90^{o}_{t}/0^{o}_{t}]_{out}$ antisymmetric cross-ply cylindrical shell under axial compression calculated by ABAQUS, Hui's postbuckling method, Koiter's general theory and curve fitting of the improved b coefficient, respectively. We can see the knock down curve calculated by the Hui's postbuckling method fits the ABAQUS result when the imperfection is up to 23% of the shell thickness. It then starts to diverge from the ABAQUS result. The result of the curve fitting is also valid when the imperfection is up to about 20% of the shell thickness. Furthermore, the knock down curve calculated by the usual b from Koiter's general theory is valid only when the imperfection is up to few percent of the shell thickness (about 5% of the shell thickness). Again, it shows a significant improvement (more than 300%) of the valid region of Hui's postbuckling method compared with the Koiter's general theory. Also we can see the improved b coefficient from curve fitting is -0.1375 compared with the usual b coefficient from Koiter's general theory, which is -0.2444. There is still an about 50% positive shift from usual b coefficient to improved b coefficient. This, again, demonstrates that the Koiter's general theory significantly overestimates the imperfection sensitivity. This also shows that the valid region is varied case by case. We can only know the valid region once we compare it with the finite element result such as ABAQUS simulation. But more or less, the valid region is the imperfection up to about 20%-30% of the shell thickness. So without the finite element simulation, it is preferred to trust the result when the imperfection is within about 20%-30% of the shell thickness. After this point, it has the risk to overestimate the buckling load significantly. Here, we need to note that, although the Hui's postbuckling method is more

accurate than the Koiter's general theory, sometimes it will slightly underestimate the buckling load. So it is good to have some safety factor which can overcome this situation.

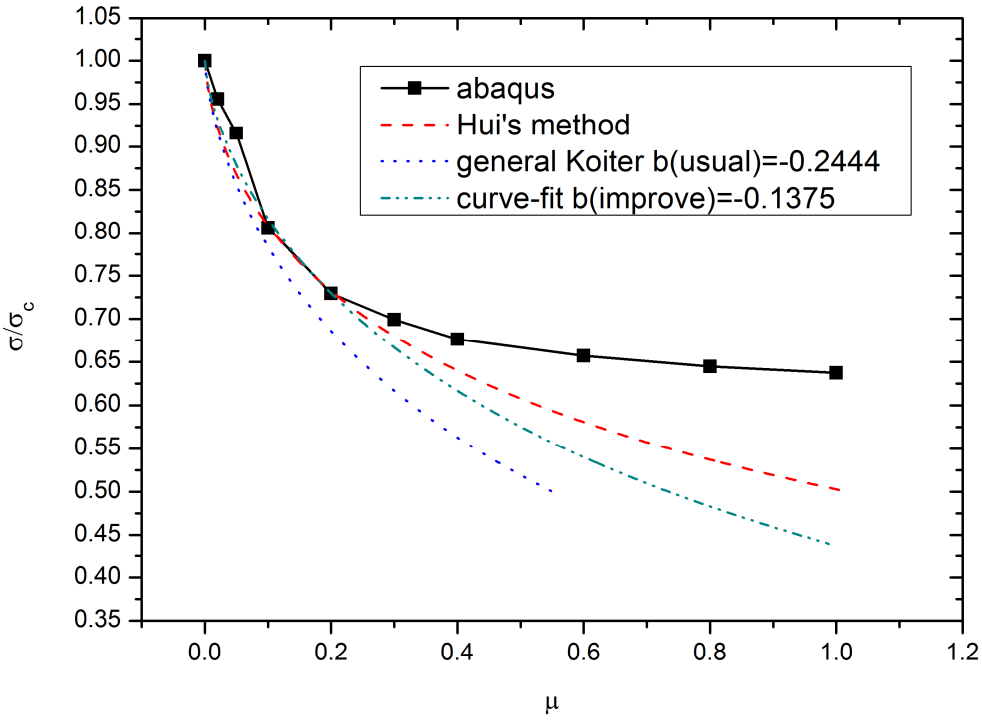

Figure 4.5 Knock down curve for $_{in}[90^{o}_{t}/0^{o}_{t}/90^{o}_{t}/0^{o}_{t}]_{out}$ antisymmetric cross-ply cylindrical shell under axial compression calculate by different method

4.4.5 $[0/90]_5$ Large laminated cylindrical shell

Figure 4.6 shows the Knock down curves for $[0/90]_5$ large antisymmetric cross-ply cylindrical shell under axial compression calculate by calculate ABAQUS, Hui's postbuckling method, Koiter's general theory and curve fitting of the improved b coefficient, respectively. In this example, the dimension is quite large and there are lots of layers. Although the length of the cylinder is quite long, the reduced Batdorf parameter is only 23.8037. This is because the shell thickness we choose is quite large. In this quite extreme case, we can see before the imperfection is less than 20% of the shell thickness, the Koiter's general curve fits the ABAQUS result better than Hui's postbuckling method. But when the imperfection increases, the Hui's postbuckling method is much closer than the Koiter's general theory. It seems that Hui's postbuckling method is tending to match the whole curve, so that it makes the first 20% of imperfection less accurate than Koiter's general theory. But after that, the Hui's postbuckling method matches the decreasing rate of the knock down curve of ABAQUS very well up to one. Again, we can see the Koiter's general theory significantly overestimates the imperfection sensitivity of the structure, by comparing the general b coefficient with the improved b coefficient which is -0.1403 and -0.0887 respectively.

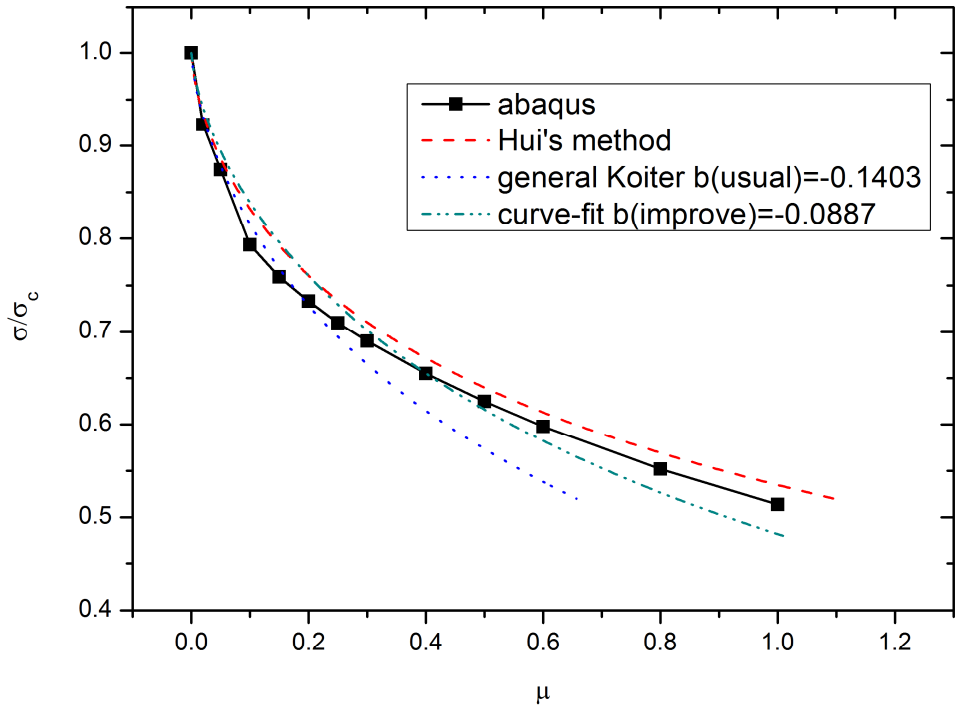

Figure 4.6 Knock down curve for $[0/90]_5$ large antisymmetric cross-ply cylindrical shell under axial compression calculate by different method, $Z_H = 23.8037$

4.5 Conclusion

In this part of the thesis, we successfully compared the Hui's postbuckling method with ABAQUS and Koiter's general theory by four cases of antisymmetric cross-ply cylindrical shell under axial compression. The result shows the valid region for Hui's postbuckling method is significantly increased compared with the Koiter's general theory. Also the Koiter's general theory significantly overestimates the imperfection sensitivity of the structures. An about 50% positive shift of postbuckling b coefficient was found through all the cases. Although the ABAQUS result is the most accurate one, the time consuming is at least 30 times more than using Hui's postbuckling method. Furthermore, ABAQUS is also an expensive commercial software, compared with no cost needed to calculate by Hui's postbuckling method using free programming language. It should be noted that, although the Hui's postbuckling method is more accurate than the Koiter's general theory, sometimes it will slightly underestimate the buckling load. So it is good to have some safety factor which can overcome this situation. Even in a very extreme condition: large dimensions; thick shell thickness; small reduced Batdorf parameters; lots of layers, the valid region of Hui's postbuckling method is much better than Koiter's general theory. Overall, Hui's postbuckling method significantly improves the valid region of Koiter's general theory, so that it is more practical to be used in a preliminary design.

CHAPTER 5

PARAMETER VARIATION STUDY ON IMPERFECTION SENSITIVITY OF STIFFENED CYLINDER USING HUI'S POSTBUCKLING MEHOD

5.1 Introduction

Here we are using the Hui's postbuckling method to analyze the postbuckling and imperfection sensitivity of stringer or ring stiffened cylindrical shell under axial compression and torsion. We are comparing the solution with the Koiter's general postbuckling theory result and also performing some parametrical variation investigation. This analysis is based on the work of Huchinson and Amazigo [40] which presents the investigation on the imperfection sensitivity of eccentrically stiffened cylindrical shells. The Donnell type non-linear partial differential equilibrium and compatibility equations of a cylindrical shell are reduced to sets of linear ordinary differential equations corresponding to the buckling and initial-postbuckling regimes by using the separation of variables technique employed by Budiansky [81]. These equations are discretized using a central-finite difference scheme (see APPENDIX A). By applying the Hui's postbuckling method, three special cares are taken, (i) the applied load in the differential equations of the second order field is using the actual value of the applied load rather than the classical buckling load, (ii) the values of first order displacement and stress function are modified with respect to the rate of the actual value of

the applied load rather than the classical buckling load, (iii) The postbuckling coefficient is also evaluated at the actual applied load. The resulting knock down curve is fitted by the least square curve fit technique for the imperfection amplitude between 0 and 0.25 to get the improved postbuckling b coefficient.

5.2 Governing Equations and First Order Field

5.2.1 Governing Equations

Koiter's theory of elastic stability is used to analyze the buckling and initial postbuckling behavior of stringer and /or ring stiffened cylindrical shells under torsion. Koiter's theory was reformulated by Budiansky and Hutchinson [79], and for brevity, it will not be redeveloped here (see Budiansky [81], Hutchinson and Amazigo [40], Hui and Du [89] [101]). For the present single-mode symmetric system, the structure is sensitive to the presence of small geometric imperfection if the postbuckling 'b' coefficient is negative, and it is not sensitive to imperfection if 'b' is positive. The extent of imperfection-sensitivity depends upon the magnitude of the b coefficient. The Koiter-style analysis is restricted to relatively small amplitudes of the imperfection. The imperfection shape is identical to that of the buckling mode.

The nonlinear Donnell-type equilibrium and compatibility partial differential equation for stiffened cylindrical shells, written in terms of an out-of-plane displacement W (positive outwards) of the 'skin' middle surface and a stress function of the 'smeared' stiffened shell are, (Hutchinson and Amazigo [40]),

$$L_D(W) + L_Q(F) = F_{,YY}\,W_{,XX} + F_{,XX}\,W_{,YY} - 2F_{,XY}\,W_{,XY} \tag{5.1}$$

$$L_H(F) - L_Q(W) = (W_{,XY})^2 - W_{,XX}\,W_{,YY} \tag{5.2}$$

In the above, X and Y are the axial and circumferential coordinates respectively and $L_D(\,)$, $L_Q(\,)$ and $L_H(\,)$ are the fourth order linear differential operators defined by Hutchinson and Amazigo [40].

5.2.2 Non-Dimensionalize

The following non-dimensional quantities are employed,

$$w = \frac{W}{h},\ \ f = \frac{F}{Eh^3},\ \ (x,y) = \frac{(X,Y)}{(Rh)^{\frac{1}{2}}}$$
$$\left[L_D\,(\,), L_Q\,(\,), L_H\,(\,)\right] = \left[Eh^3 L_d\,(\,), hL_q\,(\,), \left(\frac{1}{Eh}\right) L_h\,(\,)\right] \tag{5.3}$$

where, E is Young's modulus (taken to be the same for the skin and the stiffeners), R is the shell radius and t is the skin thickness. Thus, the non-dimensional equilibrium and compatibly equations become,

$$L_d(w) + L_d(f) = f_{,yy}\, w_{,xx} + f_{,xx}\, w_{,yy} - 2f_{,xy}\, w_{,xy} \tag{5.4}$$

$$L_h(F) - L_q(W) = \left(w_{,xy}\right)^2 - w_{,xx}\, w_{,yy} \tag{5.5}$$

The non-dimensional linear differential operators are,

$$L_d(\,) = d_{xx}(\,)_{,xxxx} + 2d_{xy}(\,)_{,xxyy} + d_{yy}(\,)_{,yyyy} \tag{5.6}$$

$$\begin{aligned} L_q(\,) = {} & q_{xx}(\,)_{,xxxx} + 2q_{xy}(\,)_{,xxyy} + q_{yy}(\,)_{,yyyy} \\ & + (\,)_{,xx} \end{aligned} \tag{5.7}$$

$$L_h(\,) = h_{xx}(\,)_{,xxxx} + 2h_{xy}(\,)_{,xxyy} + h_{yy}(\,)_{,yyyy} \tag{5.8}$$

where (equation (5.10) differs from Hutchinson and Amazigo's [40] analysis, due to the inclusion of the stiffener torsional rigidity, see APPENDIX C),

$$\begin{aligned} & (d_{xx}, d_{yy}) \\ & = \frac{\{1 + (\beta_s, \beta_r) + 12(1-v^2)[1 + (\alpha_r, \alpha_s)](\alpha_s\gamma_s^2, \alpha_r\gamma_r^2)\}}{[12(1-v^2)\alpha_0]} \end{aligned} \tag{5.9}$$

$$\begin{aligned} d_{xy} = {} & \frac{1}{12(1-v^2)}\{1 + \frac{[12v(1-v^2)\alpha_s\alpha_r\gamma_s\gamma_r]}{\alpha_0} \\ & + \frac{1}{2}(\delta_s + \delta_r)\} \end{aligned} \tag{5.10}$$

$$(q_{xx}, q_{yy}) = \frac{(v\alpha_s\gamma_s, v\alpha_r\gamma_r)}{\alpha_0} \tag{5.11}$$

$$q_{xy} = -\frac{\{\alpha_s\gamma_s[1 + (1-v^2)\alpha_r] + \alpha_r\gamma_r[1 + (1-v^2)\alpha_s]\}}{2\alpha_0} \tag{5.12}$$

$$\left(h_{xx}, h_{yy}\right) = \frac{[1 + (\alpha_s, \alpha_r)(1 - v^2)]}{\alpha_0} \tag{5.13}$$

$$h_{xy} = 1 + v - \left(\frac{v}{\alpha_0}\right) \tag{5.14}$$

In the above, v is Poisson's ratio. It is taken to be the same for the skin and the stiffeners. The stiffener cross-sectional area ratio (α_s, α_r), the stiffener out-of plane bending-stiffness ratio (β_s, β_r), the stiffener eccentricity ratio (γ_s, γ_r) and the stiffener torsional rigidity ratio (δ_s, δ_r) are,

$$\begin{gathered}(\alpha_s, \alpha_r) = \frac{(A_s, A_r)}{(d_s, d_r)h} \\ (\beta_s, \beta_r) = \frac{(E_s I_s, E_r I_r)}{D(d_s, d_r)} \\ (\gamma_s, \gamma_r) = \frac{(e_s, e_r)}{h} \\ (\delta_s, \delta_r) = \left(\frac{G_s J_s}{D d_s}, \frac{G_r J_r}{D d_r}\right)\end{gathered} \tag{5.15}$$

In order to simplify the analysis, all the stiffeners in a stiffened shell are assumed to be identical and they are equally spaced. Furthermore, (A_s, A_r) is the cross-sectional area of any stringer or ring; (d_s, d_r) is the distance between adjacent stringers or adjacent rings; (E_s, E_r) is Young's modulus of stringer or ring; (I_s, I_r) is out-of-plane bending moment of

inertia of any one stiffener with respect to its centroid; D is the flexural rigidity of the skin; (e_s, e_r) is the stiffener eccentricity and $(G_s J_s, G_r J_r)$ is the torsional rigidity of any one stringer or ring.

5.2.3 Equations for the First Order Field

According to Koiter's theory, the total displacement and the total stress function can be written as,

$$\begin{aligned} w_t &= w_0 + \xi w_I + \xi^2 w_{II} \\ f_t &= f_0 + \xi f_I + \xi^2 f_{II} \end{aligned} \tag{5.16}$$

where ξ is the amplitude of the buckling mode normalized with respect to the skin thickness and a membrane prebuckling state is assumed. The non-dimensional applied loads are,

$$\begin{aligned} (\sigma, p, \tau) &= \left(-f_{0,yy}\,, -f_{0,xx}\,, -f_{0,xy}\right) \\ &= \frac{R}{Eh^2}(N_x, N_y, N_{xy}) \end{aligned} \tag{5.17}$$

where, N_x is the axial compression force per circumferential length, N_y is the pressure, N_{xy} is the torsional force per circumferential length. Substituting w_t and f_t into nonlinear differential equations (5.4) and (5.5), then collecting terms which are linear in ξ, the equilibrium and compatibility equations for the buckling state become,

$$L_d(w_I) + L_d(f_I) + \sigma_c w_{I,xx} + p_c w_{I,yy} - 2\tau_c w_{I,xy} = 0 \tag{5.18}$$

$$L_h(f_I) - L_q(w_I) = 0 \tag{5.19}$$

5.2.4 Solve the First Order Field

Following the analysis of Budiansky(1967), the buckling mode can be written in the separable form,

$$[w_I(x,y), f_I(x,y)] = [w_c(x), f_c(x)]\cos(\bar{N}y) + [w_s(x), f_s(x)]\sin(\bar{N}y) \tag{5.20}$$

where

$$\bar{N} = n\left(\frac{h}{R}\right)^{1/2} \tag{5.21}$$

and the integer n is the number of circumferential full-waves. Substituting $w_I(x,y)$ and $f_I(x,y)$ into the linearized equilibrium equations, and then collecting terms involving $\cos(\bar{N}y)$ and $\sin(\bar{N}y)$, one obtains respectively,

$$\begin{aligned} &d_{xx}w_{c,xxxx} - 2\bar{N}^2 d_{xy}w_{c,xx} + d_{yy}\bar{N}^4 w_c + q_{xx}f_{c,xxxx} \\ &\quad - 2\bar{N}^2 q_{xy}f_{c,xx} + q_{yy}\bar{N}^4 f_c + f_{c,xx} \\ &\quad + \sigma_c w_{c,xx} - \bar{N}^2 p_c w_c - 2\tau\bar{N}w_{s,x} = 0 \end{aligned} \tag{5.22}$$

$$\begin{aligned} &d_{xx}w_{s,xxxx} - 2\bar{N}^2 d_{xy}w_{s,xx} + d_{yy}\bar{N}^4 w_s + q_{xx}f_{s,xxxx} \\ &\quad - 2\bar{N}^2 q_{xy}f_{s,xx} + q_{yy}\bar{N}^4 f_s + f_{s,xx} \\ &\quad + \sigma_c w_{s,xx} - \bar{N}^2 p_c w_s - 2\tau\bar{N}w_{c,x} = 0 \end{aligned} \tag{5.23}$$

Likewise, collecting terms involving $cos\,(\bar{N}y)$ and $sin\,(\bar{N}y)$ from the linearized compatibility equation for the buckling state, one obtains respectively,

$$\begin{aligned} & h_{xx}f_{c,xxxx} - 2\bar{N}^2 h_{xy}f_{c,xx} + h_{yy}\bar{N}^4 f_c \\ & - \left[q_{xx}w_{c,xxxx} - 2\bar{N}^2 q_{xy}w_{c,xx}\right. \\ & \left. + q_{yy}\bar{N}^4 w_c + w_{c,xx}\right] = 0 \end{aligned} \tag{5.24}$$

$$\begin{aligned} & h_{xx}f_{s,xxxx} - 2\bar{N}^2 h_{xy}f_{s,xx} + h_{yy}\bar{N}^4 f_s \\ & - \left[q_{xx}w_{s,xxxx} - 2\bar{N}^2 q_{xy}w_{s,xx}\right. \\ & \left. + q_{yy}\bar{N}^4 w_s + w_{s,xx}\right] = 0 \end{aligned} \tag{5.25}$$

For simplicity, the boundary conditions are identical at both ends of the stiffened cylindrical shell, and $w(x=0)=0$, $w(x=L/(Rt)^{(1/2)})=0$. The out-of-plane boundary conditions are either clamped $W_{,X}\,(X=0)=0$ or simply-supported $M_x^{sm}(X=0)=0$, where M_x^{sm} is the bending moment for the 'smeared' shell, which can be derived from the terms involving $\delta W_{,xx}$ in the first variation of potential energy (see APPENDIX C). The effective bending moment for the 'smeared' shell is,

$$\begin{aligned} M_x^{sm} = & -D\{(1+\beta_s)W_{,XX} + vW_{YY} \\ & - \left(\frac{e_s}{D}\right)\left[\left(1-A_{xy}\right)F_{,YY} - A_{xx}F_{,XX}\right. \\ & \left. - B_{xx}W_{,XX} - B_{xy}W_{,YY}\right]\} \end{aligned} \tag{5.26}$$

Thus, the boundary condition $M_x^{sm}(X=0)=0$ can be written in non-dimensional form,

$$\begin{aligned}&[1+\beta_s+12(1-v^2)\gamma_s\bar{B}_{xx}]w_{,xx}\,(x=0)\\&\quad-12(1-v^2)\gamma_s\big[\big(1-A_{xy}\big)f_{,yy}\,(x=0)\\&\quad-A_{xx}f_{,xx}\,(x=0)\big]=0\end{aligned}\tag{5.27}$$

The in-plane axial boundary condition is $U_{,YY}\,(X=0)=0$ or $F_{,YY}\,(X=0)=0$ and the in-plane circumferential boundary condition is $V_{,Y}\,(X=0)=0$.

Further more $U_{,YY}\,(X=0)=0$ can be obtained from equation (C.2),

$$2\varepsilon_{xy,Y}-\varepsilon_{y,X}=U_{,YY}-\left(\frac{W_{,X}}{R}\right)+W_{,X}\,W_{,YY}\tag{5.28}$$

so that the boundary condition $U_{,YY}\,(X=0)=0$ becomes,

$$\begin{aligned}&\big(vA_{xx}-A_{yx}\big)f_{,xxx}\,(x=0)\\&+\big[-2(1+v)+vA_{xy}-A_{yy}\big]f_{,xyy}\,(x=0)\\&+\big(v\bar{B}_{xx}-\bar{B}_{yx}\big)w_{,xxx}\,(x=0)\\&+\big(v\bar{B}_{xy}-\bar{B}_{yy}\big)w_{,xyy}\,(x=0)+w_{,x}\,(x=0)=0\end{aligned}\tag{5.29}$$

Finally, using $V_{,Y} = \varepsilon_y - \left(\frac{W}{R}\right) - \frac{1}{2}\left(W_{,y}\right)^2$, the $V_{,Y}(X=0) = 0$ boundary condition is (using $W(X=0) = 0, W_{,Y}(X=0) = 0, W_{,YY}(X=0) = 0$),

$$\begin{aligned} &\left(A_{yx} - vA_{xx}\right) f_{,xx}(x=0) \\ &+ \left(A_{yy} - vA_{xy}\right) f_{,yy}(x=0) \\ &+ \left(\bar{B}_{yx} - v\bar{B}_{xx}\right) w_{,xx}(x=0) = 0 \end{aligned} \tag{5.30}$$

where the non-dimensional quantities $(A_{xx}, A_{xy}, A_{yx}, A_{yy})$ and $\left(\bar{B}_{xx}, \bar{B}_{xy}, \bar{B}_{yx}, \bar{B}_{yy}\right)$ are defined by Hutchinson and Amazigo [40], which are listed in Table 5.1.

$A_{xx} = \frac{v\alpha_s}{\alpha_0}$	$A_{yy} = \frac{v\alpha_r}{\alpha_0}$	$A_{xy} = \frac{1+\alpha_r}{\alpha_0}$	$A_{yx} = \frac{1+\alpha_s}{\alpha_0}$
$\bar{B}_{xx} = \frac{\alpha_s\alpha_s(1+\alpha_r)}{\alpha_0}$	$\bar{B}_{yy} = \frac{\alpha_r\alpha_r(1+\alpha_s)}{\alpha_0}$	$\bar{B}_{xy} = \frac{v\alpha_s\alpha_r\gamma_r}{\alpha_0}$	$\bar{B}_{yx} = \frac{v\alpha_r\alpha_s\gamma_s}{\alpha_0}$
$\alpha_0 = (1+\alpha_s)(1+\alpha_r) - v^2\alpha_s\alpha_r$			

Table 5.1 Stiffened cylinder parameters

The above four ordinary differential equations and four boundary conditions at each end of the shell are discretized using the central finite difference scheme (see APPENDIX A). The resulting linear system of equations constitutes an eigenvalue problem which can be solved by using a build-in function in MATLAB or using the inverse power method (see APPENDIX B). The amplitude of the buckling mode is normalized by $[w_c(x) + w_s(x)]^{1/2} = 1$, such that the largest out-of-plane displacement of the buckling mode is unity.

5.3 Second Order Field and Postbuckling Coefficient

5.3.1 Equations for the Second Order Field

Substituting the total displacement w_t and stress function f_t into the governing nonlinear differential equations (5.4) and (5.5), and collecting terms which involve ξ^2, one obtains the equilibrium and compatibility equations for the second order fields, respectively

$$\begin{aligned} L_d(w_{II}) + L_q(f_{II}) + \sigma_a w_{I,xx} + p_a w_{I,yy} - 2\tau_a w_{II,xy} \\ = f_{I,yy}\, w_{I,xx} + f_{I,xx}\, w_{I,yy} - 2 f_{I,xy}\, w_{I,xy} \end{aligned} \tag{5.31}$$

$$L_h(f_{II}) - L_q(w_{II}) = \left(w_{I,xy}\right)^2 - w_{I,xx}\, w_{I,yy} \tag{5.32}$$

Note that instead of using p_c, σ_c and τ_c to calculate the second order field, we replace them by the actual applied load p_a, σ_a and τ_a respectively. This is one step for the Hui's postbuckling method. The actual applied load is defined to be some percent of classical buckling load, for example from 100% to 20% of the classical buckling load λ_c. So the actual applied load $\lambda_a = percent * \lambda_c$, also for each applied load the first order field must be modified like in the General Steps in section 2.2.2 (Note this is different from unstiffened cylinder in previous section which we mentioned as a special case),

$$(\overline{w}_c, \overline{w}_s, \bar{f}_c, \bar{f}_s) = percent * (w_c, w_s, f_c, f_s) \tag{5.33}$$

where $(\overline{w}_c, \overline{w}_s, \bar{f}_c, \bar{f}_s)$ is the first order field of the classical buckling state. Same procedure should be used when calculating the postbuckling b coefficient.

5.3.2 Solve the Second Order Field

Substituting the separable form of the buckling mode w_I and f_I into the right hand side of the above equations, it is clear that the second order fields can be written in the form,

$$w_{II}(x,y) = w^*(x) + w_A(x)\,cos(2\bar{N}y) + w_B(x)sin\,(2\bar{N}y) \tag{5.34}$$

$$f_{II}(x,y) = f^*(x) + f_A(x)\,cos(2\bar{N}y) + f_B(x)sin\,(2\bar{N}y) \tag{5.35}$$

Thus, the second order equations are uncoupled into two sets of ordinary differential equations involving $[w^*(x), f^*(x)]$ and $[w_A(x), w_B(x), f_A(x), f_B(x)]$ respectively. The first set of equilibrium and compatibility equations is,

$$d_{xx}w^*{}_{,xxxx} + q_{xx}f^*{}_{,xxxx} + f^*{}_{,xx} + \sigma_a w^*{}_{,xx} = -\frac{\bar{N}^2}{2}(w_s f_s + w_c f_c)_{,xx} \tag{5.36}$$

$$h_{xx}f^*{}_{,xxxx} - q_{xx}w^*{}_{,xxxx} - w^*{}_{,xx} = \frac{\bar{N}^2}{4}(w_s^2 + w_c^2)_{,xx} \tag{5.37}$$

The second set of four coupled ordinary differential equations is,

$$L_{19} = \frac{\bar{N}^2}{2}(w_{s,xx} f_s - w_{c,xx} f_c + w_s f_{s,xx} - w_c f_{c,xx} - 2w_{s,x} f_{s,x} + 2w_{c,x} f_{c,x}) \tag{5.38}$$

$$L_{20} = \frac{\bar{N}^2}{2}(-w_{c,xx} f_s - w_{s,xx} f_c - w_c f_{s,xx} - w_s f_{c,xx} + 2w_{c,x} f_{s,x} + 2w_{s,x} f_{c,x}) \tag{5.39}$$

$$L_{21} = \frac{\bar{N}^2}{2}((w_{s,x})^2 - (w_{c,x})^2 - w_s w_{s,xx} + w_c w_{c,xx}) \tag{5.40}$$

$$L_{22} = \frac{\bar{N}^2}{2}(-2w_{s,x} w_{c,x} + w_c w_{s,xx} + w_s w_{c,xx}) \tag{5.41}$$

where L_{19}, L_{20}, L_{21}, and L_{22} can be obtained from the left had side of equations (5.22) to (5.25) by replacing $\bar{N}$, w_c, w_s, f_c, f_s by $2\bar{N}$, w_A, w_B, f_A, f_B respectively. Solving the above equation sets by the Gauss Elimination, we can get the second order field.

5.3.3 Equations for the Postbuckling Coefficient

The postbuckling b coefficient (see [40] [81]) is to examine the stability of the system after initial buckling. The structure has stable postbuckling behavior (imperfection-insensitive) if b is positive; and it has unstable postbuckling behavior (imperfection-sensitive) if b is negative. The degree of imperfection sensitivity is measured by the magnitude of the postbuckling b coefficient. The equilibrium path is specified as follow,

$$b\xi^3 + \left[1 - \left(\frac{\lambda_i}{\lambda_c}\right)\right]\xi = \mu\left(\frac{\lambda_i}{\lambda_c}\right) \tag{5.42}$$

where τ is the buckling load of the imperfect system, τ_c is the classical buckling load of the perfect system, and μ is the imperfection amplitude normalized with respect to the total thickness of the cylindrical shell. Let λ_i denote the maximum value of τ when $\mu \neq 0$, Koiter first showed the relation between λ_i and μ is (valid only if $b < 0$),

$$\frac{3\sqrt{3}}{2}\mu\sqrt{-b}\left(\frac{\lambda_i}{\lambda_c}\right) = \left[1 - \left(\frac{\lambda_i}{\lambda_c}\right)\right]^{3/2} \tag{5.43}$$

The b coefficient is defined to be (Budiansky [81], Hui and Du [89]),

$$b = \frac{(C_1 + C_2)}{|D_1|} \tag{5.44}$$

where,

$$C_1 = 2\int_{y=0}^{y_0}\int_{x=0}^{Z_H}\{f_{I,yy}\,w_{I,x}\,w_{II,x} + f_{I,xx}\,w_{I,y}\,w_{II,y} - f_{I,xy}\left(w_{I,x}\,w_{II,y} + w_{I,y}\,w_{II,x}\right)\}dxdy \tag{5.45}$$

$$C_2 = \int_{y=0}^{y_0}\int_{x=0}^{Z_H}\{f_{II,yy}\,(w_{I,x})^2 + f_{II,xx}\left(w_{I,y}\right)^2 - 2f_{II,xy}\,w_{I,x}\,w_{I,y}\}dxdy \tag{5.46}$$

$$D_1 = \bar{N}^2 y_0 \int_{x=0}^{Z_H}\{\frac{1}{2}N^2 p_a(w_c^2 + w_s^2) + \frac{1}{2}\sigma_a[(w_{c,x})^2 + (w_{s,x})^2] + \tau_a N(w_s w_{c,x} - w_c w_{s,x})\}dx \tag{5.47}$$

In the above, $y_0 = 2\pi R/(Rt)^{1/2}$ and the reduced-Batdorf parameter $Z_H = L/(Rt)^{1/2}$.

Note that postbuckling b coefficient is also calculated by using the actual applied load (σ_a, p_a, τ_a). Then the b coefficient should be a function of applied load numerically. In order to compare the Hui's postbuckling method with the Koiter's general theory, we need to get one b coefficient for the Hui's postbuckling method. This is the reason for us to do the least square curve fit. By fitting the knock down curve of the Hui's postbuckling method using equation (5.43) by the least square curve fit technique in the range of imperfection amplitude form 0 to 25 percent of the shell thickness, we can get the improved b coefficient. Then we can use it to compare with the usual b coefficient calculated by the Koiter's general postbuckling theory.

5.4 Result and Discussion

5.4.1 Cases We Concerned in Here

For a stringer and/or ring stiffened cylindrical shell, the stringer and ring parameters (subscripts 's' and 'r' respectively) are the area ratio (α_s, α_r), the out-of plane bending stiffness ratio (β_s, β_r), the eccentricity to skin thickness ratio (γ_s, γ_r) and the torsional rigidity ratio (δ_s, δ_r). Further, the in-plane bending stiffness of the stiffeners is assumed to be negligible. For all the examples in this section, stringers or rings are assumed to be of rectangular shape. In this section, we use two kinds of boundary conditions which are,

$Clamp: w = w_{,x} = U_y = V_y = 0$

$Simply\ Support: w = M_x^{sm} = N_x = V_y = 0$

First, we compare the result of Hui's postbuckling method with the General Koiter's theory by analyzing the postbuckling behavior of stringer stiffened cylindrical shell under axial compression. Second, a parameter variation will be taken on stringer and/or ring stiffened cylindrical shell under torsion using both General Koiter's theory and Hui's postbuckling method. Due to the complexity of parameters which are involved in stringer or ring stiffened cylindrical shells, only three problems involving parameter variations will be considered: (i) prescribing skin thicknesses while keeping stiffeners' dimensions fixed, (ii) prescribing the number of stiffeners while keeping the area ratios α_s and α_r fixed and (iii) prescribing the reduced-Batdorf parameter. The regular b coefficient is just used for comparison purpose, since here we believe the improved b coefficient is much more accurate than regular b coefficient. The variation of Length is from Z_H=5 to 60, and step size is 1.

5.4.2 Stringer Stiffened Cylinder Under Axial Compression

For the stringer stiffened cylinder under axial compression, simply support boundary condition is applied to both ends of the cylinder, in order to compare the result with the paper presented by Huchinsion and Amazigo [40]. The data for Classical buckling load and imperfection-sensitivity of simply supported stringer stiffened cylinders under axial compression in light, medium and heavy stiffening conditions are present in Figure 5.1 to Figure 5.6 respectively. From the Figures, we can see that, both critical load and regular b coefficient are identical to the result presented by Huchinsion and Amazigo [40]. This shows our calculation for the General Koiter's theory is right. From Figure 5.1, for the light stiffening, the classical buckling load decreases rapidly when $Z_H < 15$, then the classical buckling load seems unchanged when Z_H increases. Also, when $Z_H < 12$, the classical buckling load for inside stiffening is larger than that of center stiffening. After that, center stiffening becomes larger than inside stiffening. But the outside stiffening always has the largest classical buckling load. From Figure 5.2, we can see outside stiffening is more unstable than center stiffing, which is more unstable than inside stiffening. But when Z_H increases, the imperfection sensitivity starts to be identical. We can also see, there are always some positive shifting from regular b to improved b, which means the general Koiter's theory always overestimates the imperfection sensitivity. However, when Z_H is small, the difference between regular b and improved b is large. But when the regular b goes to very small, regular b and improved b seems to be converging. So the positive shifting is depending on how large the regular b is. If the regular b is relatively large, the positive shift rate is large. The result shows that, it is very unstable for short outside light stiffening

cylinder. The imperfection sensitivity for the three cases becomes identical for long cylinder, also long cylinder is much more stable than short cylinder.

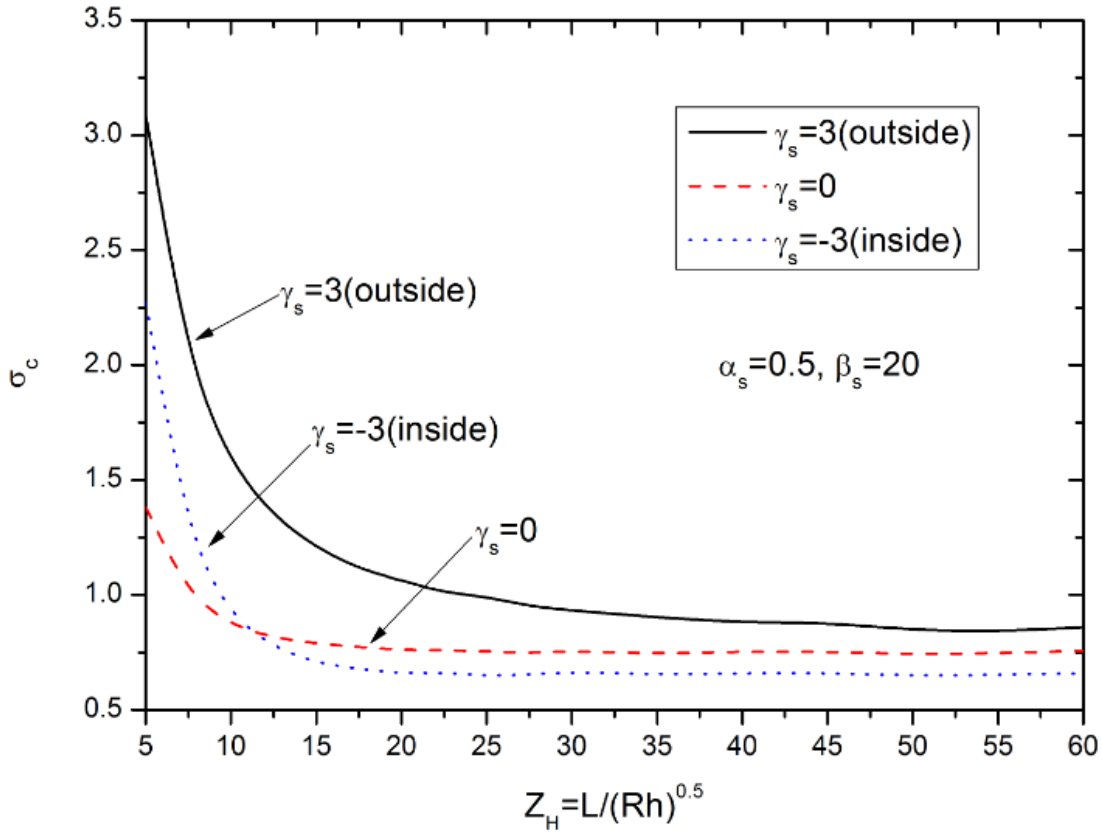

Figure 5.1 Classical buckling load of simply supported, stringer stiffened cylinders under axial compression in light stiffening condition

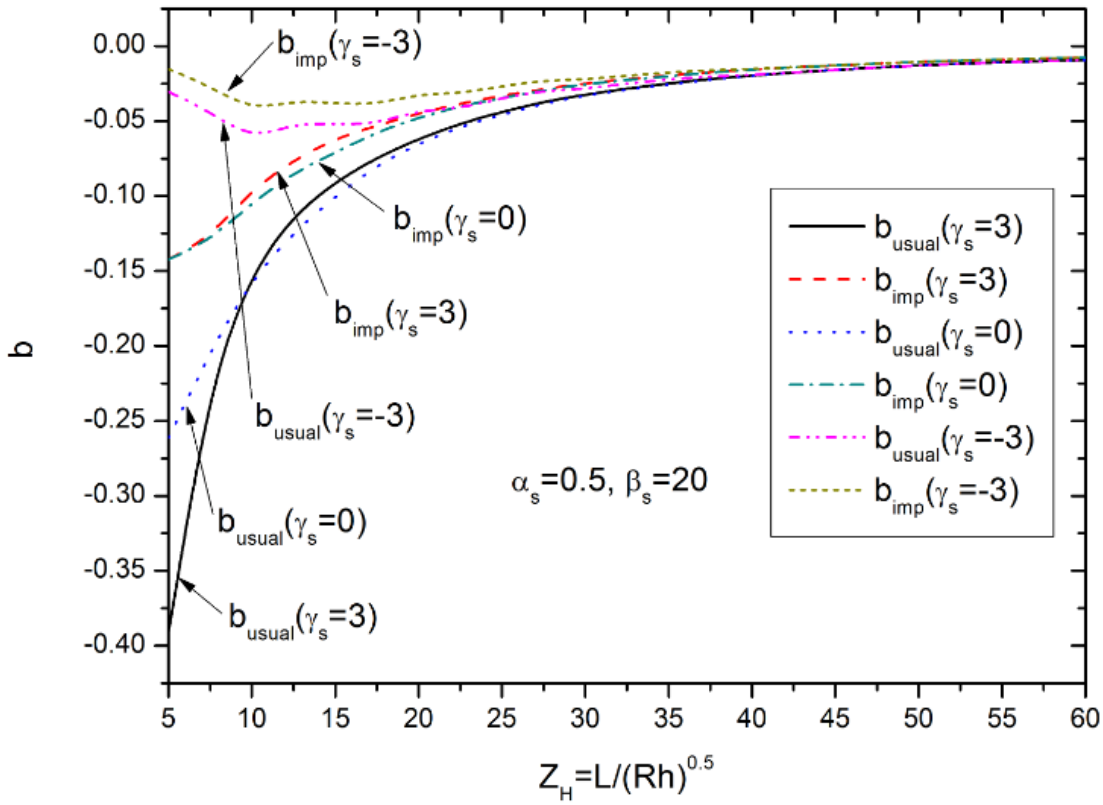

Figure 5.2 Imperfection sensitivity of simply supported, stringer stiffened cylinders under axial compression in light stiffening condition

Figure 5.3 and Figure 5.4 show the classical buckling load and the imperfection sensitivity of medium stiffening cylinder. We can see the classical buckling for medium stiffening cylinder is much higher than light stiffening cylinder. The changing tendency for the classical buckling is similar to light stiffening cylinder, but the classical buckling load for the outside and inside stiffened cylinder is similar for short cylinder when $Z_H < 10$. Again, the classical buckling load for the outside stiffened cylinder is always the largest one. From Figure 5.4, if the regular b coefficient is very negative, then the positive shift rate from regular b to improved b is very large, but if the regular b is close to zero, then the positive shift becomes very small. The reason for this is because, when b is very negative, it means that the structure is very imperfection sensitive, so the difference between classical buckling load and actual applied load is very large. That's why when we calculate the improved b coefficient with the actual applied load, the large positive shift is expected. When regular b coefficient is close to zero, the structure is not much imperfection sensitive, so the difference between classical buckling load and actual applied is very small. That's why the improved b is similar to regular b. By increasing the reduced Batdorf parameter Z_H, the improved b coefficient of outside stiffening cylinder starts close to zero at first and then rapidly changes to about -0.075, and then decreases gradually until it is close to zero. This shows that the imperfection sensitivity of outside stiffening cylinder is sensitive to the shape when the cylinder is short. Similar to light stiffening cylinder, the improved b coefficient is very small for inside stiffening. For the center stiffening, the improved b gradually decreases to almost zero. Again, when the cylinder becomes longer and longer, the structure becomes more stable except inside stiffening which is not sensitive to the reduced Batdorf parameter Z_H.

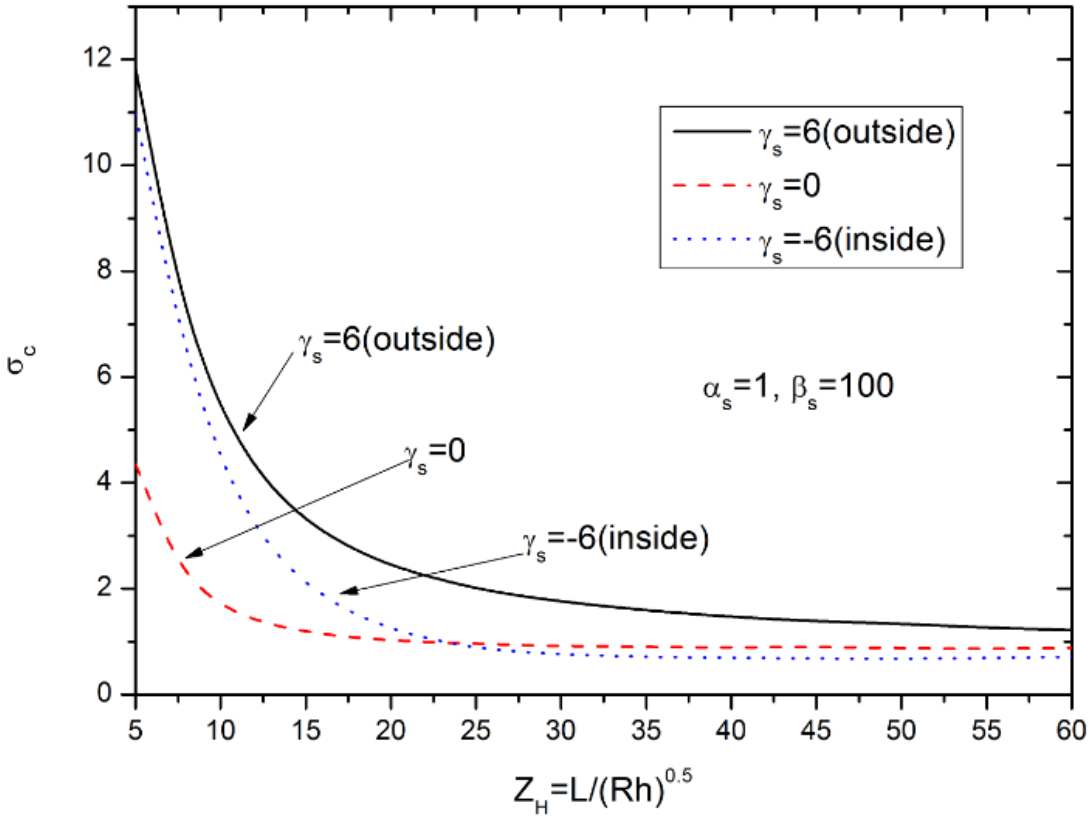

Figure 5.3 Classical buckling load of simply supported, stringer stiffened cylinders under axial compression in medium stiffening condition

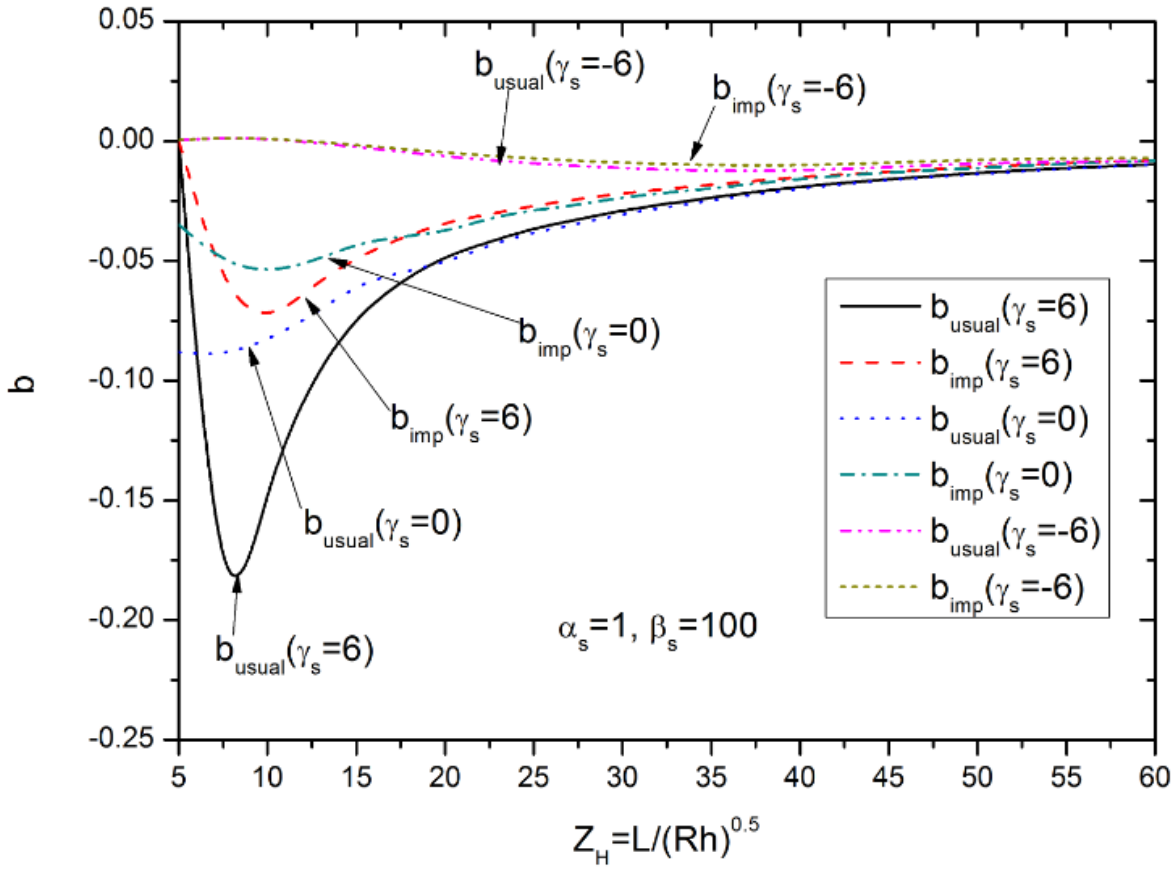

Figure 5.4 Imperfection sensitivity of simply supported, stringer stiffened cylinders under axial compression in medium stiffening condition

Figure 5.5 and Figure 5.6 show the classical buckling load and the imperfection sensitivity of heavy stiffened cylinder. At first, we can see, the classical buckling load is much larger than the previous two cases. When $Z_H < 10$, the classical buckling load for inside and outside stiffening is almost the same. Again, the decreasing tendency of classical buckling load for these three stiffened type are similar to the previous two cases. For the postbuckling b coefficient, we get similar result as we mentioned above, which is the positive shift rate changes with the magnitude of regular b coefficient. Compared with above two cases, the heavy stiffening cylinder is much more stable, since the largest magnitude of improved b is -0.027. Also, we can see for outside stiffening cylinder, the b coefficient is sensitive to the geometry when Z_H is between 10 and 20. For the inside stiffening cylinder, the improve b coefficient is always positive, which means the structure is stable, and imperfection insensitive. From the above three cases, we can make several conclusions: (1) classical buckling load increases when increasing the stiffening level; (2) classical buckling load for outside stiffened cylinder is always the largest one compared with inside and center stiffening; (3) the positive shift rate of regular b coefficient to improved b coefficient is changing with the magnitude of the regular b coefficient. When the magnitude of regular b is large, the change rate is large; otherwise, it is very small if regular b is close to zero; (4) long cylinders are more stable than short cylinders.

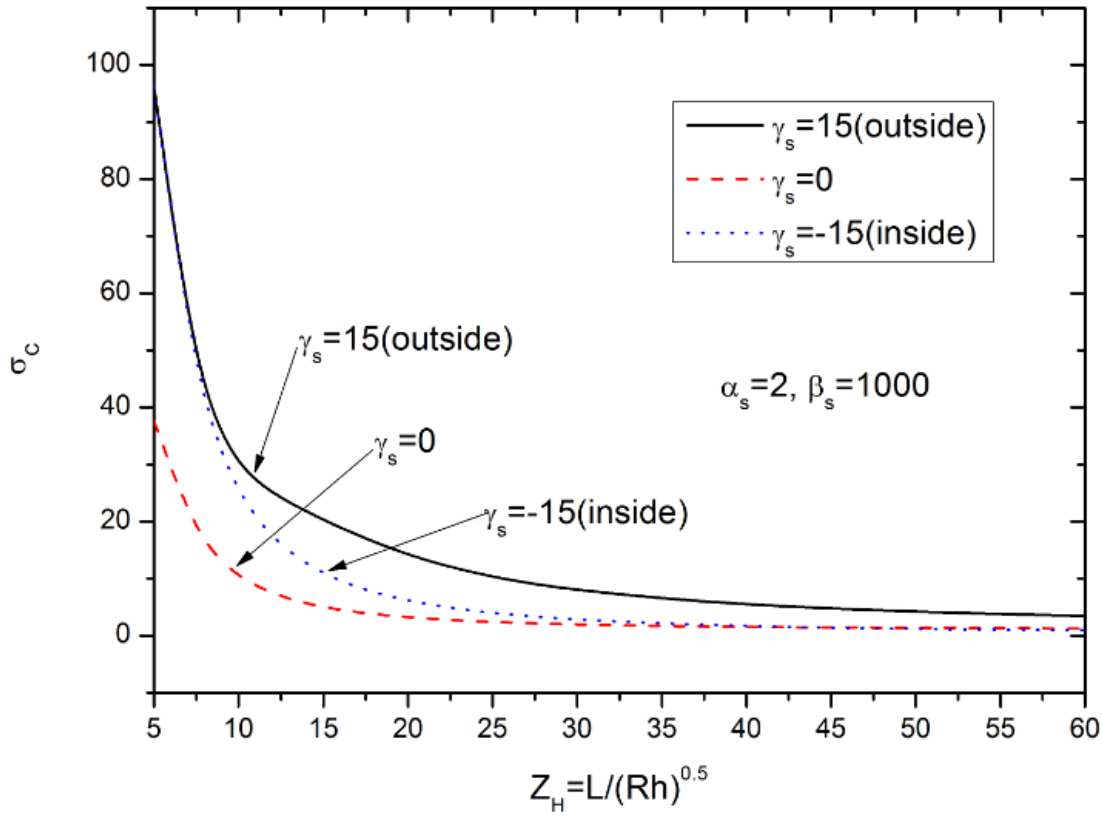

Figure 5.5 Classical buckling load of simply supported, stringer stiffened cylinders under axial compression in heavy stiffening condition

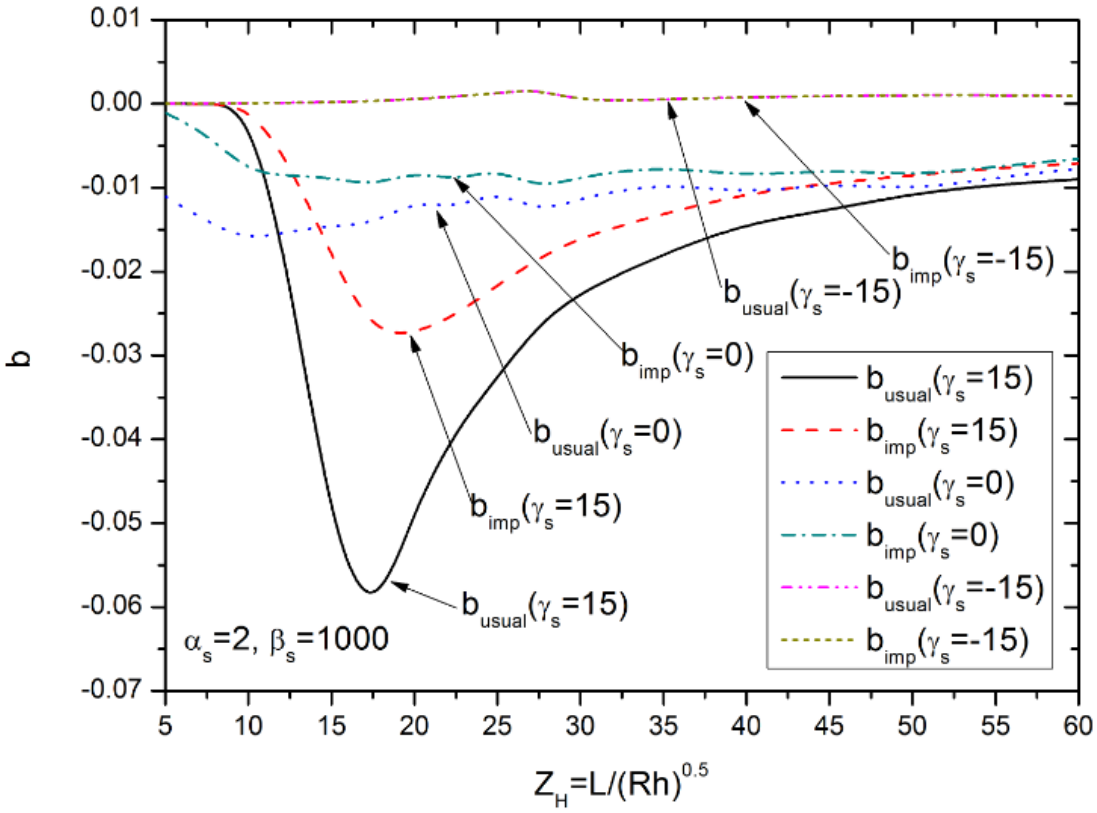

Figure 5.6 Imperfection sensitivity of simply supported, stringer stiffened cylinders under axial compression in heavy stiffening condition

5.4.3 Parameter Variation of Stringer/Ring Stiffened Cylinder Under Torsion

For the second problem, parameter variation is taken on stringer and/or ring stiffened cylindrical shell under torsion using both General Koiter's theory and Hui's postbuckling method. In this problem, we use both boundary conditions: clamp and simply support. As we mentioned above, three cases are considered in here.

In the first case, we keep the stiffeners' dimensions fixed, and changing the skin thickness. The detailed dimensional data are given in Table 5.2. The torsional buckling loads and the postbuckling b coefficients are also presented in this table. It can be seen that the classical torsional buckling load for a ring stiffened shell is much higher than a stringer reinforced one. All the postbuckling b coefficients including regular b and improve b are found to be very small, and the magnitude of b is smaller for ring stiffened shells than that for stringer stiffened ones. Since all the regular b coefficients are very small, very little positive shifting is found from regular b to improved b. Thus, the sensitivity of the buckling load to unavoidable geometric imperfection is very small. From the point of view of high buckling load and low imperfection-sensitivity, the ring stiffened shell is better than the stringer reinforced one. Also we can see, the torsional rigidity δ_s (which was ignored in Hutchinson and Amazigo's [40] analysis) of the stringers considerably raises the buckling load and also causes some changes of b coefficient (by comparing the shell with $\delta_s = 0$). This is because the stringer is under torsion so that the torsional rigidity is no more negligible. This point is proved by the result of ring stiffened shell. It shows that the influence of the torsional rigidity δ_r to both the buckling load and b coefficient is very small. This is because

the rings are under tension or compression when the cylindrical shell is under torsion, so the torsional rigidity is negligible in such conditions. In the following examples, we always use the results with torsional rigidity.

t	0.02 in	0.0254 in	0.03 in	0.035 in	0.04 in	0.05 in
α_s	1.4324	1.1279	0.9549	0.8185	0.7162	0.5730
β_s	188.0018	89.6820	55.7042	35.0890	23.5002	12.0321
γ_s	6.7500	5.4213	4.6667	4.0714	3.6250	3.0000
δ_s	43.2499	21.1142	12.8148	8.0699	5.4062	2.7680
Z_H	38.8909	34.5101	31.7543	29.3987	27.5000	24.5967
Clamp#1 $w = w_{,x} = U_y = V_y = 0$						
$\tau_c(\delta_s \neq 0)$	0.9568 (N=0.64)	0.7221 (N=0.64)	0.6055 (N=0.69)	0.5282 (N=0.75)	0.4717 (N=0.70)	0.4053 (N=0.78)
$\tau_c(\delta_s = 0)$	0.7039 (N=0.71)	0.5760 (N=0.72)	0.5124 (N=0.69)	0.4592 (N=0.75)	0.4258 (N=0.70)	0.3754 (N=0.78)
$b_{reg}(\delta_s \neq 0)$	-0.0017	-0.0024	-0.0048	-0.0058	-0.0089	-0.0110
$b_{imp}(\delta_s \neq 0)$	-0.0015	-0.0022	-0.0042	-0.0051	-0.0077	-0.0094
$b_{reg}(\delta_s = 0)$	-9.2442e-4	-0.0034	-0.0061	-0.0069	-0.0103	-0.0121
$b_{imp}(\delta_s = 0)$	-7.9944e-4	-0.0030	-0.0053	-0.0060	-0.0088	-0.0103
The following torsional buckling loads and b coefficients are for ring stiffened shells with $(\alpha_s, \beta_s, \gamma_s, \delta_s)$ being replaced by $(\alpha_r, \beta_r, \gamma_r, \delta_r)$.						
$\tau_c(\delta_s \neq 0)$	4.3833 (N=0.28)	3.1411 (N=0.32)	2.5187 (N=0.35)	2.0507 (N=0.37)	1.7212 (N=0.40)	1.2946 (N=0.45)
$\tau_c(\delta_s = 0)$	4.2327 (N=0.28)	3.0499 (N=0.32)	2.4541 (N=0.35)	2.0039 (N=0.37)	1.6858 (N=0.40)	1.2724 (N=0.45)
$b_{reg}(\delta_s \neq 0)$	-2.0459e-4	-3.5745e-4	-5.2358e-4	-7.4767e-4	-0.0010	-0.0017
$b_{imp}(\delta_s \neq 0)$	-1.9323e-4	-3.3755e-4	-4.9439e-4	-6.9328e-4	-9.4316e-4	-0.0015
$b_{reg}(\delta_s = 0)$	-2.1361e-4	-3.7004e-4	-5.3934e-4	-7.6730e-4	-0.0010	-0.0017
$b_{imp}(\delta_s = 0)$	-2.0166e-4	-3.4932e-4	-5.0913e-4	-7.1129e-4	-9.6504e-4	-0.0016

Table 5.2 Data for a stringer or ring stiffened cylindrical shell under torsion changing with shell thickness with the following parameters being held fixed, $R = 4$ in, $L = 11$ in, $E = E_s = 4 \times 10^5$ psi, $v = 0.4$, $M_s = 24$, $A_s = 0.03$ in^2, $Q_s = 0.25$ in

The shell parameters in the second case are given in Table 5.3. By keeping the area ratio constantly being 0.7, the number of stiffeners increases, the eccentricity ratio and the torsional rigidity parameter both decrease. Result shows that the classical buckling load is decreasing when the number of stiffener increases. Again, a ring stiffened shell has a much higher torsional buckling load than a stringer reinforced one. This advantage of ring over stringer stiffened shell is offset by the improved postbuckling b coefficient. From the table, we can see the first four improved b coefficients of stringer stiffened shell are positive compared with the ring stiffened ones which are negative improved b coefficients. This means, although the buckling load for the stringer stiffened shell is much lower than the ring stiffened shell, in some conditions, the stringer stiffened shell is a postbuckling stable structure under torsion, compared with all the ring stiffened shell is postbuckling unstable structure under torsion. Note that, when the structure is postbuckling stable, there is almost no difference between regular b coefficient and improved b coefficient. Although the ring stiffened shell has all negative improved b coefficients, it is always very small. So when the stringer stiffened shell changes to a postbuckling unstable structure (negative b coefficient), the advantage disappears. It is also interesting to note that the decreasing rate of the improved b coefficient of stringer stiffened shell is much more than the ring stiffened shell by increasing the number of stiffener.

M_s	6	8	10	12	14	16	18
a	1.2217	0.9163	0.733	0.6109	0.5236	0.4581	0.4072
β_s	351.0392	197.4757	126.3638	87.7814	64.4819	49.3528	38.9948
γ_s	12.7170	9.6630	7.8300	6.6090	5.7360	5.0810	4.5720
δ_s	4.5389	4.4392	4.3392	4.2400	4.1400	4.0398	3.9403
M_s	20	22	24				
a	0.3665	0.3332	0.3054				
β_s	31.5909	26.1125	21.9346				
γ_s	4.1650	3.8320	3.5540				
δ_s	3.8411	3.7422	3.6427				
Clamp#1 $w = w_{,x} = U_y = V_y = 0$							
M_s	6	8	10	12	14	16	18
τ_c	1.5419 (N=0.89)	1.0745 (N=0.78)	0.8245 (N=0.78)	0.6806 (N=0.78)	0.5884 (N=0.78)	0.5199 (N=0.67)	0.4699 (N=0.67)
b_{reg}	0.0242	0.0102	0.0057	0.0022	-5.4762e-4	-0.0052	-0.0064
b_{imp}	0.0246	0.0103	0.0057	0.0022	-4.9642e-4	-0.0045	-0.0055
M_s	20	22	24				
τ_c	0.4324 (N=0.67)	0.4034 (N=0.67)	0.3802 (N=0.67)				
b_{reg}	-0.0074	-0.0082	-0.0088				
b_{imp}	-0.0064	-0.0071	-0.0077				
The following torsional buckling loads and b coefficients are for ring stiffened shells ($\beta_s, \gamma_s, \delta_s$) being replaced by ($\beta_r, \gamma_r, \delta_r$).							
M_r	6	8	10	12	14	16	18
τ_c	5.0049 (N=0.22)	4.3501 (N=0.34)	3.7915 (N=0.34)	3.2818 (N=0.34)	2.7630 (N=0.34)	2.3952 (N=0.34)	2.1236 (N=0.35)
b_{reg}	-5.5307e-6	-1.9835e-5	-4.1819e-5	-4.2214e-4	-4.8256e-4	-5.5175e-4	-6.5928e-4
b_{imp}	-5.2525e-6	-1.9466e-5	-4.0152e-5	-3.9813e-4	-4.5538e-4	-5.2060e-4	-5.7615e-4
M_r	20	22	24				
τ_c	1.9160 (N=0.34)	1.7529 (N=0.34)	1.6217 (N=0.34)				
b_{reg}	-6.9384e-4	-7.6732e-4	-8.9300e-4				
b_{imp}	-6.4223e-4	-7.0974e-4	-7.7905e-4				

Table 5.3 Data for a stringer or ring stiffened cylindrical shell under torsion changing with stiffener number with $Z_H = 31.3050$ and $(\alpha_s = 0.7, \alpha_r = 0.7)$ and being held fixed. ($E = E_s = 4 \times 10^5$ psi, $v = 0.4, R = 4, L = 14, h = 0.05, b = 0.12$), a is the height of stiffener

Finally, in the third case, the following outside stiffened stringer parameters are held fixed: $\alpha_s = 1.0, \beta_s = 63.9687, \gamma_s = 4.8633$ and $\delta_s = 5.7150$. We will use two types of boundary conditions which are: Clamp and Simply Support. The reduced-Batdorf parameter is permitted to vary. Note that as the reduced-Batdorf parameter increases, there are three possibilities: the shell becomes longer, the radius gets smaller or the thickness of the shell becomes smaller. For ring stiffened cylindrical shells without stringer, the parameters are the same as that of the stringer-stiffened shells except that the subscript 's' is replaced by 'r'. Also, the 'simultaneous' stiffening of both stringers and rings for a reinforced cylindrical shell is considered. The volume of stingers and rings is the same, and the total volume ratio of stiffener is the same as stringer only or ring only stiffened cylindrical shells as mentioned before. So the parameter should be:

$$(\alpha_s, \alpha_r) = 0.5, (\beta_s, \beta_r) = 7.9962, (\gamma_s, \gamma_r) = 2.6817 \text{ and } (\delta_s, \delta_r) = 2.2675.$$

Figure 5.7 and Figure 5.8 show the classical buckling load and Imperfection sensitivity of stiffened cylinders under torsion with clamp boundary condition varying by reduced-Batdorf parameter. We can see when Z_H is small (Z_H <12), the buckling load for the stringer stiffened shell is larger than the ring stiffened shell. The 'simultaneous' stiffened shell is somewhere sitting between them. But when Z_H goes large (Z_H >12), which means the shell become longer, the buckling load for the stringer stiffened shell becomes much smaller than the ring stiffened one. Again, the 'simultaneous' one is in between. For the postbuckling b coefficient, we can see the stringer stiffened one is positive (stable) when Z_H is less than 24. The regular b and improved b is the same value when they are positive, comparing with

the ring stiffened one, which is negative (unstable) for all Z_H. Since the magnitude of regular b is very small, the difference between improved b and regular b is also small. Again, the 'simultaneous' one is between them, which is positive when $Z_H<9$. But when $Z_H>25$, the improved b coefficient goes much negative than both ring stiffened one and 'simultaneous' one. So combining the buckling load and improved b coefficient, we find that when $Z_H<10$, stinger stiffened one is better than 'simultaneous' one, which is better than ring stiffened one. When $10<Z_H<25$, if the buckling load is critical, then ring stiffened one is better than stringer stiffened one, which is better than 'simultaneous' one; if the improved b coefficient is the critical issue, then stringer stiffened one is better than ring stiffened one, which is better than 'simultaneous' one. For $Z_H>25$, the ring stiffened one is better than 'simultaneous' one, which is better than ring stiffened one.

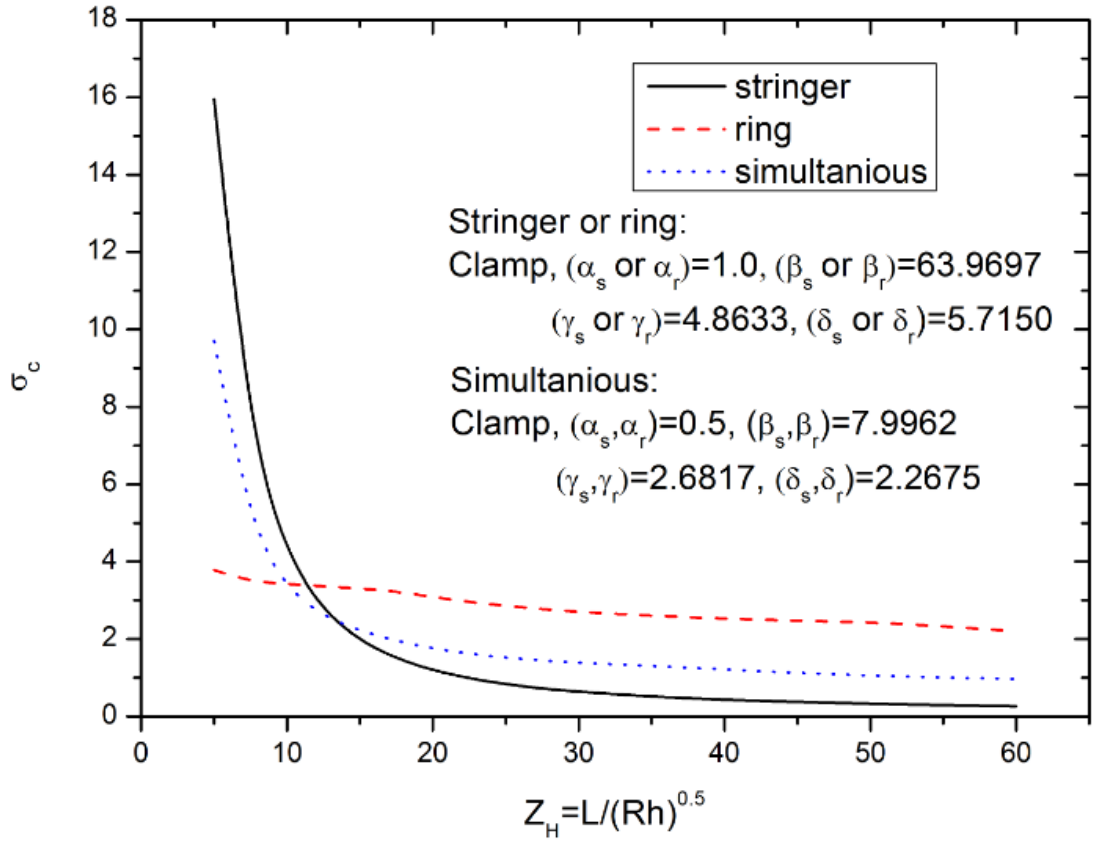

Figure 5.7 Classical buckling load of stiffened cylinders under torsion with clamp boundary condition

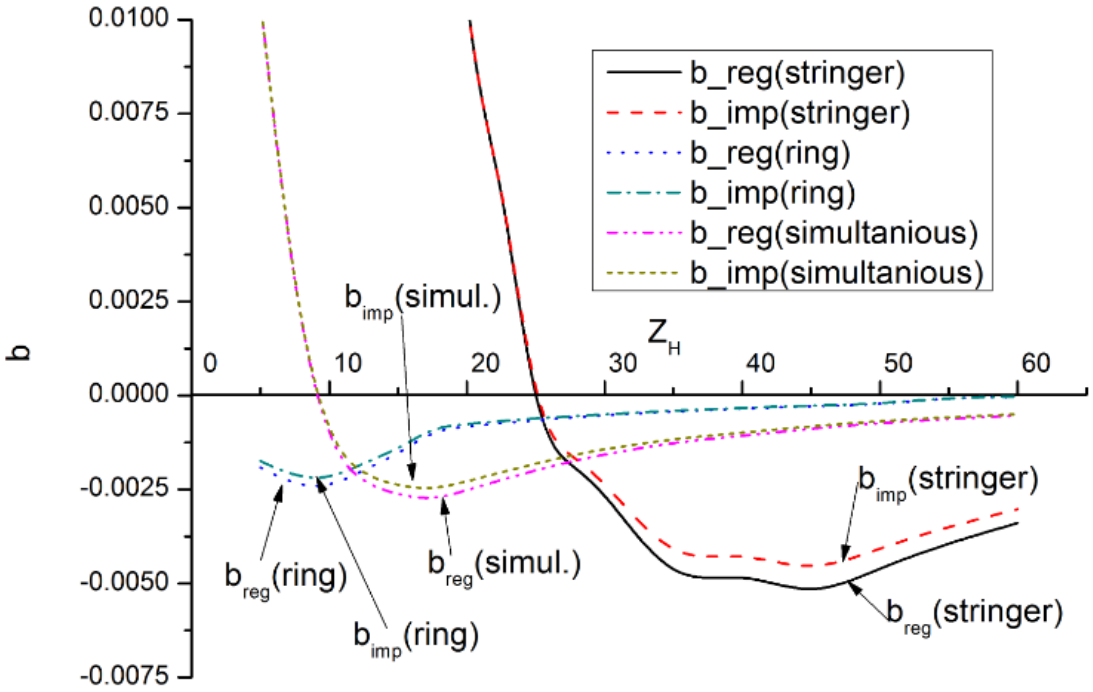

Figure 5.8 Imperfection sensitivity of stiffened cylinders under torsion with clamp boundary condition

Figure 5.9 and Figure 5.10 show the classical buckling load and Imperfection sensitivity of stiffened cylinders under torsion with simply support boundary condition varying with reduced Batdorf parameter. Since the Simply Support is much weaker than clamp boundary condition, the buckling load for stringer and 'simultaneous' reinforcement types are much lower than the clamp condition mentioned above, but the ring stiffened one did not decrease that much. From the two boundary conditions, we can see the change of buckling load for the ring stiffened one is very small compared with the other two reinforce types. Also the buckling load decreases very slowly when the shell becomes longer. In this case, the improved b coefficient for both ring and 'simultaneous' stiffened cylinders are always negative through the whole range of Z_H. When $Z_H<14$, the improved b coefficient for stringer stiffened cylinder is positive (stable). When $Z_H>17$, the improve b coefficient is more negative than the other two stiffening types. Again, because of small regular b coefficient, the difference between improved b and regular b is very small. So, here we can conclude: for pure torsional buckling of cylindrical shell, the buckling load for the ring stiffened cylindrical shell is not sensitive to the boundary conditions and the length change of cylindrical shell.

The improved b coefficient for stringer stiffened shell under Simply Support boundary condition decreases faster than Clamp case. It becomes negative before $Z_H=14$. The improved b coefficient for 'simultaneous' stiffened cylinder is much more different than Clamp one since it is always negative. Also the b coefficient for 'simultaneous' one is always smaller than the ring stiffened one under Simply Support boundary condition. So, in Simply Support boundary condition, when $Z_H<9$, Stinger stiffened one is better than 'simultaneous' one, which is better than ring stiffened one. When $9<Z_H<14$, if the buckling load is critical, then

ring stiffened one is better than stringer stiffened one, which is better than 'simultaneous' one. If the b coefficient is the critical issue, then stringer stiffened one is better than ring stiffened one, which is better than 'simultaneous' one. For Z_H>14, the ring stiffened one is better than 'simultaneous' one, which is better than ring stiffened one.

For the improved b coefficient for stringer stiffened cylinder, we find that the curve is some kind zigzag. This is because of the changing of mode number. Each zigzag represents an increase of one mode. Since we are changing the length of cylinder, once the length increases to a certain amount which can reach the minimum eigenvalue at higher mode, then the shape of buckling mode will change and this will directly influence the postbuckling b coefficient.

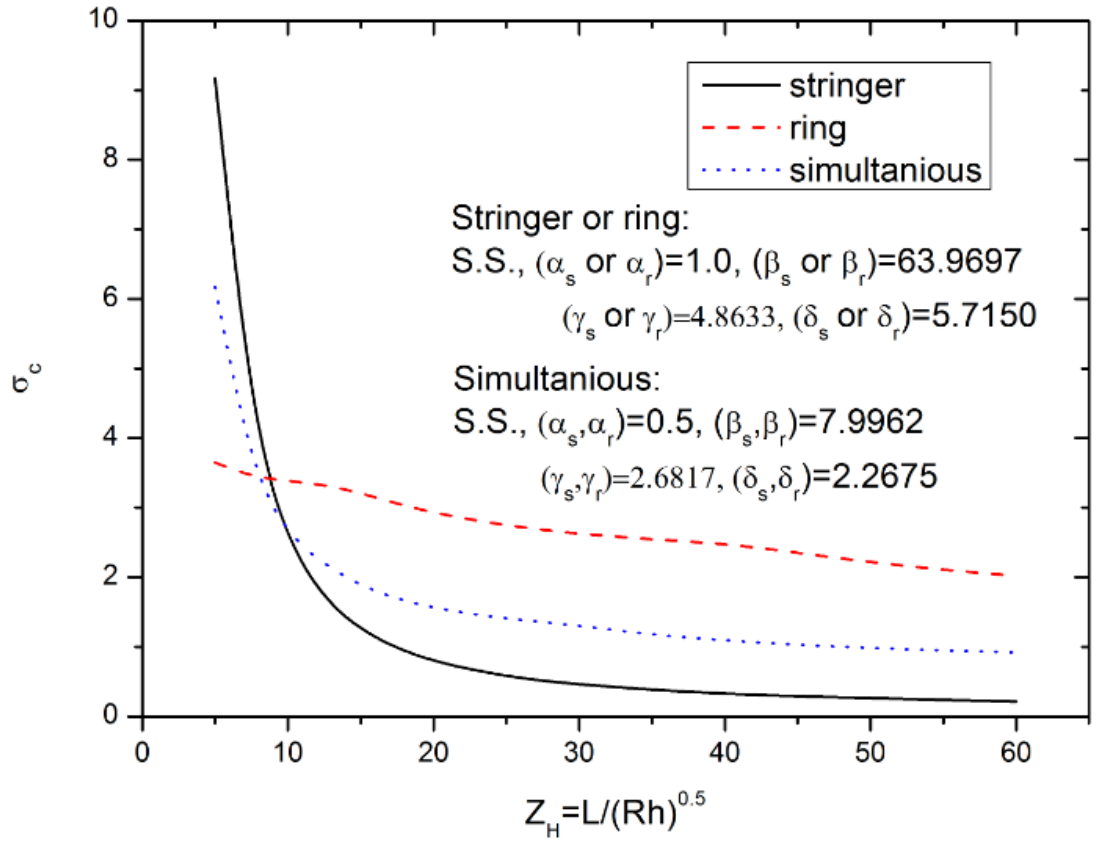

Figure 5.9 Classical buckling load of stiffened cylinders under torsion with simply support boundary condition

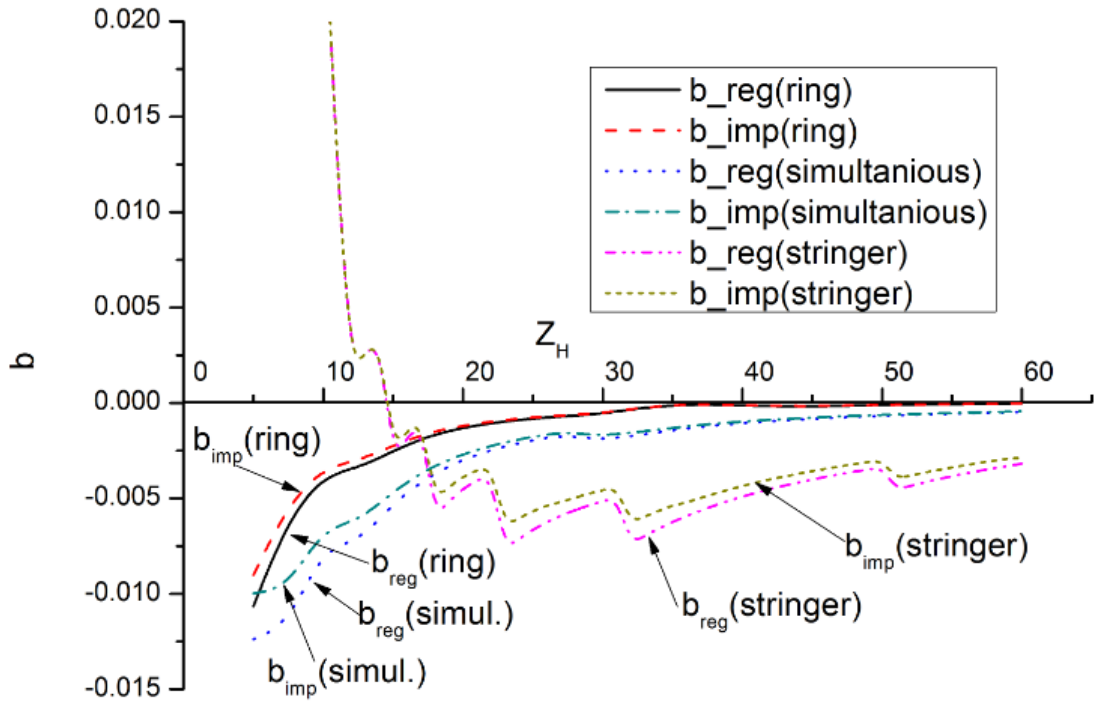

Figure 5.10 Imperfection sensitivity of stiffened cylinders under torsion with simply support boundary condition

For comparison purposes, we reproduce the torsional buckling loads of isotropic homogeneous cylindrical shells analyzed by Budiansky [81] by setting $(\alpha_s, \alpha_r) = (\beta_s, \beta_r) = (\gamma_s, \gamma_r) = (\delta_s, \delta_r) = 0$. Then compare it with the buckling loads of stringer stiffened cylindrical shells under Clamp boundary condition. The total volume of isotropic homogeneous cylindrical shell and stringer stiffened cylindrical shells is the same, so the stiffener parameters are chosen to be $\alpha_s = 1.0, \beta_s = 63.9697, \gamma_s = 4.8633$ and $\delta_s = 5.7150$ and the result is showed in Figure 5.11 and Figure 5.12. From the result we can see the buckling load for stringer stiffened shell is always larger than the unstiffened one. Especially when Z_H<20, the buckling load of stringer stiffened shell is at least 2 times larger than unstiffened one. Also for the b coefficient, the unstiffened shell is always negative, but the b coefficient for stringer stiffened shell is positive before Z_H=25. Furthermore, even when it goes to negative, it is always larger than unstiffened one. So we can conclude the stringer stiffened cylindrical shell is always better than unstiffened shell in torsional buckling.

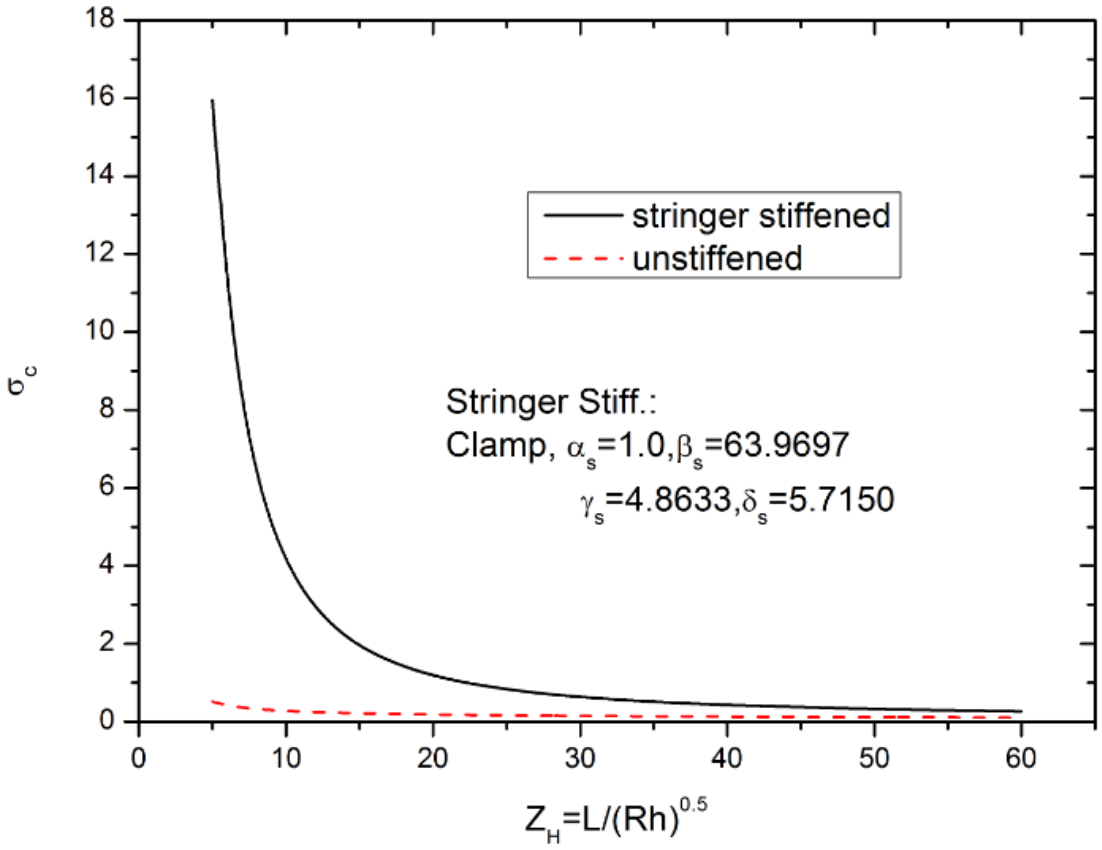

Figure 5.11 Classical buckling load of stringer stiffened cylinder and unstiffened cylinder under torsion with clamp boundary condition

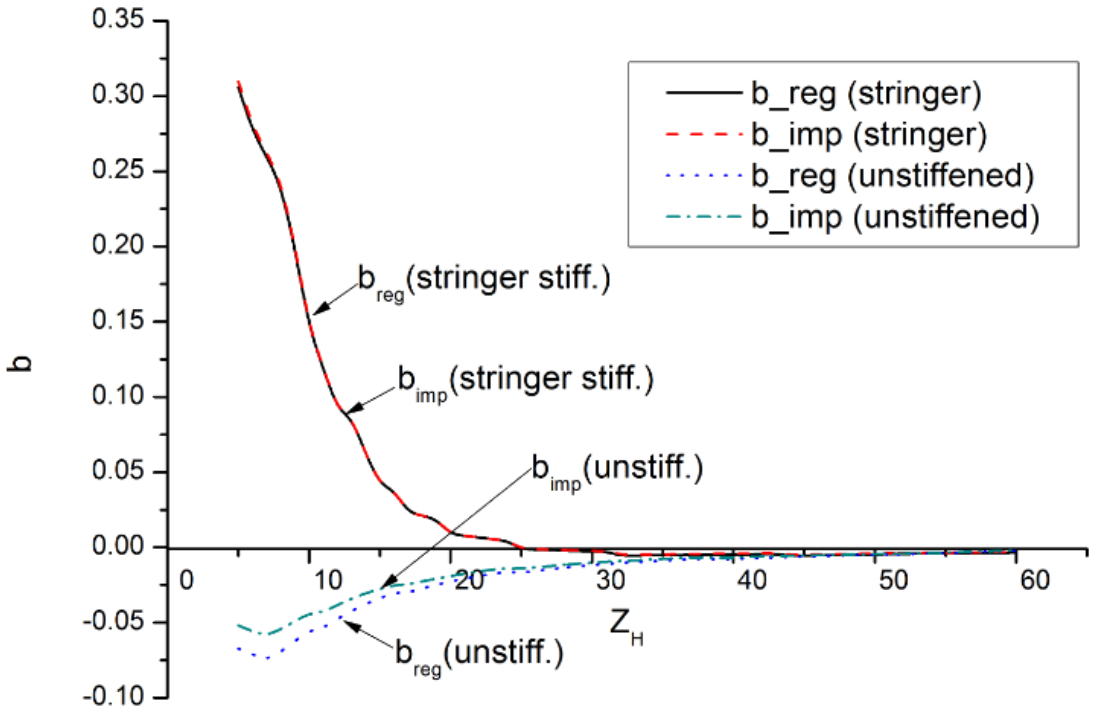

Figure 5.12 Imperfection sensitivity of stringer stiffened cylinder and unstiffened cylinder under torsion with clamp boundary condition

5.5 Conclusion

Postbuckling and imperfection sensitivity of stringer stiffened cylinder under axial compression and the torsional buckling and initial postbuckling behavior of out-side stringer and/or ring-stiffened cylindrical shells under different boundary conditions have been examined using Hui's postbuckling method. For stringer stiffened cylinder under axial compression, we found that the short cylinder is much unstable than the long cylinder. The positive shift rate from regular b coefficient to improved b coefficient depends on the magnitude of regular b coefficient. If the regular b coefficient is more negative, the positive shift is more significant. When the structure is imperfection insensitive (positive b coefficient), then there is no difference between regular b and improved b. Consider the torsional buckling and postbuckling of stringer/ring stiffened cylinder, the magnitude of b coefficient is always very small, so the positive shifting of regular b to improved b is also very small. In all cases, it is found that ring-stiffened shells are relatively insensitive to the two boundary conditions compared with other two types of reinforcements. Also, ring-stiffened shells are more effective than others for long shells. For short shells, if the boundary conditions are important, the stringer stiffened shells are more effective than the ring-stiffened one, and the 'simultaneous' one usually sits in the middle. This observation is generally valid in terms of the two criteria of having high buckling load and low imperfection-sensitivity. Nevertheless, stiffened shells are more effective against torsion than unstiffened equivalent-weight shells. It appears that an optimum design for torsional buckling of cylindrical shell would involve ‘simultaneous’ ring- and stringer-reinforced stiffeners within a certain range of the reduced-Batdorf parameter.

CHAPTER 6

SUMMARY AND FUTURE WORKS

6.1 Summary

This research is the first time to verify the Hui's postbuckling method with the finite element commercial software ABAQUS, and also it is the first time to apply this method to different kinds of closed cylindrical shells. Closed cylindrical shell is heavily used in the industry. In this research unstiffened cylinder, laminate cylinder and stiffened cylinders are considered.

Koiter's general theory has a significant deficiency: the theory is valid only when the imperfection is few percent of the shell thickness. This deficiency makes the Koiter's general theory not practical, because in the industry the imperfection is usually out of its valid range. In the industry, people usually use the commercial finite element software such as ABAQUS and ANSYS. These softwares are powerful, but expensive and need lots of computational time. Hui's postbuckling method can increase the valid region more than 200% compare with Koiter's general theory, which makes it more practical. But before this research, people do not know what is the valid region for the Hui's postbuckling method, and also how much it will improve compared with the Koiter's general theory.

For unstiffened cylindrical shells, the Hui's postbuckling method fits the finite element result very well up to the imperfection is about 40% of the shell thickness, which is much better than Koiter's general theory. And also we find the Koiter's general theory significantly overestimates the imperfection sensitivity of the unstiffened cylinders. This is because the unstiffened cylinder is a very unstable structure.

For antisymmetric cross-ply laminate cylindrical shells, the valid region for the Hui's postbuckling method varies from case to case. But all the cases show that the Hui's postbuckling method is much better than Koiter's general theory. Again, it shows that Koiter's general theory overestimates the imperfection sensitivity. But the positive shift of b coefficient of Hui's postbuckling for laminate cylindrical shells is not as much as the unstiffened one. This is because the laminate cylindrical shell is more stable than the unstiffened cylindrical shell. Also we find out that the change of the imperfection sensitivity of the laminate cylinders by increasing the reduced Batdorf parameter is getting smaller.

For stringer and ring stiffened cylindrical shells, they are very stable compared with the above two. That is the reason for the difference between Koiter's general theory and Hui's postbuckling method is very small. The result of stiffened cylindrical shell under torsion shows that when the structure is stable, there is no difference between Koiter's general theory and Hui's postbuckling method. But once the structure becomes unstable, there is always a small positive shift of Hui's postbuckling method compared with the Koiter's general theory. Not like the laminate cylinders, the stiffened cylinder will become more and more stable

when the reduced Batdorf parameter increases. So from this case, we know that the difference between Hui's postbuckling method and Koiter's general theory becomes smaller and smaller when the structure gets more and more stable. Furthermore, when the structure is imperfection insensitive, the Hui's postbuckling method and Koiter's general theory give the same result.

Generally speaking, in this research, we successfully compared the Hui's postbuckling method with Koiter's general theory and ABAQUS result. Moreover, this is the first time to point out the valid region for Hui's postbuckling method, and also the first time to apply the Hui's postbuckling method to closed cylindrical shells. The result demonstrates that Hui's postbuckling method has much better valid region compared with Koiter's general theory, and also demonstrates that the Koiter's general theory always overestimates the imperfection sensitivity of a structure.

Since Hui's postbuckling has improved a lot compared with Koiter's general theory, it makes this improved method more practical. Compared with ABAQUS, although Hui's postbuckling can only solve the problem with imperfection which is identical to the first buckling mode, the time consuming for Hui's postbuckling method is much lesser than ABAQUS. It is more than 20 times faster than finite element method. This make Hui's postbuckling method an ideal method for the optimization and preliminary design.

6.2 Suggestion for Future Works

Since this research demonstrates that correctness of Hui's postbuckling method, and shows that the valid region for this method is much better than Koiter's general theory, it opens a way to do several kinds of future research: first, we can reevaluate all the papers in the past which were using Koiter's theory; second, we can do some optimization depending on Hui's postbuckling method; last but not least, we can explore this method to be valid for other imperfection types.

APPENDIX A

FINITE DIFFERENCE METHOD

The finite difference method is one of the most often used numerical methods of solving differential equations which comes from the minimization of functional. This method is superior to the problem here, since we reduced the PDEs into ODE sets, due to its simplicity, guaranteed convergence for sufficiently small step size and efficiency in terms of computation time.

This section aims to provide a typical example of a buckling problem to be solved using the central finite difference scheme. The resulting eigenvalue problems and linear equations are solved by highly efficient MATLAB functions; also you can solve it using inverse power method and Gauss elimination method with some free program code. Moreover, for simplicity, only ordinary differential equations are considered as they are of primary concern in this thesis and extensions to partial differential equations should be relatively straight forward.

Here we are concerning the derivative up to 4th order. Then the formulas for the central difference of the derivatives of out-of-plane displacement are,

$$
\begin{aligned}
w_{,yyyy} &= \frac{1}{\Delta x^4}(w_{i+2} - 4w_{i+1} + 6w_i - 4w_{i-1} + w_{i-2}) \\
w_{,yyy} &= \frac{1}{2\Delta x^3}(w_{i+2} - 2w_{i+1} + 2w_{i-1} - w_{i-2}) \\
w_{,yy} &= \frac{1}{\Delta x^2}(w_{i+1} - 2w_i + w_{i-1}) \\
w_{,y} &= \frac{1}{2\Delta x}(w_{i+1} - w_{i-1})
\end{aligned}
\tag{A.1}
$$

where Δx is the finite difference step size.

So the governing equation such as equation (3.12) to (3.15) which can be discretize by the above formula and we will get,

$$
\begin{aligned}
&(k1\, w_{ci-2} + k2\, w_{ci-1} + k3\, w_{ci} + k2\, w_{ci+1} + k1\, w_{ci+2}) \\
&\quad + (k4\, f_{ci-1} + k5\, f_{ci} + k4\, f_{ci+1}) \\
&\quad + \sigma k6(w_{ci-1} + 2w_{ci} + w_{ci+1}) = 0
\end{aligned}
\tag{A.2}
$$

$$
\begin{aligned}
&(k1\, w_{si-2} + k2\, w_{si-1} + k3\, w_{si} + k2\, w_{si+1} + k1\, w_{si+2}) \\
&\quad + (k4\, f_{si-1} + k5\, f_{si} + k4\, f_{si+1}) \\
&\quad + \sigma k6(w_{si-1} + 2w_{si} + w_{si+1}) = 0
\end{aligned}
\tag{A.3}
$$

$$
\begin{aligned}
&(k7\, f_{ci-2} + k8\, f_{ci-1} + k9\, f_{ci} + k8\, f_{ci+1} + k7\, f_{ci+2}) \\
&\quad + (k10\, w_{ci-1} + k11\, w_{ci} + k10\, w_{ci+1}) = 0
\end{aligned}
\tag{A.4}
$$

$$
\begin{aligned}
&(k7\, f_{si-2} + k8\, f_{si-1} + k9\, f_{si} + k8\, f_{si+1} + k7\, f_{si+2}) \\
&\quad + (k10\, w_{si-1} + k11\, w_{si} + k10\, w_{si+1}) = 0
\end{aligned}
\tag{A.5}
$$

We can easily see that the above equations can be rearranged as a general eigenvalue problem,

$$(A - \sigma B)x = 0 \tag{A.6}$$

Such eigenvalue problem can be solved by the build in function ("[X V]=eig(A,B)", where X is the eigenvalues and V is the eigenvectors) in MATLAB or Shifted Inversed Power Method (see APPENXID B).

The mesh convergence also should be checked in here, to make sure the best computation efficiency. In this research we are using 121 nodes along the length of the cylinders. The following figure shows the grid independency study.

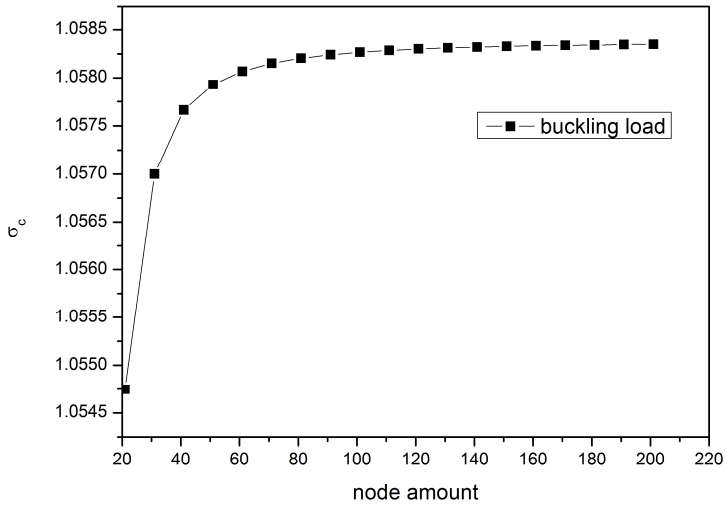

Figure A.1 Buckling load versus node amount

APPENDIX B

SHIFTED INVERS POWER METHOD

In the field of mechanical engineering, we can found the eigenvalue problem $Ax = \sigma x$ everywhere, such as buckling, vibration problems. But we usually care about the first few eigenvalues, which are the smallest, second smallest and so on. The eigenvalue problem like this is often solved by the power method which is the most efficient and well documented, and it will not be redeveloped here. The eigenvalue problems in this thesis is the general eigenvalue problem,

$$Ax = \sigma Bx \tag{B.1}$$

where the matrices A and B are real, non-symmetric matrix. We only interest in the smallest real positive eigenvalue and its eigenvector. The shifted inverse power method present by Hui(1983) are used here to find the smallest eigenvalue of the above general eigenvalue problem. For convenient, we will simply introduce the algorithm in here for someone who cannot access the MATLAB.

Take the initial guess of the lower bound of all the eigenvalues,

$$\sigma_{guess} = const. \tag{B.2}$$

Then the general eigenvalue problem can be expressed as follow,

$$Ax = (\sigma + \sigma_{guess})Bx \tag{B.3}$$

which implies the actual eigenvalue is

$$\sigma_{acual} = \sigma + \sigma_{guess} \tag{B.4}$$

Equation A3 can be re-arranged in the form as,

$$\left(A - \sigma_{guess}B\right)\left[\left(\frac{1}{\sigma}\right)x\right] = Bx \tag{B.5}$$

Then the algorithm for the shifted inverse power method is:

i. Compute $(A - \sigma_{guess}B)$ and assume an initial guess for the eigenvector so that $x = x_{guess}$

ii. Compute Bx and then solve for y in the following equation,

$$\left(A - \sigma_{guess}B\right)y = Bx \tag{B.6}$$

iii. Suppose that the largest element (in magnitude) of y found in step (ii) is d_0, then set x to be, $x = y/d_0$, Repeat steps (ii) and (iii) until the eigenvector x converges.

iv. The smallest eigenvalue is $\sigma_{smallest} = (1/d_0) + \sigma_{guess}$. Alternatively, it can also be

computed in a more laborious way $\sigma_{smallest} = (x^T Ax)/(x^T Bx)$ without the inclusion of σ_{guess}.

In general, the above algorithm will converge to the smallest eigenvalue. It is safe to choose the initial guess which would be the lower bound of all the eigenvalues. If the initial guess is not available, one can simply set

$$\sigma_{guess} = 0 \tag{B.7}$$

$$x_{guess} = \frac{1}{\sqrt{n}}(1,1,1,\ldots,1) \tag{B.8}$$

where n is the dimension of the square matrix A so that the norm of x is one. Furthermore, it should be noted that the convergence of the eigenvector implies the convergence of the corresponding eigenvalue whereas the converse is not true. Thus, convergence of the eigenvector in steps (ii) and (iii) will guarantee the convergence of the eigenvalue in step (iv). In general, convergence of the eigenvalue to half a percent is achieved in only a few iterations and it is not unusual that one or two iterations will suffice. Moreover the case when the matrix B is singular does not affect the above algorithm.

APPENDIX C

EQUILIBRIUM EQUATION IN CORPORATING STIFFENER TORSIONAL RIGIDITY

This appendix aims to derive the out-of-plane governing equilibrium equation of stringer and/or ring stiffened cylindrical shells. In particular, the important effects of stringer and/or ring torsional rigidity are incorporated in the analysis which was previously ignored by Huchinson and Amazigo [40].

The potential energy of the stiffened cylindrical shell consists of the sum of an area integral for the skin and two single integrals for the stringer and rings respectively (all symbols not defined in the appendix are defined in the body of the paper),

$$
\begin{aligned}
P.E. = \frac{1}{2}\int_{Y=0}^{2\pi R}\int_{X=0}^{L} \{ & N_x\varepsilon_x + N_y\varepsilon_y + 2N_{xy}\varepsilon_{xy} \\
& + M_x^{sk}(-W_{,XX}) + M_y^{sk}(-W_{,YY}) \\
& + 2M_{xy}^{sk}(-W_{,XY})\}dXdY \\
& + \frac{M_s}{2}\int_{X=0}^{L} \{E_sA_s(\varepsilon_s)^2 + E_sI_s(W_{,XX})^2 \\
& + G_sJ_s(W_{,XY})^2 + E_sI_t^s(V_{,XX})^2\}dX \\
& + \frac{M_r}{2}\int_{X=0}^{L} \{E_rA_r(\varepsilon_r)^2 + E_rI_r(W_{,YY})^2 \\
& + G_rJ_r(W_{,XY})^2 + E_rI_t^r(U_{,YY})^2\}dY
\end{aligned}
\tag{C.1}
$$

In the above expression, (I_t^s, I_t^r) is the in-plane bending moment of inertia of stringer or ring with respect to its centroid; the in-plane strains at the skin middle surface $(\varepsilon_x, \varepsilon_y, \varepsilon_{xy})$ are related to the axial, circumferential and out-of plane displacements of the skin middle surface (U, V, W) by,

$$\begin{aligned} \varepsilon_x &= U_{,X} + \frac{1}{2}(W_{,X})^2 \\ \varepsilon_y &= V_{,Y} + \frac{W}{R} + \frac{1}{2}(W_{,Y})^2 \\ \varepsilon_{xy} &= \frac{1}{2}(U_{,Y} + V_{,X}) + \frac{1}{2} W_{,X} W_{,Y} \end{aligned} \tag{C.2}$$

The bending stress resultants of the 'skin' (superscript 'sk') are,

$$\begin{aligned} M_x^{sk} &= -D(W_{,XX} + \nu W_{,YY}) \\ M_y^{sk} &= -D(W_{,YY} + \nu W_{,XX}) \\ M_{xy}^{sk} &= -D(1-\nu) W_{,XY} \end{aligned} \tag{C.3}$$

and (N_x, N_y, N_{xy}) are the membrane stress resultants of the skin. Further, $(\mathrm{M_s}, \mathrm{M_r})$ are the number of equally spaced stringers or rings such that $M_s d_s = 2\pi R$ and $M_r d_r = L$.

The strains for the stringer and ring are,

$$\begin{aligned} \varepsilon_s &= \varepsilon_x - e_s W_{,XX} + \frac{e_s^2}{2}(W_{,XY})^2 \\ \varepsilon_r &= \varepsilon_y - e_r W_{,YY} + \frac{e_r^2}{2}(W_{,XY})^2 \end{aligned} \tag{C.4}$$

The stress function of a 'smeared-out' cylindrical shell is defined:

$$F_{,YY} = N_x + N_s$$
$$F_{,XX} = N_y + N_r \tag{C.5}$$
$$F_{,XY} = -N_{xy}$$

where

$$N_s = \frac{E_s A_s \varepsilon_s}{d_s}$$
$$N_r = \frac{E_r A_r \varepsilon_r}{d_r} \tag{C.6}$$

Introducing the membrane stress resultant of the skin $(\mathrm{N_x}, \mathrm{N_y})$ in terms of W and F (see Hutchinson and Amazigo [40]).

$$N_x = A_{xx}F_{,XX} + A_{xy}F_{,YY} + B_{xx}W_{,XX} + B_{xy}W_{,YY} \tag{C.7}$$

$$N_y = A_{yy}F_{,YY} + A_{yx}F_{,XX} + B_{yy}W_{,YY} + B_{yx}W_{,XX} \tag{C.8}$$

Using the principal of virtual work, assuming that the in-plane bending stiffness of the stiffeners is negligible, the in-plane equilibrium equations with respect to U and V vanish. The out-of-plane equilibrium equation can be obtained by setting the integrand of the following integral to zero:

$$\delta P.E. = \int_{Y=0}^{2\pi R}\int_{X=0}^{L}\Big\{\frac{F_{,XX}}{R} - F_{,YY}\,W_{,XX} - F_{,XX}\,W_{,YY} + 2F_{,XY}\,W_{,XY} + e_s A_{xx}F_{,XXXX} + e_r A_{yy}F_{,YYYY} + \left[e_s\left(A_{xy}-1\right) + e_r(A_{yx}-1)\right]F_{,XXYY} + \left[e_s B_{xx} + D\left(1+\frac{E_s I_s}{D d_s}\right)\right]W_{,XXXX} + \left[e_r B_{yy} + D\left(1+\frac{E_r I_r}{D d_r}\right)\right]W_{,YYYY} + \Big[e_s B_{xy} + e_r B_{yx} + D\left(2+\frac{G_s J_s}{D d_s}+\frac{G_r J_r}{D d_r}\right)\Big]W_{,XXYY} + e_s^2 D[(F_{,YY} - N_x)W_{,XY}]_{,XY} + e_r^2 D\big[\big(F_{,XX} - N_y\big)W_{,XY}\big]_{,XY}\Big\}\delta W\,dX\,dY \tag{C.9}$$

Ignoring the small terms involving e_s^2 and e_r^2, it can be seen that the effects of stiffener torsional rigidity can be incorporated in Hutchinson-Amazigo's(1967) formulation by redefining,

$$d_{xy} = \frac{1}{12(1-v^2)}\{1 + \frac{[12v(1-v^2)\alpha_s\alpha_r\gamma_s\gamma_r]}{\alpha_0} + \frac{1}{2}(\delta_s + \delta_r)\} \tag{C.10}$$

where δ_s and δ_r are defined in equation 12.

Finally, the strains at the skin middle surface can be written in the form,

$$\begin{aligned}
\varepsilon_x &= \frac{1}{Et}\left(N_x - vN_y\right) \\
&= \frac{1}{Et}\left[\left(F_{,YY} - N_s\right) - v\left(F_{,XX} - N_r\right)\right] \\
\varepsilon_y &= \frac{1}{Et}\left(N_y - vN_x\right) \\
&= \frac{1}{Et}\left[\left(F_{,XX} - N_r\right) - v\left(F_{,YY} - N_s\right)\right] \\
\varepsilon_{xy} &= \frac{1}{Et}(1+v)N_{xy} = -\frac{1}{Et}(1+v)F_{,XY}
\end{aligned} \tag{C.11}$$

It can be seen that the compatibility equation,

$$\begin{aligned}
&\varepsilon_{x,YY} + \varepsilon_{y,XX} - 2\varepsilon_{xy,XY} \\
&\qquad = \left(W_{,XY}\right)^2 - W_{,XX}\,W_{,YY} + \frac{W_{,XX}}{R}
\end{aligned} \tag{C.12}$$

is unaffected by the stiffener torsional rigidity.

REFERENCE

[1] R. Lorenz, "Achsensymmetrische Verzerrungen in dunnwandigen Hohlzylinder," *Z Ver deut Ingr 52,* pp. 1766-1793, 1908.

[2] R. Lorenz, "Die nicht achsensymmetrische Knickung dunnwandiger Hohlzylinder," *Phy Z Leipzig J 13,* pp. 241-260, 1911.

[3] S. P. Timoshenko, "Einige Stabilitatsprobleme der Elastizitatstheorie," *Z Math Phys 58,* pp. 337-357, 1910.

[4] S. P. Timoshenko, "Buckling of cylinders (exact title unknown)," *Bull Electrotech Inst St Petersburg XI,* 1914.

[5] R. V. Southewll, "On the general theory of elastic stability," *Phil Trans Roy Soc London Ser A 213,* pp. 187-202, 1914.

[6] A. Robertson, "The strength of tubular struts," *ARC rep and memno 1185,* 1929.

[7] W. Flugge, "Die Stabilitat der Kreiszylinderschale," *Ing Arch,Bd III 5,* pp. 463-506, 1932.

[8] W. M. Wilson and N. M. Newmark, "The strength of thin cylindrical shells as columns,," *Bull no 255, Eng Exp Station, Univ of Illinois,* 1933.

[9] E. E. Lundquist, "Strength tests of thin-walled duralumin cylinders in compression," *NACA TR-473,* 1933.

[10] M. Stein, "The effect on the buckling of perfect cylinders of prebuckling deformations and stresses induced by edge support," *Collected papers on instability of shell structures, NASA TN D-1510,* pp. 217-226, 1962.

[11] G. N. Fisher, "Uber den Einfluss der gelenkigen Lagerung auf die Stabilitat diinnwandiger Kreiszylinderschalen unter Axial- und Innendruck," *Z Flugwissenschaften 11(3),* pp. 111-116, 1963.

[12] M. Stein, "The influence of prebuckling deformations and stresses on the buckling of perfect cylinders," *NASA TR R-190,* 1964.

[13] H. Ohira, "Local buckling theory of axially compressed cylinders," *Proceedings of the eleventh Japan national congress of applied mechanics, Tokyo,* pp. 37-40, 1961.

[14] W. Nachbar and N. J. Hoff, "On edge buckling of axially compressed circular cylindrical shells," *Q Appl Math 20,* pp. 267-271, 1962.

[15] N. J. Hoff and L. W. Rehfield, "Buckling of axially compressed circular cylindrical shells at stresses smaller than the classical critical value," *J Appl Mech 32,* pp. 533-538, 1965.

[16] N. J. Hoff and T. C. Soong, "Buckling of circular cylindrical shells in axial compression," *Int J Mech Sci 7,* pp. 489-495, 1965.

[17] T. von Karman and H. S. Tsien, "Buckling of axially compressed circular cylindrical shells at stresses smaller than the classical critical value," *J Appl Mech 32,* pp. 533-538, 1965.

[18] D. M. A. Leggett and R. P. N. Jones, "The behavior of a cylindrical shell under axial compression when the buckling load has been exceeded," *ARC rep and mem no 2190,* 1942.

[19] H. F. Michielsen, "The behavior of thin cylindrical shells after buckling under axial compression," *J Aero Sci 15(12),* pp. 739-744, 1948.

[20] J. Kempner, "Postbuckling behavior of thin cylindrical shells," *J Aero Sci 21(5),* pp. 329-334, 1954.

[21] B. O. Almroth, "Postbuckling behavior of axially compressed circular cylinders," *AIAA J 1(3),* pp. 630-633, 1963.

[22] A. Sobey, "The buckling strength of a uniform circular cylinder loaded in axial compression," *ARC rep and mem no 3366,* 1964.

[23] L. H. Donnell, "A new theory for the buckling of thin cylinders under axial compression," *Trans ASME 56,* pp. 795-800, 1934.

[24] L. H. Donnell and C. C. Wan, "Effects of imperfections on buckling of thin cylinders and columns under axial compression," *Trans ASME 72(1),* pp. 73-78, 1950.

[25] T. T. Loo, "Effects of large deflections and imperfection on the elastic buckling of cylinders under torsion and axial compression," *Proc. Second U. S. Nat. Cong. Appl. Mech. 1954,* pp. 345-357, 1954.

[26] L. H. Lee, "Effects of modes of initial imperfections on the stability of cylindrical shells under axial compression," *Collected papers on stability of shell structures, NASA TN D-1510,* pp. 143-152, 1962.

[27] K. Y. Narasimhan and N. J. Hoff, "Snapping of imperfect thin-walled circular cylindrical shells of finite length," *J Appl Mech 38(1),* pp. 162-171, 1971.

[28] J. Arbocz and E. E. Sechler, "On the buckling of axially compressed imperfect cylindrical shells," *J Appl Mech 41(3),* pp. 737-743, 1974.

[29] I. Sheinman and G. J. Simitses, "Buckling analysis of geometrically imperfect stiffened cylinders under axial compression," *AIAA J 15(3),* pp. 374-382, 1977.

[30] W. T. Koiter, "On the stability of elastic equilibrium," *Doctoral Thesis, Delf, The Netherlands; English translations: NASA TT F-10, 833, 1967 and AFFDL-TR-70-25, 1970,* 1945.

[31] J. W. Huthinson and W. T. Koiter, "Postbuckling theory," *ASME Appl. Mech. Rev. 23,,* pp. 1353-1366, 1970.

[32] B. Budiansky and J. W. Hutchinson, "Buckling: progress and challenge," *In Proc. of Trends in Solid Mechanics (Edited by J. F. Besseling and A. M. A. van der Heijden),University Press, Delft.,* pp. 93-116, 1979.

[33] G. J. Simitses, "Buckling and postbuckling of imperfect cylinderical shells: A review," *In Proc. of ASME Joint Pressure Bessels Piping and Computer Engineering Divisions, Chicago, 20-24 July,* 1986.

[34] W. A. Nash, "An experimental analysis of buckling of thin initially imperfect cylindrical shells subjected to torsion," *Proc. of Society of Experimental Stress Analysis, Vol. 16,* pp. 55-68, 1959.

[35] V. I. Weigarten, "The effect of internal pressure and axial tension on the buckling of cylindrical shells under torsion," *Proc. of 4th U.S. National Congress of Applied Mechanics, published by ASME, Volume 2,* pp. 827-842, 1962.

[36] N. Yamaki and S. Kodama, "Perturbation analysis for the postbuckling and imperfection sensitivity of circular cylindrical shells under torsion," *Theory of Shells, Proc. of the Third IUTAM Symposium on Shell Theory, Tbilisi, U.S.S.R., August 22-28, 1978, edited by Koiter, W. T. and Mikhailov, G. K., North-Holland Publishing Co., Amsterdam,,* pp. 635-668, 1980.

[37] S. Kodama, K. Otomo and N. Yamaki, "Postbuckling behavior of pressurized circular cylindrical shells under torsion, Part 1: Experiment," *Int. J. of Non-linear Mechanics, Vol. 16, No 3/4, 1981,* pp. 337-353, 1981.

[38] W. F. Thielemann and M. E. Esslinger, "On the postbuckling behavior of thin-walled axially

compressed circular cylinders of finite length," *Proceedings of 70th anniversary symposium on the theory of shells to honor L H Donnell, Univ of Houston, Houston TX, D Muster, Ed,* pp. 433-479, 1967.

[39] W. F. Thielemann and M. E. Esslinger, "On the postbuckling equilibrium and stability of thin-walled circular cylinders under axial compression," *Proceedings of second IEST AM symposium on the theory of thin shells, F I Niordson, Ed, Springer-Verlag, Berlin,* pp. 264-293, 1967.

[40] J. W. Huthinson and J. C. Amazigo, "mperfection-sensitivity of eccentrically stiffened cylindrical shells," *AIAA Journal, Vol. 5, No. 3,* pp. 392-401, 1967.

[41] J. Singer, M. Baruch and O. Harari, "On the stability of eccentrically stiffened cylindrical shells under axial compression," *Int. J. of Solids and Structures, Vol. 3,* pp. 445-470, 1967.

[42] J. Singer, "Buckling of integrally stiffened cylindrical shells-a review of experiment and theory," *Contributions to the Theory of Aircraft Structures, presented to A. van der Neut, Delft University Press,* pp. 325-357, 1972.

[43] I. Sheinman and G. J. Simitses, "Buckling of imperfect stiffened cylinders under destabilizing loads, including torsion," *AIAA Journal, Vol. 15, No. 12,* pp. 1699-1703, 1977.

[44] V. V. Kostyrko and V. L. Krasovsky, "Pre-buckling deformation of axially compressed longitudinally reinforced shells," *Theoretical Foundations of Civil Engineering,* p. 87–96, 1995.

[45] V. V. Kostyrko and V. L. Krasovsky, "Investigation of influence of load eccentricity to the stability of stringer shells. Dnepropetrovsk: DGU," *Gidroaeromehanika i Teoriya Uprugosti [in Russian],* p. 75–81, 1988.

[46] V. L. Krasovsky, "Stability of isotropic and reinforced cylinders under axial compression," *Theoretical Foundations of Civil Engineering,* p. 123–32, 1997.

[47] V. L. Krasovsky, "Pre-buckling deformation and buckling of isotropic and reinforced thin-walled cylinders under axial compression," *Proceedings of the PGASA,Dnepropetrovsk,* p. 19–28, 1998.

[48] V. L. Krasovsky and V. V. Kostyrko, "The investigation of effect of axial compressive load eccentricity on the stability of stringer shells," *Proceedings of the VIII symposium on stability of structures, Zakopane (Poland),* p. 137–142, 2000.

[49] J. Singer, J. Arbocz and T. Weller, "Buckling experiments, shells, built-up structures, composites and additional topics," *New York: Wiley,* 2002.

[50] I. Y. Amiro and V. A. Zarutskii, "Experimental study of the stability of stiffened shells (Review)," *International Applied Mechanics, 32(9),* p. 659–668, 1996.

[51] A. I. Manevitch, "Stability and optimal design of reinforced shells," *KievDonetzk: Visha Shkola,* 1972.

[52] A. I. Manevitch, "Coupled instability of cylindrical shells stiffened with thin ribs (theoretical models and experimental results)," *In: Zaras J Kowal-Michalska K, Rhodes J, editors. Thin-walled structures Advances and developments. Proceedings of the third international conference thin-walled structures. London: Elsevier,* p. 683–691, 2001.

[53] A. C. Walker, A. Andronniko and S. Stridharan, "Experimental investigation of the buckling of stiffened shells using small scale models," *Buckling of the Shells in off-shore Structures. Granada: London et al,* p. 45–71, 1982.

[54] C. P. Ellinas and J. G. A. Croll, "Experimental and theoretical correlations of elastic buckling of axially compressed stringer stiffened cylinders," *Journal of Strain Analysis for Engineering Design, 18(1),* p. 41–67, 1983.

[55] E. Byskov and J. C. Hansen, "Postbuckling and imperfection sensitivity analysis of axially stiffened cylindrical shells with mode interaction," *Journal of Structural Mechanics, 8(2),* p. 205–224, 1980.

[56] M. Stein, "Some recent advances in the investigation of shell buckling," *AIAA Journal, 6(12),* p. 2339–2345, 1968.

[57] J. Singer, "Stiffened cylindrical shells,In: Teng JG, Rotter JM, editors," *Buckling of thin metal structures. London: Spon,* p. 286–343, 2004.

[58] I. V. Andrianov, V. Verbonol and J. Awrejcewicz, "Buckling analysis of discretely stringer-stiffened cylindrical shells," *International Journal of Mechanical Sciences, 48,* p. 1505–1515, 2006.

[59] G. J. Simitses, "Buckling of eccentrically stiffened cylinders under combined loads," *A/AA J., 7,* pp. 335-337, 1969.

[60] J. G. A. Cross, "Stiffened cylindrical shells under axial and pressure loading," *Shell Structures." Stability and Strength, ed. R. Narayanan. Elsevier Applied Science Publishers, Barking,* pp. 19-56, 1985.

[61] R. C. Tennyson, "The effect of shape imperfection and stiffening on the buckling of circular cylinders," *Buckling of Structures. ed. B. Budiansky Springer-Verlag, Berlin,* pp. 251-273, 1976.

[62] H. S. Shen, P. Zhou and T. Y. Chen, "Postbuckling Analysis of Stiffened Cylindrical Shells under Combined External Pressure and Axial Compression," *Thin - Walled Structures, 15,* pp. 43-63, 1993.

[63] R. C. Tennyson, H. K. Chan and D. B. Muggeridge, "The effect of axisymmetric shaped imperfections on the buckling of laminated anisotropic circular cylinders," *Transactions of the Canadian Aeronautics and Space Institute (CASI), Vol. 4,* pp. 335-360, 1971.

[64] R. C. Tennyson and D. B. Muggeridge, "Buckling of laminated anisotropic imperfect circular cylinders under axial compression," *J. Spacecraft, 10,* p. 143–148, 1973.

[65] H. S. Shen, "Post-buckling analysis of imperfect stiffened laminated cylindrical shells under combined external pressure and axial compression," *Comput Struct, 63,* p. 335–348, 1997.

[66] H. S. Shen, "Postbuckling of shear deformable cross-ply laminated cylindrical shells under combined external pressure and axial compression," *Int J Mech Sci, 43,* p. 2493–2523, 2001.

[67] H. S. Shen, "Boundary layer theory for the buckling and postbuckling of an anisotropic laminated cylindrical shell. Part I: Prediction under axial compression," *Composite Structures, 82,* p. 346–361, 2008.

[68] H. S. Shen, "Boundary layer theory for the buckling and postbuckling of an anisotropic laminated cylindrical shell, Part II: Prediction under external pressure," *Composite Structures, 82,* p. 362–370, 2008.

[69] H. S. Shen, "Boundary layer theory for the buckling and postbuckling of an anisotropic laminated cylindrical shell, Part III: Prediction under torsion," *Composite Structures, 82,* p. 371–381, 2008.

[70] G. J. Simitses, "Buckling of moderately thick laminated cylindrical shells: a review," *Composites Part B, 27B,* pp. 581-587, 1996.

[71] C. Hühne, R. Rolfes, E. Breitbach and J. Teßmer, "Robust design of composite cylindrical shells under axial compression — Simulation and validation," *Thin-Walled Structures, 46,* p. 947–962, 2008.

[72] R. Degenhardt, A. Kling, J. Orf, L. Kärger, R. Zimmermann, K. Rohwer and A. Calvi, "Investigations on imperfection sensitivity and deduction of improved knock-down factors for unstiffened CFRP cylindrical shells," *Composite Structures, 92,* p. 1939–1946, 2010.

[73] S. Castro, R. Zimmermann, M. Arbelo and R. Degenhardt, "Exploring the constancy of the global buckling load after a critical geometric imperfection level in thin-walled cylindrical shells for less conservative knock-down factors," *Thin-WalledStructures, 72,* p. 76–87, 2013.

[74] C. A. Schenk and G. I. Schuëller, "Buckling analysis of cylindrical shells with random geometric imperfections," *International Journal of Non-Linear Mechanics, 38,* p. 1119 – 1132, 2003.

[75] C. A. Schenk and G. I. Schuëller, "Buckling analysis of cylindrical shells with cutouts including random boundary and geometric imperfections," *Comput. Methods Appl. Mech. Engrg., 196,* p. 3424–3434, 2007.

[76] V. Papadopoulos and P. Iglesis, "The effect of non-uniformity of axial loading on the buckling behaviour of shells with random imperfections," *International Journal of Solids and Structures, 44,* p. 6299–6317, 2007.

[77] D. Hui and Y. Chen, "Imperfection-sensitivity of cylindrical panels under compression using Koiter's improved postbuckling theory," *Int. J. Solids Structures, 23(7),* pp. 969-982, 1987.

[78] D. Hui, "Postbuckling behavior of infinite beams on elastic foundations using Koiter's improved theory," *Int. J. Non-Linear Mechanics, 1988, Vol. 23, No. 2,* pp. 113-123, 1988.

[79] B. Budiansky and J. W. Hutchinson, "Dynamic buckling of imperfection-sensitive structures," *Proceedings of 11th Int. Congress of Applied Mechanics, Munich (Edited by H. Gortler) 1964, Springer, Berlin,* pp. 636-651, 1966.

[80] J. Arbocz and J. M. A. M. Hol, "Collapse of axially compressed cylindrical shells with random imperfections," *Thin-Walled Structures, 23,* pp. 131-158, 1995.

[81] B. Budiansky, "Post-buckling behavior of cylinders in torsion," *Theory of Thin Shells, IUTAM Symposium, Niordon, F. L., ed., SpringerVerlag, 1969,* pp. 212-233, 1967.

[82] D. Hui, "Asymmetric postbuckling of symmetrically laminated short cylindrical panels under compression," *Composite Structures, Vol. 3, 1985,,* pp. 81-95, 1985b.

[83] D. Hui, "Effects of geometric imperfections on frequency-load interaction of biaxially compressed antisymmetric angle ply rectangula plates," *ASME Journal of Applied Mechanics, 1985, Vol. 52,,* pp. 155-162, 1985a.

[84] D. Hui, "Imperfection sensitivity of axially compressed laminated flat plates due to bending-stretching coupling," *Int. J. Solids Structures,1986, Vol. 22, No. 1,* pp. 13-22, 1986a.

[85] J. R. Fitch, "The buckling and post-buckling behavior of spherical caps under concentrated load," *Int. J. Solids Structures 4,* pp. 421-446, 1968.

[86] W. T. Koiter and M. Pignataro, "A general theory for the interaction between local and overal buckling of stiffened panels," *Delft University of Technology Report WTHD 83, April 1976; also Problemi Attuali de Mecanica Teorica e Applicata, Atti del Convegno Internazionale a Ricordo di Modesto Panetti, Torino 1977,* pp. 179-222, 1976.

[87] W. A. Nash, "Buckling of initially imperfect cylindrical shells subject to torsion," *J. Appl. Mech. 24,,* pp. 125-130, 1957.

[88] M. Booton, "Buckling of imperfect anisotropic cylinders under combined loading," *University of Toronto Institute for Aerospace Studies (UTIAS), Report N0. 203.,* 1976.

[89] D. Hui and I. H. Y. Du, "Initial postbuckling behavior of imperfect antisymmetric cross-ply cylindrical shells under torsion," *ASME Journal of Applied Mechanics, 1987, Vol. 54,* pp. 174-180, 1987a.

[90] R. C. Tennyson, "Buckling of laminated composite cylinders: A review," *Composites, Vol. 1,* pp. 17-24, 1975.

[91] A. Van der Neut, "General instability of stiffened cylindrical shells under axial compression," *National Luchtvaartlaboratorium, Holland, Vol. 13, Rept. S 314,* 1947.

[92] J. M. Hedgepeth and D. B. Hall, "Stability of stiffened cylinders," *AIAA J. 3,* pp. 2275-2286, 1965.

[93] M. Baruch and J. Singer, "Effect of eccentricity of stiffeners on the general instability of stiffened cylindrical shells under hydrostatic pressure," *J. Mech. Eng. Sci. 5,* p. 23, 1963.

[94] D. Hui, "Interaction between local and overall buckling modes in axially stiffened cylindrical shells," *university of Toronto Institute for Aerospace Studies, UTIAS Report No. 247, November (CN ISSN 0082-5255),* 1983.

[95] W. T. Koiter, "The non-linear buckling problem of a complete spherical shell under uniform external pressure," *In Proc. of Koninklijke Nederlandse Akademie Van Wetenschappen, Series B, Vol. 72,* pp. 40-123, 1969.

[96] W. T. Koiter, "General theory of mode interaction in stiffened plate and shell structures," *Delft University of Technology, Report WTHD 91, September.,* 1976.

[97] R. L. Citerley, "Imperfection sensitivity and postbuckling behavior of shells," *In Pressure Vessels and Piping: Design Technology, a Decade of Progress (Edited by S. Y. Zamrik and D. Dietrich), ASME, New York.,* pp. 27-46, 1982.

[98] R. L. Citerley, "A review of imperfection sensitivity of stiffened shells," *Air Force Wright Aeronautical Laboratory, AFWAL_TR-84-3006.,* 1984.

[99] R. L. Citerley, "Computer programs for sensitivity analysis of stiffened cylindrical shells," *Welding Research Concil, WRC Bulletin 313, April, 17,* 1986.

[100] D. Hui, "Imperfection-sensitivity of elastically supported beams and its relation to the double-cusp instability model," *Proc. R. Soc. Lond. A, 1986, 405,,* pp. 143-158, 1986b.

[101] D. Hui and I. H. Y. Du, "Imperfection-sensitivity of long antisymmetric cross-ply cylindrical panels under shear loads," *ASME Journal of Applied Mechanics, 1987, Vol. 54,,* pp. 292-298, 1987b.

[102] R. C. Tennyson, M. Booton and D. Hui, "Changes in cylindrical shell buckling behavior resulting from system parameter variations," *Proceedings of the 15th International Congress,* 1980.

VITA

Hailan Xu was born in Chongqing, China, on June 4th, 1985, the only child in his family. He got his Bachelor degree in mechanical engineering in 2008 in Shenzhen University. In 2009 he attended University of New Orleans as a master student in mechanical engineering and also worked as a research assistant in the department. In 2010 he changed the program from master to PhD program. In 2011 spring semester he received the M.S. degree in mechanical engineering in the second year of the PhD program in University of New Orleans. Currently, he is working as the Teaching Assistance of the Department of Mechanical Engineering in the University of New Orleans.